Developing the Hydrologic Model of the Laurel Creek Watershed Including the Water Infrastructure

by

Lindsay Kathleen Bowman

A thesis
presented to the University of Waterloo
in the fulfillment of the
thesis requirement for the degree of
Master of Science
in
Earth Sciences

Waterloo, Ontario, Canada, 2016

Author's Declaration

I hereby declare that I am the sole author of this thesis. This is a true copy of the thesis, including any required final revisions, as accepted by my examiners.

I understand that my thesis may be made electronically available to the public.

Abstract

Continued growth of the Canadian economy has led to an increased population, which resulted in the progressive urbanization of Canada's watersheds. Additionally, as infrastructure ages, an increasing percentage of drinking water is lost due to leakage from the distribution system. Conversely, groundwater infiltrates into sanitary sewer systems, which results in additional inflow to wastewater treatment plants and increased cost to consumers. Municipal infrastructure asset management is an essential tool to efficiently manage the water and wastewater distribution networks.

To support asset management strategies for the City of Waterloo, the primary goal of this thesis was to create an integrated groundwater-surface water model for the Laurel Creek Watershed, with the inclusion of sanitary sewer infrastructure. Data was made available by the City of Waterloo, and a simplified version of the sanitary sewer network was created and added to the Laurel Creek Watershed model, which had been updated with a new digital elevation model, hydraulic conductivity field, land use files, and vegetation and evapotranspiration parameters. The model created in this thesis was constructed as a foundational prototype, and is intended for use as the basis of future work, which will include model enhancements and calibration.

A 2-D mesh was created based on a 10 m DEM of the Laurel Creek Watershed. The mesh had 25 m spacing along the stream network, and 100 m spacing in all other areas. A 3-D mesh was created using the bedrock as the bottom layer, and the 10 m DEM as the top layer. The upper 22 layers were created based on the 10 m DEM and the bottom 17 layers were generated using the Waterloo Moraine model created by Sousa (2013). An additional layer was added to incorporate the sanitary sewer network in order to ensure the network had a continually decreasing elevation to allow for gravity drainage of the sanitary sewers.

Four steady state simulations were created using HydroGeoSphere. Two simulations ran with 25% precipitation and no evapotranspiration, with one including the sanitary sewer infrastructure. The next two simulations ran with 100% precipitation and evapotranspiration, with one including the sanitary sewer infrastructure. The model results were also compared to measured stream flow data; a steady state model was compared to data collected over four years from 10 sites, and a transient model was compared to data from a 2014 storm event for five sites. While no calibration was conducted for the model, the steady state model produced results that were similar

to the measured data. The transient model produced very high peak flows for storm events, but it is expected that model calibration would mitigate this.

This thesis concludes that sewer infrastructure can be input into an integrated groundwater-surface water model using HydroGeoSphere, on the condition that it depends on the geometry of the 3-D mesh. It also resolves that the updated Laurel Creek Watershed model is able to simulate transient flows, though it must be calibrated in order to accurately represent measured stream flows.

Acknowledgements

First and foremost, I would like to express my sincere gratitude to my supervisor Andre Unger for providing me with the opportunity to study under his advisement. I am grateful for the opportunity to work within the SWIFT research group, gaining a multidisciplinary understanding of hydrologic modeling. Throughout my research, your feedback was always insightful, practical, and supportive. I would also like to thank you for the opportunity to speak at the 2014 American Geophysical Union Fall Meeting in San Francisco to present my research. The experience was inspiring and unforgettable.

Thank you also to my second supervisor, Jon Paul Jones. Without your help and constant encouragement, the experience of carrying out this thesis would have been vastly different, particularly in the beginning stages while I was learning the ropes. Your advice and feedback were invaluable, and your humour was always appreciated.

To Mark Knight, Carl Haas, and all the members of the SWIFT research group – thank you for introducing me to the world of municipal asset management. The work you are doing is incredibly valuable, and I am grateful I was given the opportunity to contribute a small portion.

For all of your expertise and advice regarding HydroGeoSphere, I would like to thank everyone at Aquanty Inc. In particular, thank you to Young-Jin Park for providing a deeper insight into HydroGeoSphere, and for the number of occasions you met with me to discuss my model.

Thank you to the members of my committee, and to all of the professors I have had the privilege of working with throughout my time at UW in the Faculty of Engineering and the Faculty of Science. In a relatively short amount of time, I have learned an incredible amount, qualitatively and quantitatively, from all of you. If knowledge is power, then I have met quite a few superheroes over the years.

I would also like to thank the University of Waterloo and the Department of Earth Sciences for the scholarships that were awarded to me: The Science Domestic Graduate Student Award, The University of Waterloo Graduate Scholarship, the Komex Graduate Scholarship in Earth Sciences, and the Steven Fritz Memorial Scholarship.

To my friends: Victoria and Megan – thank you for your never-ending camaraderie throughout the grad school process. Cailin – in times of darkness, thank you for showing me that the light at the end of the tunnel exists. Steph – thank you for defining the meaning of friendship, for leading by example when times get tough, and for your endless advice, encouragement, and positivity.

Finally, to Jaime: thank you for riding my highs with me, for digging me out of the lows, and for putting up with my shenanigans. Most importantly, thank you for opening my eyes to a brightness that I never knew existed.

Table of Contents

List of Figures

List of Tables

Chapter 1: Introduction

"The need for physically-based hydrologic models is growing, as regulators and stakeholders are only just now beginning to realize that it is imperative for them to integrate the regional-scale hydrologic budget into their groundwater and surface water management plans. In addition, forecasting the future supply of surface and groundwater resources in the advent of potential climate (and consequently precipitation and infiltration) change and uncertain population growth dynamics are an increasing concern confronting scientists and planners." Li et al., 2008

Continued growth of the Canadian economy has led to an increased population, which has resulted in the progressive urbanization of Canada's watersheds. Urbanization leads to an increased demand on the water and wastewater distribution networks. Given that water is a public good in Canada, all costs associated with the water and wastewater networks are paid for by the consumers. In order to minimize costs to the consumer, and to efficiently manage the networks, an asset management system is essential. An asset management system is put in place to: Assess the current condition of the water and wastewater distribution systems, schedule operation and maintenance activities according to this assessment, and predict the likely performance of the infrastructure under various development and water demand scenarios.

In 2009, the reported average residential water use for Canadians was 274 litres per capita per day (lpcd) (Environment Canada, 2011). High water use can contribute to environmental and economic problems, including the drawdown of aquifers, water shortages, and increased energy consumption for pumping and treatment; so it is important to have efficient maintenance of the municipal infrastructure.

As the infrastructure ages, a higher percentage of drinking water is lost to leakage in the distribution system. From 2006 to 2009, leakage rose from 12.8% to 13.3% of metered water (Environment Canada, 2011). The Canadian Water and Wastewater Association (CWWA) estimated that Canada would require $88.5 billion to update existing water and wastewater infrastructure and build new water and wastewater systems between 1997 and 2012 (CWWA, 1998). According to Statistics Canada (2007), investments in water systems "barely compensated for the aging of existing equipment from 1993 to 2002." Therefore, it is essential to develop

infrastructure asset management strategies to foster efficient use of our water and wastewater systems.

1.1 Objectives

This thesis aims to create an integrated groundwater-surface water model of the Laurel Creek Watershed, using the previous model created by Jones (2005) as a guide. The new model will be created using a new digital elevation model, hydraulic conductivity field, updated land use files, and new vegetation and evapotranspiration properties.

Following the model update, the primary objective of this thesis is to use data from the City of Waterloo concerning the location and operation of its water main and sanitary sewer network to model the flow through a simplified version of the water infrastructure within the integrated Laurel Creek Watershed groundwater-surface water model. The development of this model will demonstrate the merits of including subsurface infrastructure in groundwater-surface water models for urbanized watersheds. A full hydrologic model is necessary because the flow through water mains and sanitary sewers is of the same order of magnitude as other features in the watershed, such as evapotranspiration. These features are responsible for a large amount of water consumption, making a full hydrologic model essential for practical application.

Steady state and transient versions of the model will also be compared to existing stream flow data. The purpose of this comparison is to determine the correctness of the model. The results will provide a starting point for model calibration to be conducted in the future. The comparison of the model to stream flows will determine the impact of infrastructure on the surface flow and groundwater flow.

1.2 Technical Approach

The steps required for accomplishing the objectives described in Section 1.1 are as follows:

1. Update the integrated Laurel Creek Watershed groundwater-surface water model using the model created by Jones (2005) as a guideline, and include evapotranspiration.
2. Introduce sanitary sewer infrastructure into the model with plans to include water mains and storm sewers in future models.

3. Compare model to stream flow and monitoring well data to determine the impact of infrastructure on surface flow and groundwater flow both locally at specific streams and on a macro scale.
4. Utilize the model results for operational asset management strategies for a municipality.

1.3 Scope

The model created in this thesis focused only on the Laurel Creek Watershed. No-flow boundary conditions were utilized in the model, and isotropy was assumed throughout the porous media. Infrastructure data was made available only from the City of Waterloo, which comprises 66% of the surface area of the Laurel Creek Watershed. In order to test the capabilities of HydroGeoSphere and to decrease computation time, a simplified version of the sanitary sewer infrastructure was created, which was comprised of 3.2% of the total length of the sanitary sewer system. The simplified version was representative of the trunk lines within the sanitary sewer network. Only the sanitary sewer system was modeled in this thesis.

The model was compared to measured stream flows for steady state and transient flow simulations, but no calibration was conducted due to time constraints. Simulations were conducted for the months between April and October, with no consideration for snowfall, snowmelt, or the freeze-thaw cycle. Additionally, the model was limited by the capabilities of HydroGeoSphere; infrastructure was dependent on the mesh geometry, and information regarding the exchange flux between the subsurface and infrastructure domains could not be collected while simultaneously collecting stream flow data.

The model produced in this thesis created a path toward constructing a practical asset management tool for use by a municipality. The model is intended for use as a foundational prototype. More work is required in order for this model to be fully functional.

1.4 Thesis Organization

This thesis is comprised of six chapters: 1) Introduction, 2) Background, 3) Methodology, 4) Results, 5) Conclusions, and 6) Recommendations for Future Work. All citations referred to in the chapters can be found in References. Each chapter is written in such a way that it will be easy to follow by future graduate students and researchers in order to aid in the continuation of this project.

Chapter 2: Background

2.1 Literature Review

2.1.1 Groundwater-surface water interaction

Historically, groundwater and surface water have been treated as separate entities for the purposes of scientific study and engineering design. While they do behave differently, the interaction between groundwater and surface water has significant effects on the hydrologic cycle. It is important to understand and quantify the exchange between groundwater and surface water in order to maintain water resources.

There are numerous methods used for the measurement of groundwater-surface water interaction, some of which include direct measurement, and others that are indirect. Direct measurements may include seepage meters (Lee, 1977), heat tracers (Winter et al., 1998), or the utilization of Darcy's Law (Darcy, 1856), which requires field-testing for the hydraulic gradient, hydraulic conductivity, groundwater velocity, and porosity. Finally, the mass balance approach involves the measurement of gains and losses in surface water, using methods such as dilution gauging (Kilpatrick and Cobb, 1985) and the subsequent calculation of change in groundwater (Kalbus et al., 2006).

Physically based, numerical modeling is an indirect way to measure the groundwater-surface water interaction of a watershed. Freeze and Harlan (1969) created the original 'blueprint' for a physically-based hydrologic model, with the primary purposes of the models being:

- To synthesize past hydrologic events.
- To predict future hydrologic events and to evaluate, for design purposes, combinations of hydrologic events occurring rarely in nature.
- To evaluate the effects of artificial changes imposed by man on the hydrologic regime.
- To provide a means of research for improving our understanding of hydrology in general, and the runoff process in particular.

(Freeze and Harlan, 1969)

The predictive capacity of this approach makes numerical modeling an attractive technique for the measurement of groundwater-surface water interaction. The 'blueprint' created by Freeze and

Harlan (1969) provided a framework for future work in hydrogeology. Within this framework, models can be created using externally coupled and iteratively coupled approaches with respect to the compatibility of land surface interface fluxes and pressure heads (Jones, 2005). However, these methods require the application of boundary conditions at the groundwater-surface water interface. To eliminate the requirement of boundary conditions at the interface, the interface fluxes between groundwater and surface water can be solved simultaneously by using a fully-integrated approach.

VanderKwaak (1999) created an integrated physically-based numerical model of surface and subsurface hydrologic response to precipitation and chemical transport within coupled hydrologic systems, called the Integrated Hydrology Model (InHM). Jones et al. (2008) assessed InHM's ability to simulate transient flow processes at a large scale by creating a physically-based surface/variably saturated subsurface flow model for the hydraulically complex Laurel Creek Watershed, which is the same watershed studied here. Following calibration with stream flow and observation wells, and validation with two sets of rainfall data, Jones et al. (2008) found that the level of agreement between the computed and observed hydraulic head and drainage patterns captured the groundwater and surface water characteristics of the watershed. The paper ultimately showed that fully-integrated groundwater-surface water models are useful for predicting steady state and transient flow at the watershed scale.

Sudicky et al. (2008) created a fully-integrated hydrologic model of the Laurel Creek watershed using InHM based on the work of Jones (2005). The objectives were to analyze the integrated physically-based numerical model's ability to simulate integrated groundwater-surface water flow processes when applied to a hydraulically complex, but reasonably well-characterized subcatchment, and to investigate the near-stream water flow and contaminant exchange fluxes resulting from the use of different temporal averages of precipitation as input when simulating a surficial contaminant plume discharging into a stream. The simulation strategy was to: 1) simulate a steady-state subsurface plume for 30 years with the use of a the steady-state groundwater-surface water flow system, and 2) to use the steady-state flow system as the initial condition for the subsequent transient flow and transport simulations for a one-year duration, in which synthetic precipitation rates were input on annual, monthly, and daily time scales. The authors found that although there were issues related to model parameterization and numerical implementation that should be considered in future studies, the model was generally capable of simulating fully-integrated groundwater-surface water flow and transport flow. The authors

believed that this fully-integrated approach to watershed simulation has the potential to improve upon previous conventional simulation strategies, which either consider groundwater and surface water separately or join them in a weakly coupled manner.

HydroGeoSphere was developed after InHM, based on the code for FRAC3DVS (Therrien, 1992). FRAC3DVS was designed to simulate variably saturated groundwater flow and the advective-dispersive solute transport in porous media and discretely fractured porous media. Given that FRAC3DVS was a groundwater model, a surface water flow component was added, and thus HydroGeoSphere (formally HydroSphere) was created (Therrien et al., 2003).

Li et al. (2008) used HydroGeoSphere to examine the hydrologic budget of the Duffins Creek Watershed, which has an area of 286.6 km^2. Prior to this study, no applications had examined the influence of seasonal precipitation variations as it relates to groundwater-surface water flow at the watershed scale. This study shows the utility of HydroGeoSphere to simulate three-dimensional hydrologic responses of the groundwater and surface water flow systems in a large-scale watershed, driven by multi-seasonal precipitation events. The authors identified data gaps that contribute to reduction in the predictive capacity of the model. Results indicated that while the model reproduced annual average stream flows it was unable to reproduce detailed features for individual hydrographs. The authors predicted that in order to generate accurate simulations from one year to the next, the evapotranspiration parameters should be adjusted.

Goderniaux et al. (2009) used HydroGeoSphere to estimate the impacts of climate change on groundwater resources, where the physically-based groundwater-surface water flow model was combined with advanced climate change models for the Geer watershed in Belgium. Contrary to previous studies by Jones (2005), Sudicky et al. (2008) and Li et al. (2008), Goderniaux et al. (2009) used a large discretization in order to provide an accurate representation of the components of water balance at all points during the simulation. Had a fine discretization been used, as in previous studies, the results would have been overrepresented at the riverbed scale (Goderniaux et al., 2009). Ultimately, this study provides methodology that can be used to assess impacts of climate change on groundwater reserves, and the uncertainties regarding these impacts.

2.1.1.1 Modeling Fractured Media

Blessent et al. (2008) developed a new modeling approach to represent groundwater flow and contaminant transport through fractured media. Fractures have a high permeability and low storage because they have a lower contribution to total porosity of the rock mass. The approach used coupled geological and numerical models. The fractures were incorporated into the mesh generation using 2-D models and then modeled in 3-D using HydroGeoSphere. The authors showed that this approach was successful at modeling flow through fractured media.

2.1.2 Municipal Infrastructure Asset Management

The development of municipal water and wastewater infrastructure in Canada began over 150 years ago. As Canadian cities grew, the infrastructure systems continued to expand in order to support the population (Federation of Canadian Municipalities, 2002). Water and wastewater infrastructure networks have long service lives, and are commonly in use for 80 to over 100 years (Felio, 2012). Given that components of municipal infrastructure are constructed and maintained at different times, have varying service lives, and deteriorate at different rates depending on design, construction, and maintenance, it is critical to properly plan and manage these assets. While governments struggle to catch up to the infrastructure needs, the needs of the community continue to grow as aging infrastructure exceeds its lifespan and the growing population continues to require new infrastructure (Felio, 2012). Additional pressures such as climate change, sustainability, and environmental protection put more stress on municipalities to maintain their assets. Canadian municipalities are entering an era during which a significant percentage of water and wastewater infrastructure are nearing the end of their life cycle (Federation of Canadian Municipalities, 2002). As a result, asset management strategies have become increasingly important for Canadian municipalities.

Despite the need for asset management strategies, there have been few Canadian standards or guidelines for municipal infrastructure asset management. In 2002, the Canadian Institute of Chartered Accountants (CICA) explored alternatives for financial reporting of infrastructure as assets, and the Public Sector Accounting Board of CICA suggested that senior levels of government adopt private sector accounting practices for financial reporting (Federation of Canadian Municipalities, 2004). This method would involve the capitalization and depreciation of tangible capital assets, as opposed to the practice of expensing the assets. Also in 2002, the government of Ontario passed Bill 175 (Sustainable Water and Sewage Systems Act), making it

mandatory for municipalities in Ontario to assess and report the full costs of providing water and sewage services, and to prepare and implement plans for the recovery of those costs (Federation of Canadian Municipalities, 2004).

2.1.2.1 Objectives and Benefits of Asset Management

Asset management involves long-term comprehensive planning for the management of new and existing infrastructure on a life-cycle basis. It includes the inventory and condition assessment of all current assets, and the development of maintenance and risk management programs, as well as a financial and investment strategy (Stewart, 2012). Municipalities have a wide range of assets, all with different ages and varying life cycles and differing requirements according to the public and council. Therefore, municipal asset management plans must be flexible in order to adapt to change and still achieve the desired results. Because every municipality has different expectations for their community, there is no singular approach to asset management. However, the basic framework can be summarized with the following seven questions:

1) What do you have and where is it? (Inventory)
2) What is it worth? (Cost/replacement rates)
3) What is its condition and expected remaining service life? (Condition and capability analysis)
4) What is the level of service expectation, and what needs to be done? (Capital and operating plans)
5) When do you need to do it? (Capital and operating plans)
6) How much will it cost and what is the acceptable level of risk(s)? (Short- and long-term financial plan)
7) How do you ensure long-term affordability? (Short- and long-term financial plan)

(Federation of Canadian Municipalities, 2004)

The implementation of municipal infrastructure asset management plans can reduce life cycle costs of the assets, increase accuracy in financial planning, increase data management efficiency, and lead to more effective communication between taxpayers and elected officials.

2.1.2.2 Challenges of Asset Management

Asset management has the potential to be highly effective. However, without meaningful and comprehensive communication between municipal staff, elected officials, and the public, efficiency of the program could decrease. Implementation of an asset management plan is challenging if it is not well endorsed by all stakeholders. Additionally, there are significant challenges related to the development of a current database of all infrastructure inventory and condition due to the large number of municipal assets (Federation of Canadian Municipalities, 2004).

2.1.2.3 Strategic, Tactical, and Operational Models

An asset management plan should look at three types of plans: strategic, tactical, and operational. The strategic plan gives a high level analysis of the asset life cycle, providing a 50 to 100 year outlook. The strategic model includes the creation of development plans for renewal, rehabilitation, and sustainable projections of the assets.

The tactical model includes the development of capital programs to ensure the best health of the assets over the long-term, 3-10 years. It includes programs such as infrastructure management systems, capital program development and prioritization, and asset risk and criticality analysis.

The operation model is the 1-3 year plan, which provides a detailed capital budget, and lists individual projects. (Stantec et al., 2014)

2.1.3 Water-Energy Nexus

Water and energy scarcity are growing challenges that are facing society today, and they are linked to each other. Meeting future energy needs is dependent on the availability of water, and energy is required for the production of future water needs (Zhou et al., 2013). As urban populations grow, water and energy supplies are exceeded and imports from distant areas are required (Perrone et al., 2011).

Perrone et al. (2011) created a tool to quantify the amount of water and energy used by a community to help assess resource flows. They computed the amount of energy required to produce water for a community in Tuscon, Arizona, as well as the amount of water required to produce energy for the same community. This analysis showed that it is more efficient for

Tuscon to import their water from an upstream watershed than to use their own groundwater resources. However, this method of using upstream watersheds for the water source of urban centres can lead to desertification in rural areas.

Perhaps the solution is to reduce urban water consumption in order to reduce the amount of energy used and thus decrease desertification in rural areas. Zhou et al. (2013) suggest that optimization of water supply systems would reduce energy demands and greenhouse gas emissions in the municipal water sector. Urban water systems, including supply, distribution, end use, and wastewater treatment together use 2-3% of the worlds' energy supply for consumers and industry. A decrease in urban water use directly correlates to a decrease in the amount of energy required to produce the water, and thus a decrease in the amount of water required to produce that energy. In fact, a 20% efficiency increase in Ontario could result in a potential 34% energy reduction (Power Applications Group, 2008). Zhou et al. (2013) established a water flow analysis framework using life cycle analysis to determine water flow in municipalities, and the related energy consumption using an input-output analysis. They applied this water flow analysis, which neglects evapotranspiration and soil moisture, to Changzhou, China. They found that energy used for water production was 10% of the total energy use, and that the wastewater treatment was the most energy-intensive stage.

Reducing inflow and infiltration into the sanitary sewer network would reduce the amount of wastewater treatment required, which would therefore reduce the amount of energy required for treatment. Inflow and infiltration are defined as the components of sewer flow, which enter the sewer conduit from surface water or groundwater sources, respectively (Chin, 2014). Chin (2014) shows that by efficiently managing water resources, we are not only conserving water supplies for the future of our municipalities; we can also reduce the amount of energy required.

Goderniaux et al. (2009) used HydroGeoSphere to create a physically-based and spatially-distributed groundwater-surface water model for the Geer Basin (465 km^2) in Belgium. They simulated six regional climate model scenarios to assess the effects of climate change on the watershed. The model was calibrated to hydraulic heads and surface flow rates from 1967-2003. Then six climate change scenarios were applied to the model for the years 2071-2100. The scenarios were based on the European Union Fifth Framework Programme (FP5) PRUDENCE project (Prediction of Regional scenarios and Uncertainties for Defining European Climate change risks and Effects) (Christensen et al., 2007). The simulations showed that groundwater

levels and river flow rates are expected to decrease significantly during the future simulation period: 2071-2100. The results provide further incentive to improve efficiency within the water-energy nexus.

2.2 Site Description

2.2.1 Laurel Creek Watershed

The Laurel Creek Watershed is 75.8 km^2, resides within the Region of Waterloo inside the Grand River Watershed (Figure 1). The watershed contains both rural and urban land uses, with primarily agricultural/forested areas in the West, and residential, commercial, or industrial areas within the City of Waterloo in the East.

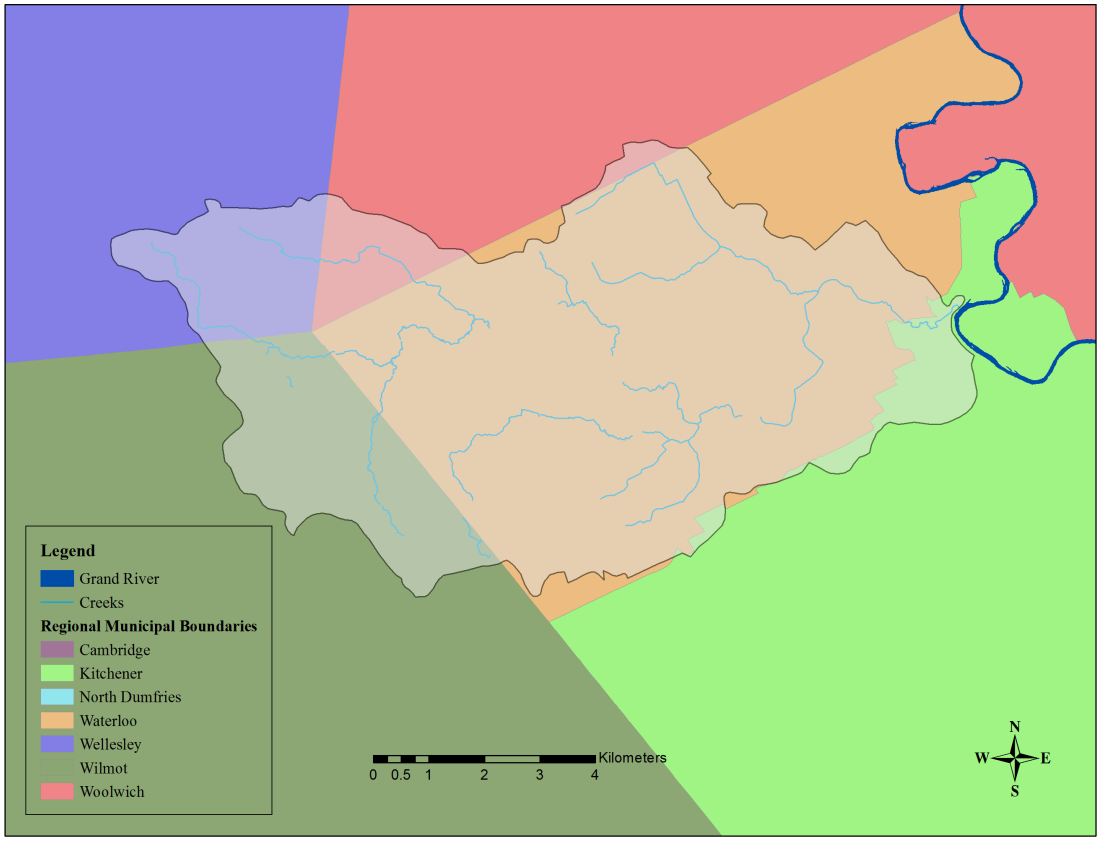

Figure 1 Location of the Laurel Creek Watershed within the Region of Waterloo

The watershed is within the Waterloo Moraine. The Waterloo Moraine occupies an area of 600 km^2, and has rolling topography with elevations between 330 to 400 m above sea level (asl) (Bajc et al., 2014). Figure 2 shows the Grand River Watershed, with the Waterloo Moraine shaded. The Laurel Creek Watershed location within the Waterloo Moraine is shown in Figure 3.

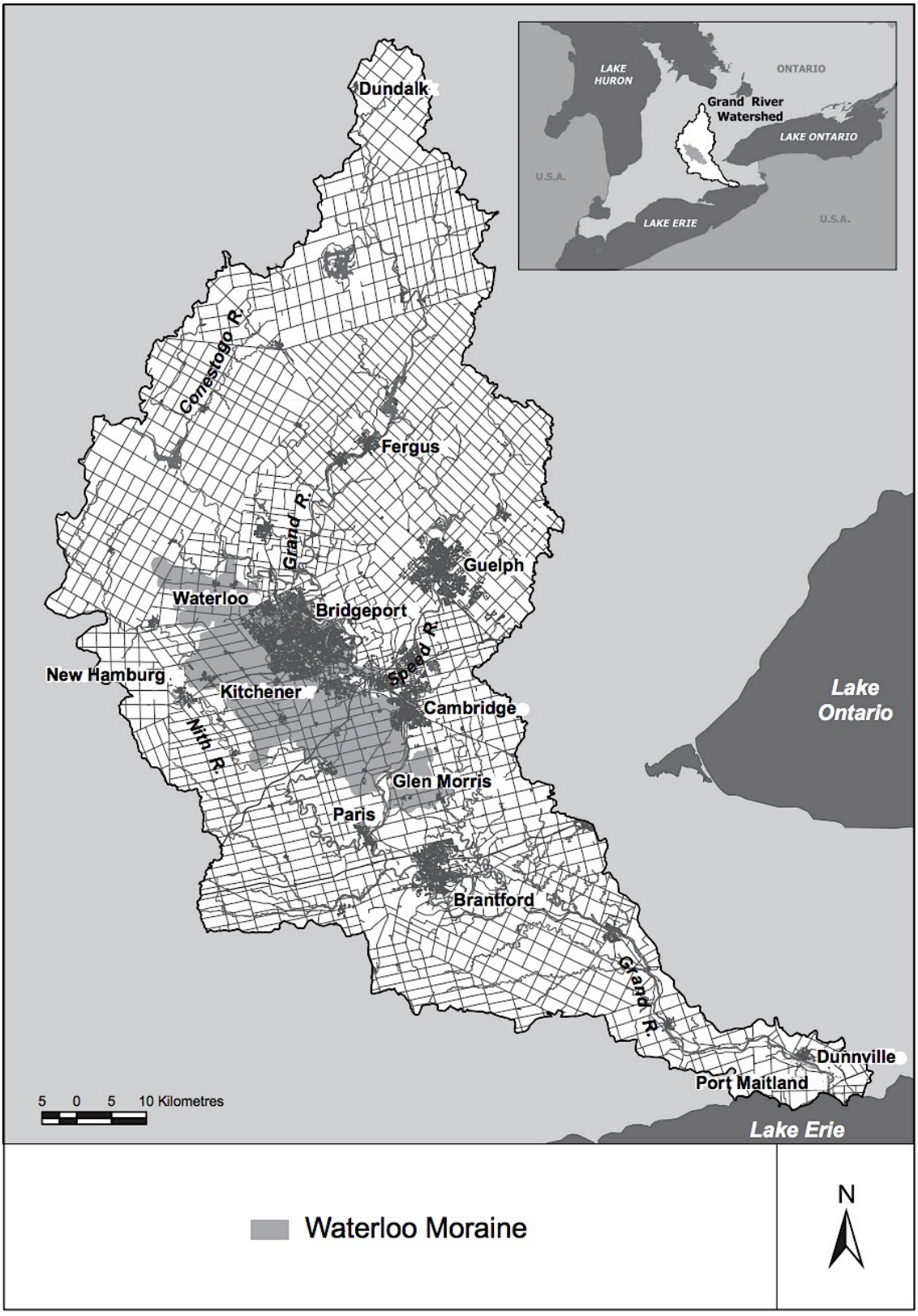

Figure 2 The Grand River Watershed, with the Waterloo Moraine indicated by shading (Veale et al., 2014)

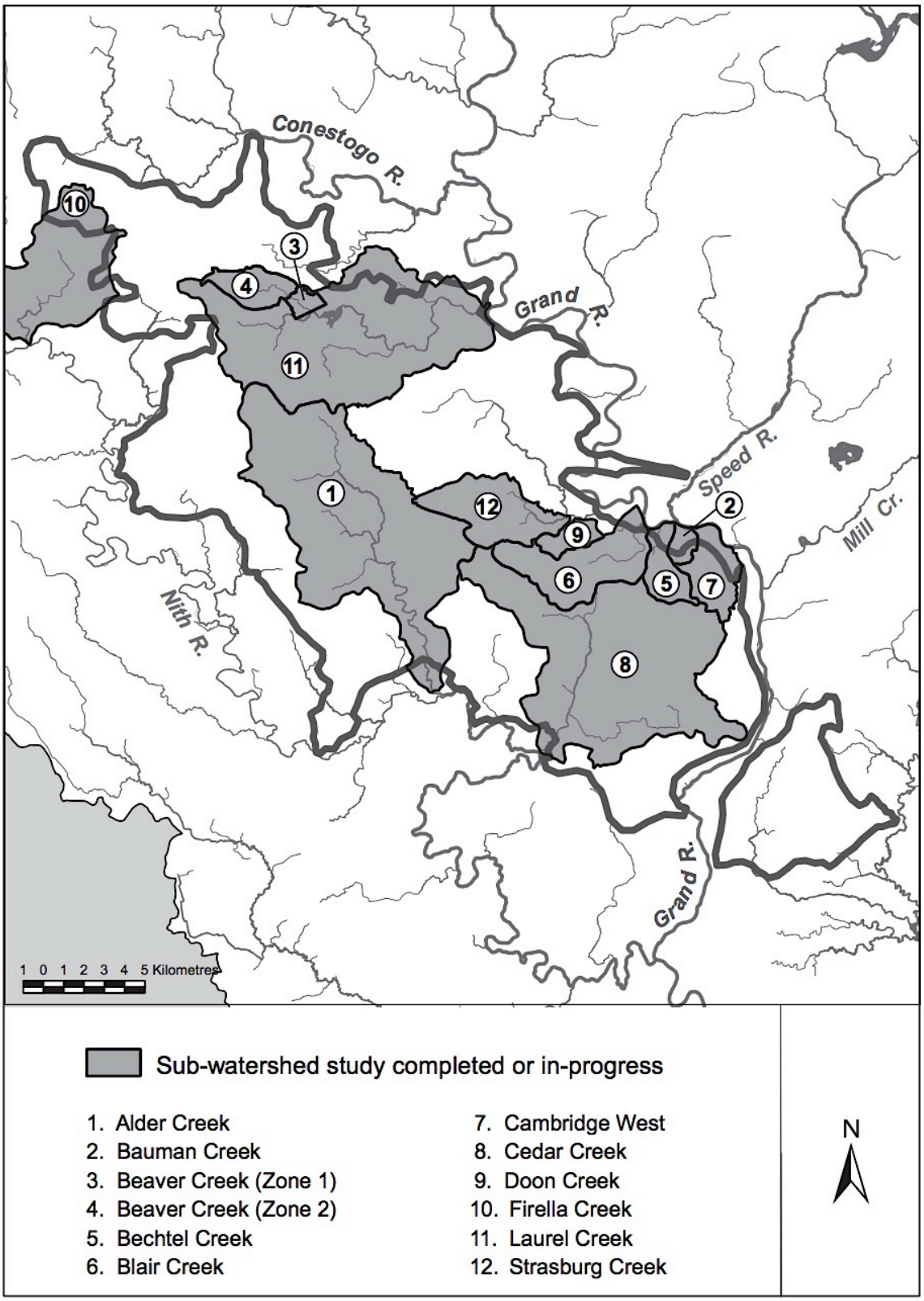

Figure 3 Sub-watersheds of the Grand River Watershed, showing the Laurel Creek Watershed as #11 (Veale et al., 2014)

2.2.2 Climate

Southern Ontario experiences four distinct seasons, with temperatures ranging from an average of -6.5°C in the winter to 20°C in the summer. The average annual precipitation, between the period of 1981-2010 was 916 mm, with the months with the lowest and highest amounts of precipitation occurring in February and July, respectively Environment Canada, 2015). The average amount of recharge is between 200 mm/year and 450 mm/year, depending on the underlying geology (Blackport et al., 2014).

2.2.3 Geology

The Laurel Creek Watershed, within the Waterloo Moraine, is composed of the Mornington, Tavistock, Upper Maryhill, and Port Stanley Tills in the upper layers. In the subsurface, it is composed of Catfish Creek Till, Pre-Catfish Creek Till glaciofluvial deposits, Canning sediment, and Pre-Canning glaviofluvial deposits, as outlined in Figure 4 (Bajc et al., 2014). The formations are described in Table 1. The bedrock is made of dolostone, shale, gypsum, and limestone from the Silurian Salina formation (Bajc et al., 2014; Jones, 2005).

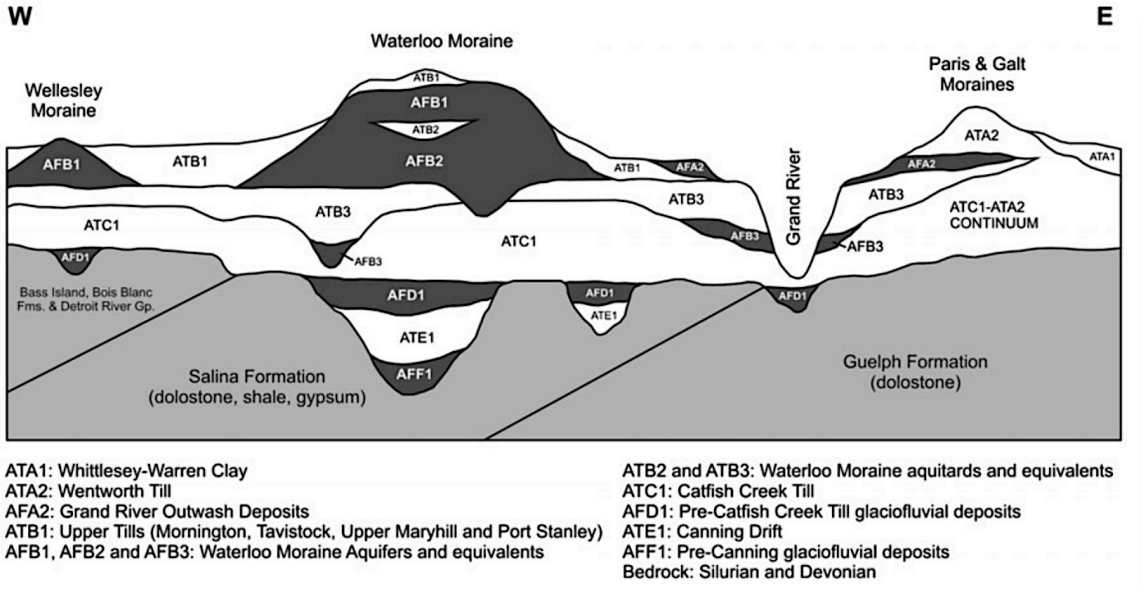

Figure 4 Idealized conceptual geological model for the Waterloo Moraine. Aquitard units are light, aquifer units are dark, and bedrock is grey. (Bajc et al., 2014)

Table 1 Characteristics of the important hydrostratigraphic units modeled in the Waterloo Moraine (Bajc et al., 2014)

Stratigraphic Units	Ontario Geological Survey hydro-stratigraphic class	Thickness (m)	Sediment Characteristics
Mornington Till, Port Stanley Till, Tavistock Till, Upper Maryhill Till	ATB1	<30	Pebbly, sandy silt to stone-poor, silty clay to clayey silt diamictons, massive to laminated
Waterloo Moraine Aquifer	AFB1	<80	Bedded to massive silt, sand and gravel, silt- to clay-rich diamicton and glaciolacustrine deposits with granules and isolated pebbles, sharp-based fining upward successions
Middle Maryhill Till	ATB2		
Waterloo Moraine Aquifer	AFB2		
Lower Maryhill Till	ATB3		
Waterloo Moraine Aquifer	AFB3		
Catfish Creek Till	ATC1	<30	Massive to laminated, pebbly to cobbly sandy silt and sand mud diamicton with minor silt, sand and gravel interbeds
Pre-Catfish glaciofluvial deposits	AFD1	<20	Bedded sand and gravel
Canning sediment	ATE1	<15	Massive to laminated silt and clay and stone-poor silty to clayey diamicton, minor sand
Pre-Canning glaciofluvial deposits	AFF1	<30	Bedded sand and gravel
Silurian and Devonian bedrock	Bedrock		Dolostone, shale, gypsum, cherty limestone

2.3.4 Surface Water

The primary surface water feature in the Laurel Creek Watershed is Laurel Creek, which runs from West to East and discharges into the Grand River. There are several tributaries to Laurel Creek, as shown in Figure 1. Many of the tributaries are lined with riprap, which influences their

natural rainfall-runoff responses. The Laurel Creek Reservoir and Columbia Lake, as well as the wetlands in the Western side of the watershed, also represent significant surface water features. The reservoir and the lake both have controlled discharges that are used to mitigate flooding during the spring.

In Southern Ontario, significant changes in stream stage, >0.5 m, occur for short durations of 1-2 weeks during spring melt and storm events. Beyond these periods of significant change, the stream stage fluctuation is less than 0.5 m (Meyer et al., 2014). Therefore, it can be assumed for modeling purpose that the stage fluctuations are short and that the stage can be represented by a long-term average value for all streams within the watershed.

2.3.5 Hydrogeology

The aquifer system in the Laurel Creek Watershed is complex due to the discontinuous nature of the multi-level aquitard and aquifer units (Bajc et al., 2014). In the Region of Waterloo, 80% of the municipal water needs are supplied by groundwater resources from over 100 active groundwater supply wells, with the remaining 20% coming from the Grand River. Blackport et al. (2014) describe the hydrogeology of the Region of Waterloo with a focus on the major municipal water supply aquifers and the key aquitards that comprise the Waterloo Moraine. There are three primary aquifer units (Figure 4, Table 1).

Due to the implementation of the *Clean Water Act* (Province of Ontario, 2006), stemming from the Walkerton Inquiry (O'Connor, 2002), the Ontario Geological Survey initiated a program to provide geoscience information with the goal of protecting and preserving Ontario's groundwater resources (Blackport et al., 2014). Three-dimensional mapping of the overburden units beneath the Region of Waterloo were created as a result of this goal. Additionally, the Region initiated the Integrated Urban System Supply Optimization and Expansion Project. The goal of the project was to develop additional water supplies from existing, underutilized municipal supply wells (Blackport et al., 2014). Further technical studies have since been conducted to examine potential threats to water quality and quantity within the Regional groundwater supply. As studies evolve and more data becomes available, more detailed interpretations of the hydrostratigraphic units may change. According to Blackport et al. (2014), "although [our understanding of] the general stratigraphic structure of the Waterloo Moraine has not evolved dramatically over the past few decades, the conceptual understanding of the groundwater flow system has been refined,

particularly with respect to hydraulic interconnections between the primary aquifers, and between the upper aquifer and the surface water features."

Generally, the Laurel Creek Watershed is highly heterogeneous and anisotropic, with hydraulic conductivity ranging from 1×10^{-11} m/s to greater than 1×10^{-02} m/s. The Upper Waterloo Moraine aquifers consist of a thick saturated and unsaturated sand and gravel unit that is typically greater than 45 m in thickness. The total amount of water permitted for removal from the aquifer using the four major well fields in the Waterloo Moraine is 773 L/s, with an average pumping rate of 427 L/s (Blackport et al., 2014). The four major well fields are Mannheim West, Mannheim East, Erb Street, and Wilmot Centre (Blackport et al., 2014). The recharge rates in areas where the Upper Maryhill Till aquitard is absent are as high as 200 mm/year to 450 mm/year (Blackport et al., 2014). However, due to urbanization, there is a high amount of runoff in the Eastern part of the Watershed.

2.3.6 Infrastructure

The City of Waterloo currently has 465.6 km and 431.6 km of water mains and sanitary sewers, respectively. A map of the water main and sanitary sewer network is given in Figure 5, with the Laurel Creek Watershed mesh also shown. Figure 6 shows the water main and sanitary sewer network in the City of Waterloo urban core.

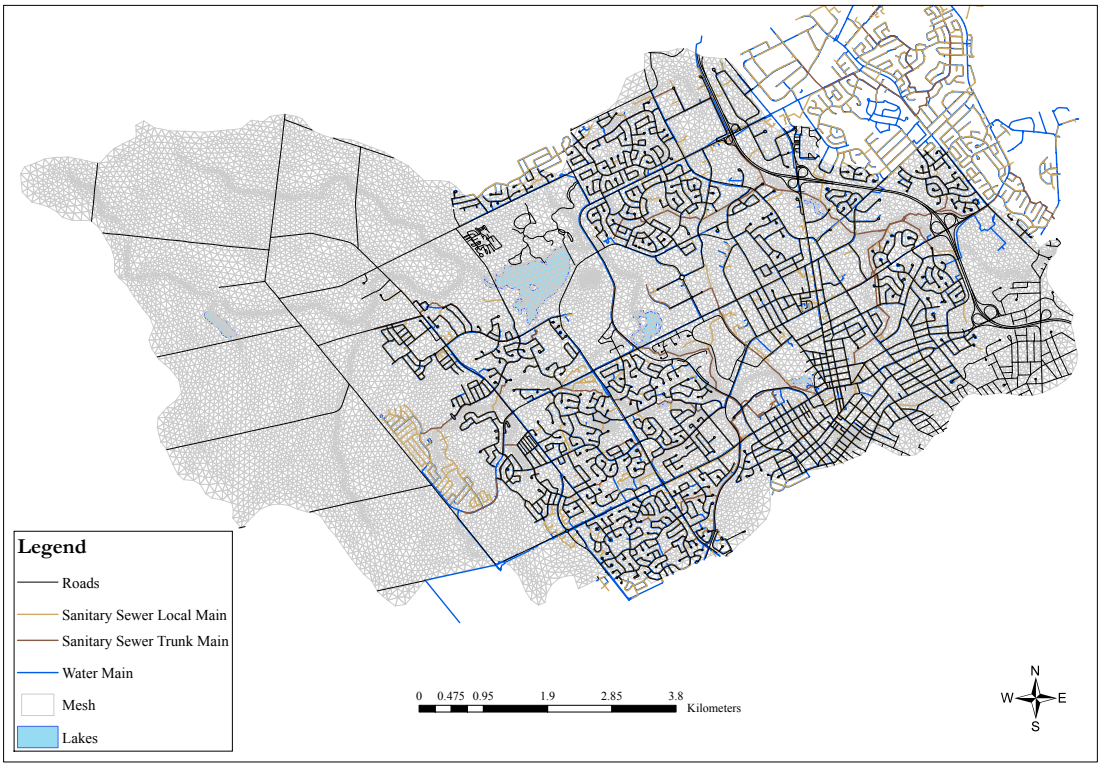

Figure 5 Water main and sanitary sewer network in the City of Waterloo

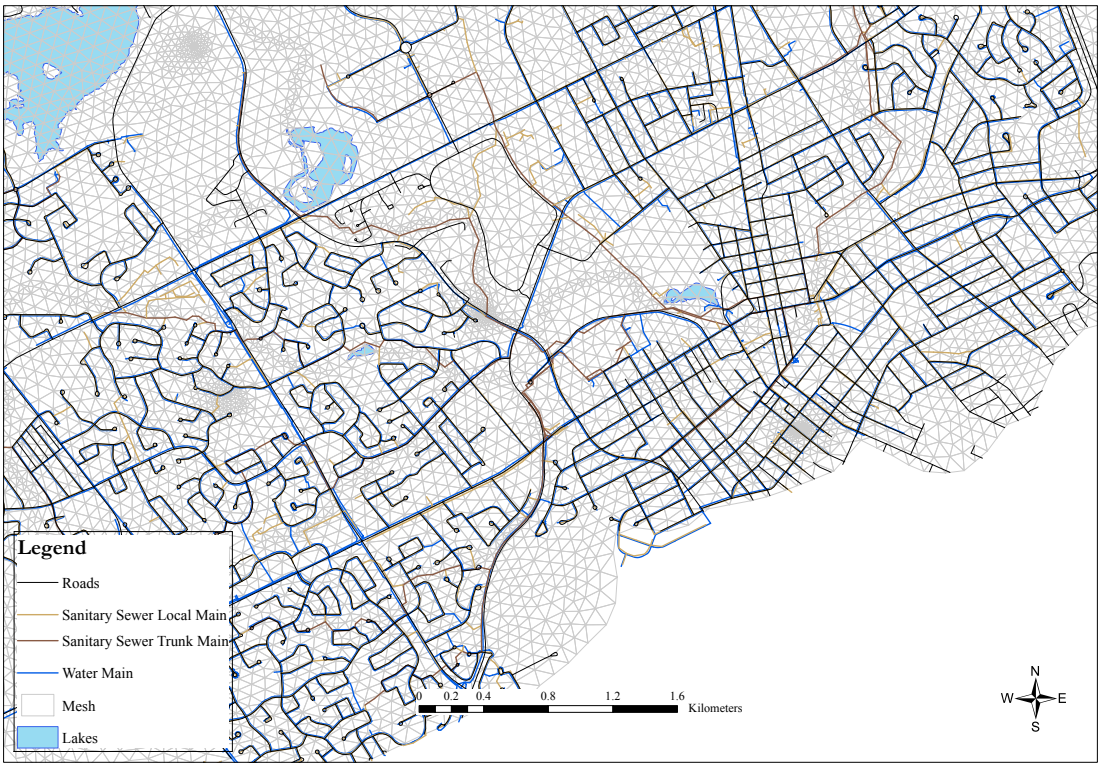

Figure 6 City of Waterloo water main and sanitary sewer infrastructure in the urban core

Chapter 3: Methodology

3.1 Discretization

To create the two-dimensional (2-D) mesh, Grid Builder was used. Grid Builder is a pre-processor for 2-D triangular element and finite-element programs (McLaren, 2011). An irregular finite-element grid was created. The finite-element approach allows for mesh refinement at local features, such as the local stream network, without affecting other areas of the mesh. The outer boundary of the Laurel Creek Watershed was imported into Grid Builder to define the outer boundary of the mesh. The Laurel Creek Watershed stream network was also imported to allow for more mesh refinement along the stream network. A sensitivity analysis was conducted to determine the optimal node spacing. Ultimately, a node spacing of 100m was used, with 25m spacing along the stream network. The final 2-D mesh is given in Figure 7. The topography of the model was established using a 10m digital elevation model (DEM). The 2-D mesh with hydraulic head is shown in Figure 8.

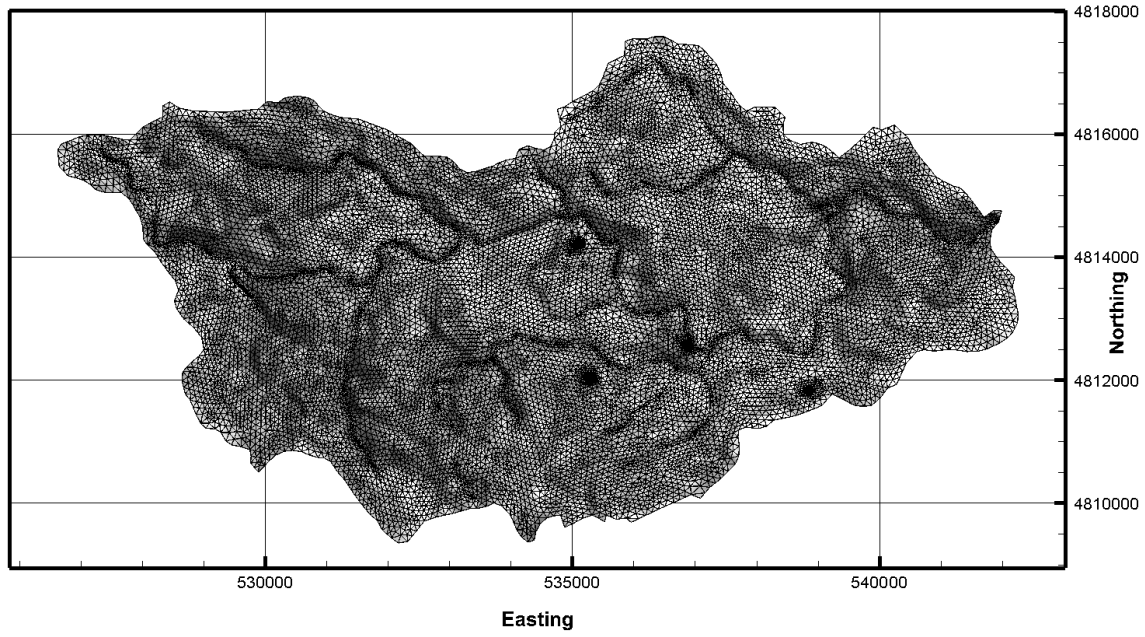

Figure 7 2-Dimensional mesh

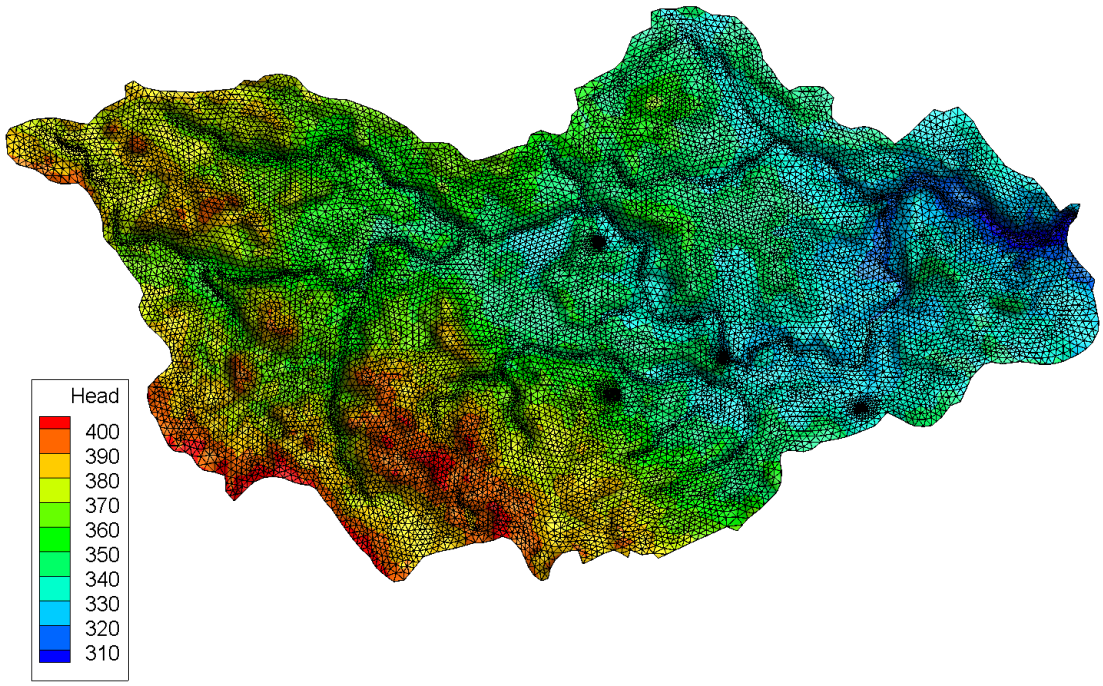

Figure 8 2-Dimensional mesh with hydraulic head (m)

The three-dimensional (3-D) mesh was created using the bedrock as the bottom layer, and a 10 m DEM as the surface topography layer. The bottom 17 layers were generated using the Waterloo Moraine model created by Sousa (2013). The upper layers were created based on the 10 m DEM.

The 3-D mesh contained 22 upper layers, with a layer adjusted to accommodate the sanitary sewer network. This adjustment was necessary because the geometry of the sanitary sewer is dependent on the geometry of the 3-D mesh. Therefore, in order for the sanitary sewers to continually flow with a decreasing elevation instead of following the surface topography, the adjusted layer needed to be created. The 10 uppermost layers had 0.1 m spacing. Following this uniform layering, there were five layers from 1 m to 2 m BGS. The next layer, at 3 m BGS contained adjustments to accommodate the sanitary sewer network. Below this layer, there were six layers with 1.0 m spacing to 10.0 m BGS. Table 2 gives the total number of nodes, elements, and layers for the 2-D and 3-D meshes. Figure 9 shows a side view of the 3-D mesh.

Table 2 Number of nodes, elements, and layers in each mesh

	2-D Mesh	3-D Mesh
Nodes	15,525	605,475
Elements	30,661	1,165,118
Layers	1	39

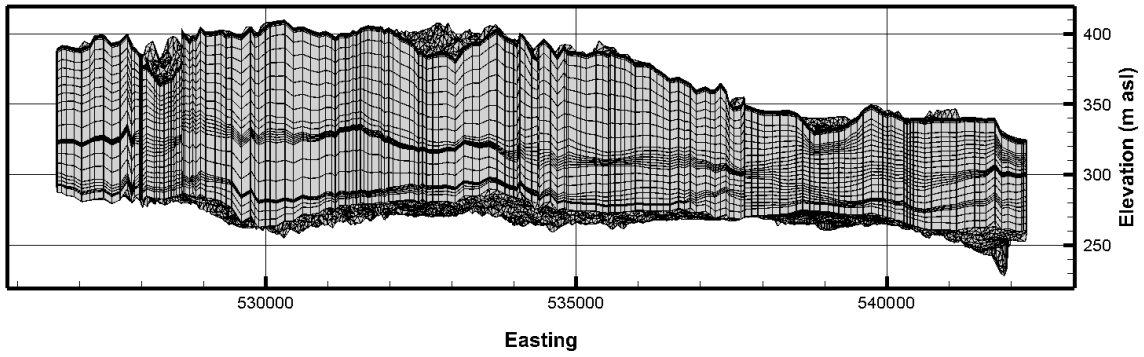

Figure 9 3-Dimensional mesh, looking North

3.2 HydroGeoSphere Governing Equations

3.2.1 Subsurface Flow

The following assumptions are made for subsurface flow:

- The fluid is incompressible
- The porous medium and fractures are non-deformable
- The system is under isothermal conditions
- The air phase is infinitely mobile

HydroGeoSphere uses a modified form of Richard's equation to describe the 3-D transient subsurface flow in a variably-saturated porous medium (Aquanty Inc., 2013):

$$-\nabla \cdot (w_m q) + \sum \Gamma_{ex} \pm Q = w_m \frac{\partial}{\partial t}(\theta_s S_w) \quad (1)$$

where w_m [dimensionless] is the volumetric fraction of the total porosity occupied by the porous medium. It is always equal to 1.0 unless a second porous continuum is considered for a

simulation, such as when representing fractures or macropores in the subsurface. The fluid flux, q [L T^{-1}], is given by Darcy's Law:

$$q = -k_{rw} \frac{\rho_w g}{\mu_w} k \nabla(\Psi_p + z) \quad (2)$$

where k_{rw} [dimensionless] is the relative permeability of water, ρ_w [M L^{-3}] is the density of water, g [L T^{-2}] is the gravitational constant, μ_w [M L^{-1} T^{-1}] is the viscosity of water, k is the intrinsic permeability vector of the porous medium[L^2], Ψ_p [L] is the pressure head, and z [L] is the elevation head.

From Equation 1, Γ_{ex} [L^3 L^{-3} T^{-1}] is the volumetric fluid exchange rate between the subsurface domain and all other domains in the model, expressed per unit volume of the other domain types. These other domain types could be surface flow, wells, tile drains, discrete fractures, and/or dual continuum. Γ_{ex} is positive for flow into the porous medium, and is dependent on the conceptualization of the fluid exchange between the domains.

In Equation 1, Q [L^3 L^{-3} T^{-1}] is a volumetric fluid flux per unit volume, which represents a source (positive) or sink (negative) flow into or out of the porous medium, respectively.

For nonlinear flow, the primary variable of solution is the pressure head, Ψ_p, which must be related to S_w and k_{rw}, where S_w [dimensionless] is water saturation and is expressed as:

$$S_w = \frac{\theta}{\theta_s} \quad (3)$$

where θ [dimensionless] is the water content of the porous medium, and θ_s [dimensionless] is the saturated water content of the porous medium, which is assumed to be equal to porosity.

The relative permeability of water may be expressed either in terms of pressure head or water saturation. HydroGeoSphere incorporates the functions presented by Brooks and Corey (1964) and Van Genuchten (1980) to relate the variables. Further explanation of these functions is given by Aquanty Inc. (2013). The HydroGeoSphere model can also relate k_{rw} and S_w as a tabular data input. It should be noted that the current HydroGeoSphere model is not capable of modeling the effects of hysteresis.

The storage term on the right hand side of Equation 1 relates the change in storage in the saturated zone to a change in fluid pressure through compressibility terms. It is assumed that the bulk compressibility of the medium is constant for saturated and variably-saturated conditions. Where unsaturated conditions exist, it is assumed that the compressibility on the storage of water is negligible. The storage term can be expressed as follows (Cooley, 1971; Neuman, 1973):

$$\frac{\partial}{\partial t}(\theta_s S_w) \approx S_w S_s \frac{\partial \Psi}{\partial t} + \theta_s \frac{\partial S_w}{\partial t} \quad (4)$$

3.2.2 Surface Flow

Surface flow is modeled in HydroGeoSphere as a 2-D depth-averaged flow equation. It is the diffusive-wave approximation of the Saint Venant equation for surface flow, given below. A full derivation of this equation can be found in Aquanty Inc. (2013).

$$\frac{\partial \phi_o h_o}{\partial t} - \frac{\partial}{\partial x}\left(d_o K_{ox} \frac{\partial h_o}{\partial x}\right) - \frac{\partial}{\partial y}\left(d_o K_{ox} \frac{\partial h_o}{\partial y}\right) + d_o \Gamma_o \pm Q_o = 0 \quad (5)$$

where ϕ_o [unitless] is the surface flow domain porosity, d_o [L] is the depth of flow, h_o [L] is the water surface elevation equal to the sum of the land surface elevation and the depth of flow, Γ_o [L^3 L^{-3} T^{-1}]is the fluid exchange rate, and Q_o [L T^{-1}] is the volumetric flow rate per unit area representing external sources and sinks. K_{ox} and K_{oy} [L T^{-1}] are the surface conductances that approximate friction slopes. K_{ox} and K_{oy} can be calculated with the Manning's Equation, the Chezy Equation, or the Darcy-Weisbach Equation, as specified by the user. The equations are explained further in Aquanty Inc. (2013).

Surface runoff is calculated using the Saint Venant equations for unsteady shallow water, which consists of three equations – the mass balance equation, and the equations for momentum in the x-direction and the y-direction, respectively (Aquanty Inc., 2013). The bed and friction slopes are approximated using the Manning, Chezy, or Darcy-Weisbach equations. These equations are written and explained by Aquanty Inc (2013). Substituting variations of these equations into the continuity equation to obtain the diffusive wave approximation creates the final equation solved by HydroGeoSphere:

$$\frac{\partial \phi_o h_o}{\partial t} - \frac{\partial}{\partial x}\left(d_o K_{ox} \frac{\partial h_o}{\partial x}\right) - \frac{\partial}{\partial y}\left(d_o K_{oy} \frac{\partial h_o}{\partial y}\right) + d_o \Gamma_o \pm Q_o = 0 \quad (6)$$

This equation assumes depth-averaged flow velocities, hydrostatic pressure distribution vertically, mild slope, and dominant bottom shear stresses along the surface.

The storage and flow terms in Equation 6 include rill (depression) storage and obstruction storage terms. If runoff occurs over a flat plane, without rill and obstruction storage parameters specified, then the surface flow domain porosity will be equal to one. Rill storage represents the amount of storage that must be filled before lateral surface flow can occur. Contrarily, obstruction storage is the amount of storage that is reduced by the presence of urban features, such as buildings.

HydroGeoSphere does not presently have the ability to simulate hydraulic control features, such as weirs and dams. It can accommodate for a weir discharge coefficient for open channel flow if the Manning's Equation is used. For features that are manually controlled, such as reservoirs or stormwater management ponds, the absence of hydraulic control features can impact model results.

3.2.3 One-Dimensional Hydraulic Features

One-dimensional (1-D) hydraulic features such as rivers, subsurface wells, water supply lines, and drain pipes, are simulated in HydroGeoSphere by using a general 1-D equation to describe the flow in terms of the Hagen-Poiseuille Equation, Manning's Equation, or the Hazen-Williams Equation, as specified by the user. Interactions can by simulated using the common node or dual node approach.

Flow along the axis, s, of 1-D features is described by the generalized version of the continuity formula integrated over the flow area perpendicular to the principle axis, A_f, as explained in Aquanty Inc. (2013).

$$-\frac{\partial}{\partial s}(Q_{1D}) + Q_w \delta(s - s_p) = \frac{\partial}{\partial t}[A_f] \quad (7)$$

$$Q_{1D} = A_f \cdot q_{1D} \quad (8)$$

where Q_{1D} [L^3 T^{-1}] is the fluid flux along the 1-D medium, q_{1D} is the linearly averaged velocity over the cross-sectional flow area, A_f [L^2], and Q_w [L^3 T^{-1}] is the rate of addition or extraction of water at $s = s_p$. In pipe flow, the flow area is defined as a function of saturation:

$$A_f = A_{1D} S_{1D} \tag{9}$$

where A_{1D} is the saturated pipe area, and S_{1D} is the pipe saturation.
The 1-D fluid flux along the hydraulic feature, Q_{1D}, is described by this generalized formula:

$$Q_{1D} = -C \cdot A_f \cdot (R_H)^p \cdot \left[\frac{\partial h_w}{\partial s}\right]^q \tag{10}$$

where C [dimensionless] is a proportionality constant, p and q [dimensionless] are fitting exponents, and R_H [L] is the hydraulic radius. C, p, and q are determined by the equation chosen to describe the flow – Hagen-Poiseuille, Manning's, or Hazen-Williams.

3.2.4 Flow Through Pressurized Subsurface Pipe Systems

Water mains are a form of pressurized subsurface pipe system and are designed using empirical equations based on experimental measurements of fluid flow under a range of conditions. The equation used by HydroGeoSphere for pressurized flow is the Hazen-Williams equation, which was developed for flow in pipes with a diameter, $D \geq 5$ cm with a velocity, $V \leq 3$ m/s (Houghtalen, 2010). The Hazen-Williams equation used in HydroGeoSphere is as follows (Aquanty Inc., 2013):

$$Q_{1D} = -k \cdot C_{HW} \cdot A_f \cdot (R_H)^{0.63} \cdot \left[\frac{\partial h_p}{\partial s}\right]^{0.54} \tag{11}$$

$$\frac{\partial}{\partial s}\left(-k \cdot C_{HW} \cdot A_f \cdot (R_H)^{0.63} \cdot \left[\frac{\partial h_p}{\partial s}\right]^{0.54}\right) + Q_p \delta(s - s_c) = \pi r_p^2 S_{sp} \frac{\partial h_p}{\partial t} \tag{12}$$

where h_p [L] is the hydraulic head at a given location, s [L], along the pipe, S_{sp} [L^{-1}] is the specific storage, Q_p [L^3 T^{-1}]is the rate of water consumption at the location s_c [L], and R_H [L] is the hydraulic radius of the pipe defined as the cross-sectional area of the pipe divided by the wetted perimeter ($R_H = A_f/P_f$). C_{HW} [dimensionless] is the Hazen-Williams roughness

coefficient. The roughness coefficient has a strong dependence on the Reynold's number, and is most applicable to smooth pipes. A typical roughness coefficient for a concrete pipe is 120 (Chin, 2013).

Pressurized pipes in the subsurface often lose a portion of their water through cracks or deficiencies in the pipe. This is particularly apparent when the pipes begin to age, as will be discussed further in a later section. In HydroGeoSphere, the leakage of water is assumed to follow a first-order leakance relationship (Aquanty Inc., 2013).

$$\Gamma_{p\rightarrow pm} = -2\pi r_p K_{exch(pm.p)} \frac{h_p - h}{l_{exch(pm,p)}} \tag{13}$$

Since the head in the pressurized pipe, h_p [L], should be significantly greater than the surrounding head, h, the water will leak from the pipe into the subsurface, as shown by the notation $\Gamma_{p\rightarrow pm}$. Equation 13 can be substituted into Equation 12 to give Equation 14 below.

$$\frac{\partial}{\partial s}\left(-k \cdot C_{HW} \cdot A_f \cdot (R_H)^{0.63} \cdot \left[\frac{\partial h_p}{\partial s}\right]^{0.54}\right) + Q_p \delta(s - s_c) + \Gamma_{p\rightarrow pm} = \pi r_p^2 S_{sp} \frac{\partial h_p}{\partial t} \tag{14}$$

3.2.5 Flow Through Subsurface Gravity Flow Sewer Systems

Sanitary sewers flow via gravity drainage in the subsurface. Flow in sanitary sewers is characterized by the Manning's Equation (Chin, 2013):

$$Q = \frac{1}{n} \cdot A_f \cdot (R_H)^{\frac{2}{3}} \cdot S^{\frac{1}{2}} \tag{15}$$

$$\frac{\partial}{\partial s}\left(-\frac{1}{n} \cdot A_f \cdot (R_H)^{\frac{2}{3}} \cdot \left[\frac{\partial h_{ss}}{\partial s}\right]^{\frac{1}{2}}\right) = B_T \frac{\partial h_{ss}}{\partial t} \tag{16}$$

where n [dimensionless] is the Manning's roughness coefficient, and S [dimensionless] is the slope of the pipe calculated as the change in elevation of the pipe (∂h) [L] divided by the length of the pipe (∂s) [L]. B_T [L] is the top width of the water in the pipe.

Similar to pressurized pipe systems, leakage will occur between the porous medium and the sanitary sewer. Sanitary sewers are modeled in the same way as channel flow. Because sanitary

sewers are in the subsurface, leakage between overland flow and sanitary sewer is not considered. Leakage between the porous medium (pm) and the sanitary sewer (ss) is calculated as follows (Aquanty Inc., 2013):

$$\Gamma_{pm \to ss} = -P_f (k_r)_{exch(pm,ss)} K_{exch(pm,ss)} \frac{h_{ss} - h}{l_{exch(pm,ss)}} \tag{17}$$

Therefore, the final calculation for head in the sanitary sewer over time is found by substituting Equation 17 into Equation 16, given below in Equation 18.

$$\frac{\partial}{\partial s}\left(-\frac{1}{n} \cdot A_f \cdot (R_H)^{\frac{2}{3}} \cdot \left[\frac{\partial h_{ss}}{\partial s}\right]^{\frac{1}{2}} \right) + \Gamma_{pm \to ss} = B_T \frac{\partial h_{ss}}{\partial t} \tag{18}$$

3.2.6 Flow Through Subsurface Wells

Groundwater wells are used for the extraction or monitoring of groundwater. Assuming laminar flow conditions in the well, and that the cross-sectional area of the well casing is much smaller than the length of the well, the Hagan-Pouiseulle formula can be used to estimate the flow in fully saturated wells, given by Equations 19 and 20 (Aquanty Inc., 2013).

$$Q_{1D} = -(\pi r_w^2) \left(\frac{r_w^2 \rho g}{8\mu} \right) \frac{\partial h_w}{\partial s} \tag{19}$$

$$\frac{\partial}{\partial s}\left(\pi r_w^4 \frac{\rho g}{8\mu} \frac{\partial h_w}{\partial s} \right) + Q_w \delta(s - s_p) + \Gamma_{pm \to w} = \pi r_w^2 S_{sw} \frac{\partial h_w}{\partial t} \tag{20}$$

where r_w [L] is the radius of the well, μ [L^2 T^{-1}] is the viscosity of water, $S_{sw} = \rho g \beta$ is the specific storage of the well [L^{-1}] with ρ [M L^{-3}], g [L T^{-2}], and β [L T^2 M^{-1}] being the density of water, gravitational acceleration, and compressibility of water, respectively.

Wells may also be partially saturated. As such, Equation 19 and Equation 20 can be modified to accommodate the reduction in flow area and water volume to produce the equations below (Aquanty Inc., 2013).

$$Q_{1D} = -k_{rw}(S_{ww} \pi r_w^2) \left(\frac{r_w^2 \rho g}{8\mu} \right) \frac{\partial h_w}{\partial s} \tag{21}$$

$$\frac{\partial}{\partial s}\left(k_{rw}S_{ww}\pi r_w^4\frac{\rho g}{8\mu}\frac{\partial h_w}{\partial s}\right)+Q_w\delta(s-s_p)=\pi r_w^2 S_{ww}S_{sw}\frac{\partial h_w}{\partial t}+\pi r_w^2\frac{\partial S_{ww}}{\partial t} \quad (22)$$

where S_{ww} [dimensionless] and k_{rw} [dimensionless] are the degree of saturation and relative permeability of the well, respectively, and can range between 0 and 1 with 0 being completely dry and 1 between fully-saturated.

The fluid exchange between the well and the porous medium is characterized by the following equations.

$$\Gamma_{pm\rightarrow w}=-2\pi r_w(k_r)_{exch(pm,w)}K_{exch(pm,w)}\frac{h_w-h}{l_{exch(pm,w)}} \quad (23)$$

$$\frac{\partial}{\partial s}\left(k_{rw}S_{ww}\pi r_w^4\frac{\rho g}{8\mu}\frac{\partial h_w}{\partial s}\right)+Q_w\delta(s-s_p)+\Gamma_{pm\rightarrow w}=\pi r_w^2 S_{ww}S_{sw}\frac{\partial h_w}{\partial t}+\pi r_w^2\frac{\partial S_{ww}}{\partial t} \quad (24)$$

$\Gamma_{pm\rightarrow w}$ is the fluid exchange between the porous medium and the well with an exchange thickness ($l_{exch(pm,w)}$) [L], a hydraulic conductivity ($K_{exch(pm,w)}$) [L/T], giving a relative permeability ($(k_r)_{exch(pm,w)}$) [dimensionless].

3.2.7 Flow Coupling

Flow coupling is the definition of water exchange terms (Γ_{ex}), and is represented in HydroGeoSphere with the common node approach or the dual node approach (Aquanty Inc., 2013). The common node approach assumes continuity of hydraulic head between two domains, providing instantaneous equilibrium between the domains.

The dual node approach uses the equation for Darcy flux to characterize the transfer of water by computing the hydraulic head difference between the domains. It assumes that a thin layer of porous material across which the exchange occurs separates the domains. The exchange term for surface-subsurface coupling when the dual node approach is chosen is as follows (Aquanty Inc., 2013).

$$d_o\Gamma_o=\frac{k_r K_{zz}}{l_{exch}}(h-h_o) \quad (25)$$

A positive value of Γ_o represents flow from the subsurface into the surface system. K_{zz} [L T-1] is the vertical saturated hydraulic conductivity of the underlying porous media and l_{exch} [L] is the coupling length.

3.3 Subsurface Characterization

Hydraulic conductivity (K) [L/T] is a property of porous media that describes the relationship between the specific discharge (q) [L/T] and the hydraulic gradient (dh/dL) [dimensionless], as described by Darcy's law (Fetter, 2001):

$$q = -K(\frac{dh}{dL}) \tag{26}$$

The hydraulic conductivity is a function of both the fluid and of the porous medium through which it flows. Hydraulic conductivity can be measured empirically based on grain size distribution, or experimentally with the use of Darcy's Law (Chin, 2013). Coarse-grained materials usually have a higher hydraulic conductivity than fine-grained materials. A typical hydraulic conductivity classification is given in Figure 10. From the figure, it is evident that there is a range of values for hydraulic conductivity for each type of soil classification, and some soil types may have overlapping hydraulic conductivity values. Therefore, the estimation of hydraulic conductivity can be difficult.

For this work, the hydraulic conductivity field was based on research conducted by Sousa (2013). The groundwater flow model that created a basis for the research by Sousa (2013) was the Waterloo Moraine model created by Martin and Frind (1998). The purpose of their study was to create three-dimensional conceptual hydrogeological model based on geological characteristics of the multi-aquifer Waterloo Moraine system in order to define susceptibility to contamination and create a basis for management and protection strategies (Martin and Frind, 1998). The system consists of eight hydrostratigraphic layers – three aquifer layers, four aquitard layers, and the bedrock layer (Figure 11). The authors used 2044 borehole logs to give continuous interpretation of the stratigraphy. The lithological units were grouped into 17 categories and representative hydraulic conductivity values were assigned to each unit based on literature values and previous pumping and slug tests conducted in the well field areas.

Sousa (2013) updated the original hydraulic conductivity distribution with new data from the Regional Municipality of Waterloo and refined the model discretization to give a total of 29 layers, ~ 1,300,000 nodes, and ~ 2,500,000 elements. The author then used three hydrologic flow models to assess uncertainty in spatial distribution of recharge. He calibrated the recharge data to 42 observation wells in the study area (Figure 12). Hydraulic conductivity was used as a calibration parameter and was allowed to vary within one order of magnitude, which is consistent with error bounds for field tests at this scale (Sousa, 2013).

The hydraulic conductivity results from Sousa (2013) were mapped onto the Laurel Creek Watershed three-dimensional finite element mesh. The nodes in the model were assigned a soil type according to their hydraulic conductivities. The soil types were assigned based on the research by Jones (2005). Porosity and specific storage were assigned to the soil types, based on the research by Jones (2005). The hydraulic properties assigned to the 13 soil types are presented in Table 3. Isotropy is assumed throughout the porous medium. Future versions of the model should consider anisotropy.

Table 3 Hydraulic properties

Soil Type	Hydraulic Conductivity (K) [L/T]	Specific Storage (S_s) [L^{-1}]	Porosity
Silty clay	1.0×10^{-10}	9.751×10^{-04}	0.450
Clayey silt	1.0×10^{-09}	2.303×10^{-04}	0.450
Sandy clay	1.0×10^{-08}	9.751×10^{-04}	0.430
Gravelly clay	5.0×10^{-08}	9.751×10^{-04}	0.420
Silt	8.0×10^{-08}	2.303×10^{-04}	0.430
Sandy silt	5.0×10^{-07}	2.303×10^{-04}	0.410
Gravelly silt	1.0×10^{-06}	2.303×10^{-04}	0.410
Clayey sand	5.0×10^{-05}	1.617×10^{-04}	0.395
Silty sand	5.0×10^{-04}	1.617×10^{-04}	0.370
Fine sand	1.0×10^{-03}	1.617×10^{-04}	0.380
Medium sand	5.0×10^{-03}	1.186×10^{-04}	0.360
Coarse sand	1.0×10^{-02}	7.448×10^{-05}	0.375
Gravel	5.0×10^{-02}	1.102×10^{-05}	0.280

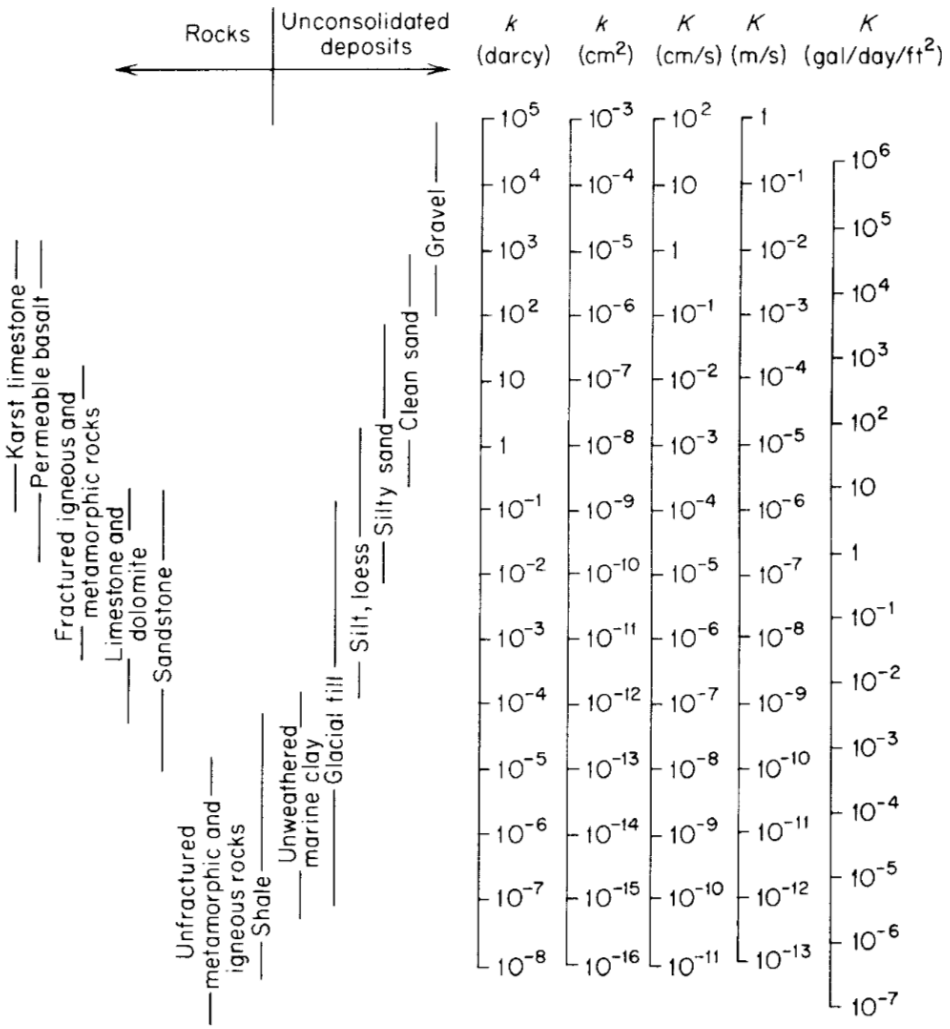

Figure 10 Range of values for hydraulic conductivity (K) and permeability (k) (Freeze and Cherry, 1979)

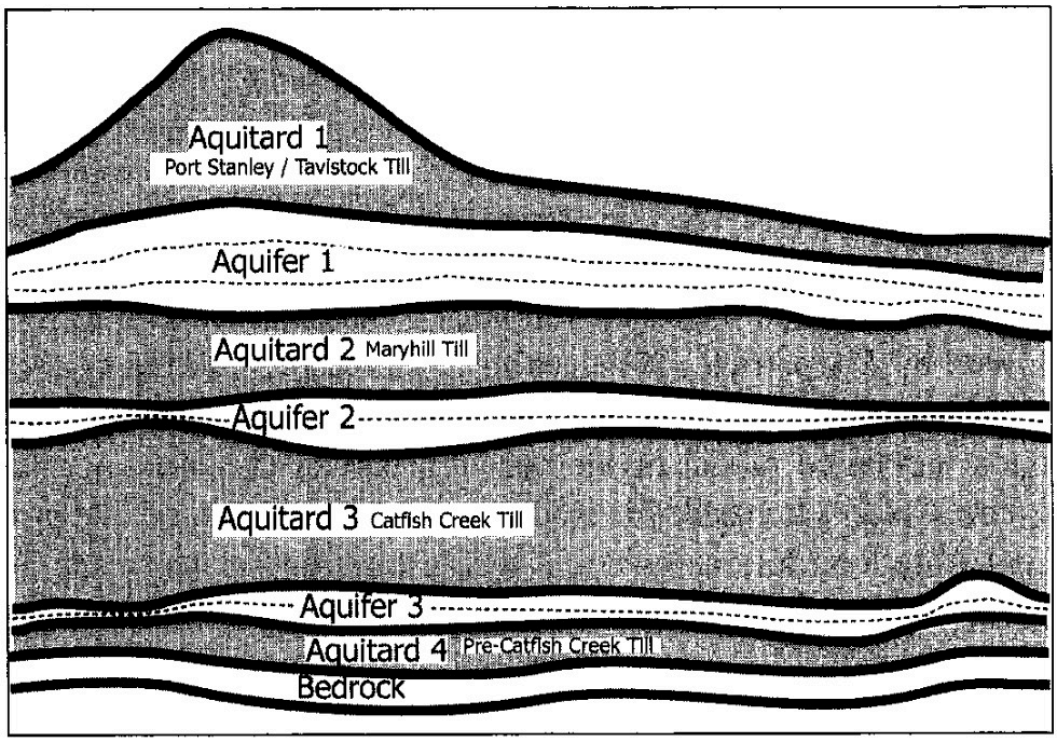

Figure 11 Hydrostratigraphic layers of the Waterloo Moraine (Martin and Frind, 1998)

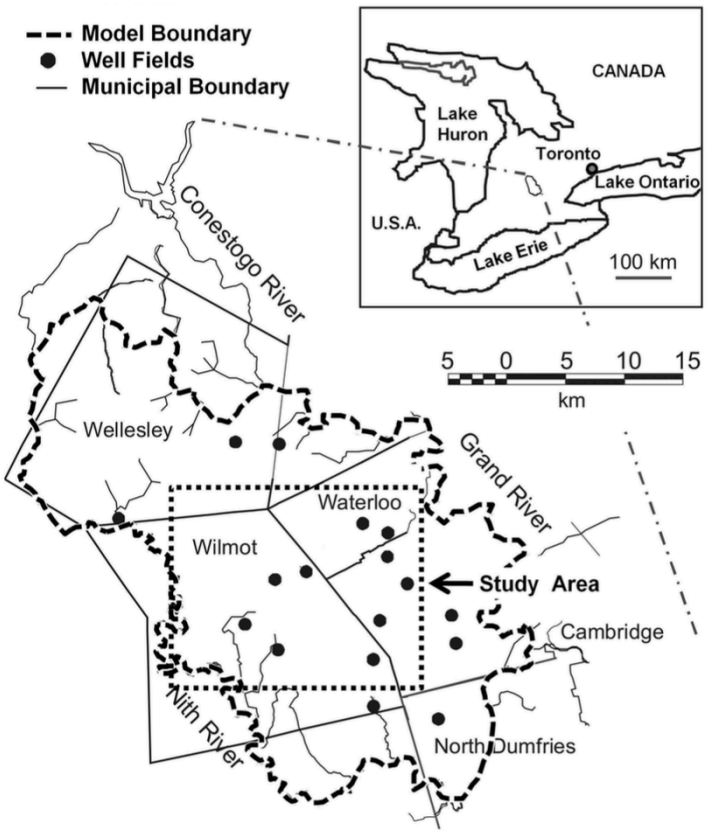

Figure 12 Recharge study area in Waterloo Moraine model (Sousa, 2013)

3.4 Surface Characterization

Surface flow parameters are designated according to land use. Figure 13 shows the land use in the Laurel Creek Watershed.

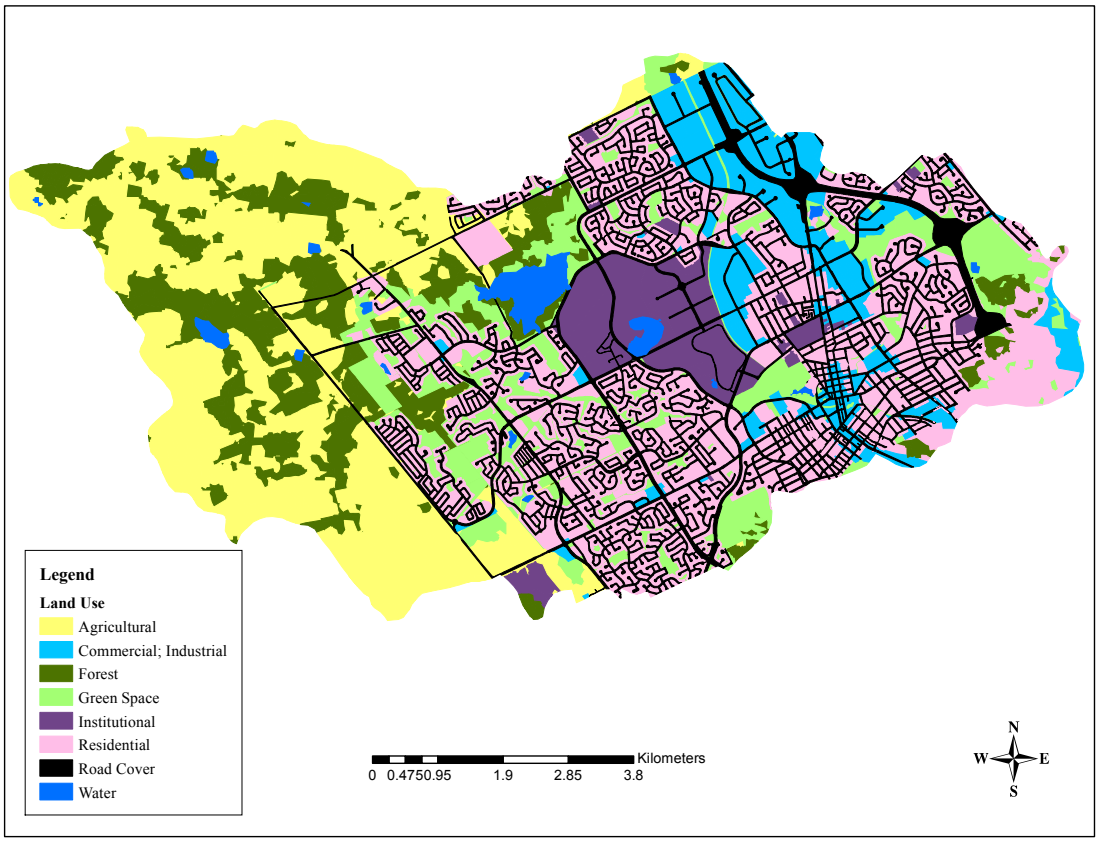

Figure 13 Land use in the Laurel Creek Watershed

Most of the Western part of the watershed is characterized as agricultural and forested land, whereas the central and Eastern parts of the watershed have a mix of residential, commercial, industrial, and institutional land uses. When characterizing the watershed for surface flow, the commercial and industrial land uses were combined. The institutional land use was expanded to include the landfill and service stations. Table 4 gives the overland flow properties associated with each of the land use types. The overland flow properties were adapted from Jones (2005).

Table 4 Overland flow properties according to land use

Land Use	X Friction Factor	Y Friction Factor	Rill Storage Height (m)	Obstruction Storage Height (m)	Coupling Length (m)
Agricultural	0.2	0.2	1.0×10^{-4}	0.0	1.0×10^{-4}
Commercial; Industrial	0.012	0.012	1.0×10^{-4}	0.0	1.0×10^{-4}
Forest	0.6	0.6	1.0×10^{-4}	0.0	1.0×10^{-4}
Green Space	0.15	0.15	1.0×10^{-4}	0.0	1.0×10^{-4}
Institutional	0.15	0.15	1.0×10^{-4}	0.0	1.0×10^{-4}
Residential	0.012	0.012	1.0×10^{-4}	0.0	1.0×10^{-4}
Road Cover	0.012	0.012	1.0×10^{-4}	0.0	1.0×10^{-4}
Water	0.04	0.04	1.0×10^{-4}	0.0	1.0×10^{-4}

3.5 Evapotranspiration

Evapotranspiration [L/T] is the largest consumptive use of water and is an important quantity in regional water budgets as it can consume around 70% of rainfall annually (Chin, 2013). Evapotranspiration is the combination of evaporation and transpiration. Evaporation is the process of water moving from the liquid to the vapor phase and transpiration is the process by which water moves through plants and evaporates through leaf stomata. The term potential evapotranspiration (E_p) [L/T] represents the water loss that will occur if at no time there is a deficiency of water in the soil for the use of vegetation (Fetter, 2001). Actual evapotranspiration is the term used to describe the amount of evapotranspiration occurring under field conditions. Actual evapotranspiration is calculated based on the potential evapotranspiration and a variety of other parameters, as explained in this section.

Potential evapotranspiration was calculated based on the Hargreaves equation, given below as Equation 27. The Hargreaves equation was chosen for the calculation of potential evapotranspiration based on its simplicity and reliability. Compared to the Penman-Monteith equation, which requires additional inputs such as wind speed, long wave and short wave radiation, and soil heat flux, and humidity, the reduction in data required for the Hargreaves equation makes it an optimal choice for a large area such as the Laurel Creek Watershed. Where

field estimates of E_p are not feasible and historical data quality is missing or not available, the Hargreaves equation provides a reliable estimate of E_p (Hargreaves, 2003).

$$E_p = 0.0023(T_{mean} + 17.8)(T_{max} - T_{min})^{0.5} \times R_a \quad (27)$$

All temperatures (T) are expressed in °C as the daily mean, maximum, and minimum air temperatures, respectively. R_a [L/T] is the daily water equivalent of extraterrestrial solar radiation. Using historic temperature data from the University of Waterloo weather station (Seglenieks, 1998), and solar radiation was calculated based on data from Doorenbos (1977). The E_p was calculated for each month based on changing temperatures and solar radiation values. They were then averaged to give the annual average E_p of 2.26 mm/day (2.616×10^{-8} m/s). Figure 14 shows the monthly average potential evapotranspiration.

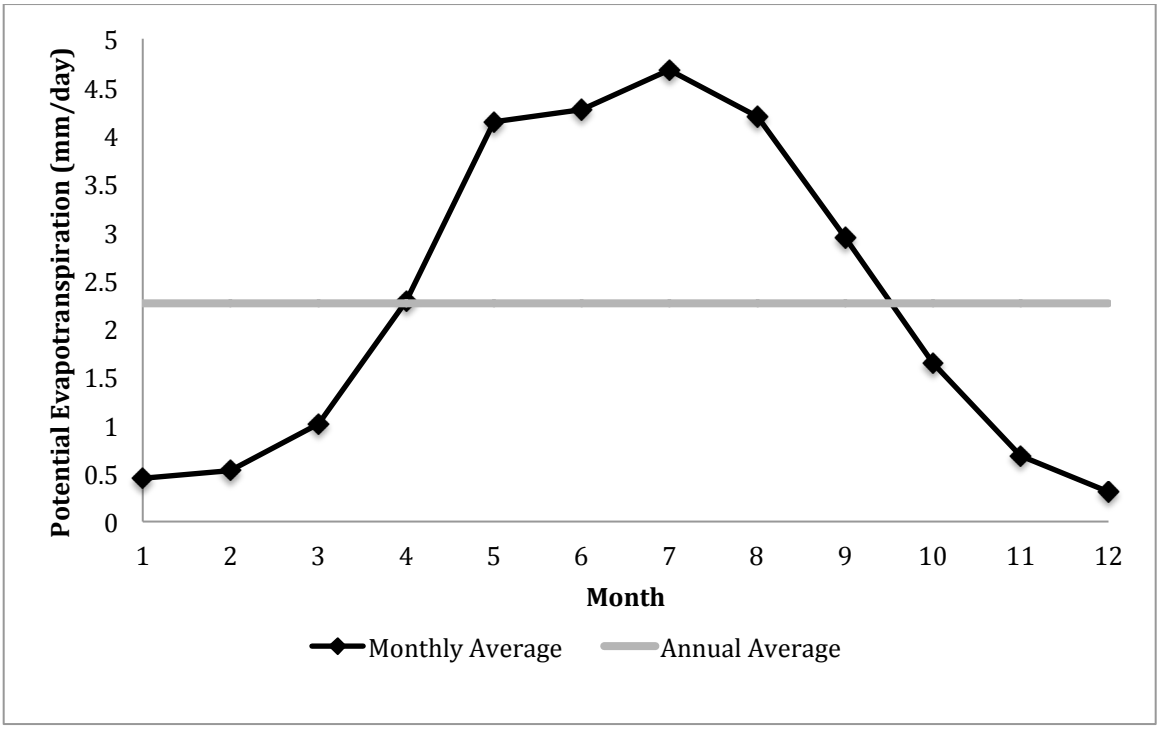

Figure 14 Monthly and annual potential evapotranspiration (mm/day)

Using the annual average EP value that was calculated using Hargreaves equation, HydroGeoSphere calculates the actual evapotranspiration (ET) using the following series of equations (Aquanty Inc., 2013) as a combination of plant transpiration and evaporation.

$$T_p = f_1(LAI) f_2(\theta) RDF[E_p - E_{can}] \quad (28)$$

Where T_p is the rate of transpiration and E_{can} [L/T] is the canopy evaporation. Transpiration from vegetation occurs within the root zone of the subsurface, which will vary depending on the type of vegetation and may be above or below the water table. f_1 is a function of the leaf area index (LAI) [dimensionless], f_2 is a function of the nodal water content (θ) [dimensionless], and RDF is the time-varying root distribution function. Each of these values are given by the following equations:

$$f_1(LAI) = \max\{0, \min[1, (C_2 + C_1 LAI)]\} \quad (29)$$

$$RDF = \frac{\int_{z_1'}^{z_2'} r_F(z')dz'}{\int_0^{L_r} r_F(z')dz'} \quad (30)$$

$$f_1(\theta) = \begin{cases} 0 \; for \; 0 \le \theta \le \theta_{wp} \\ f_3 \; for \; \theta_{wp} \le \theta \le \theta_{fc} \\ 1 \; for \; \theta_{fc} \le \theta \le \theta_o \\ f_4 \; for \; \theta_o \le \theta \le \theta_{an} \\ 0 \; for \; \theta_{an} \le \theta \end{cases} \quad (31)$$

$$f_3 = 1 - \left[\frac{\theta_{fc} - \theta}{\theta_{fc} - \theta_{wp}}\right]^{C_3} \quad (32)$$

$$f_4 = 1 - \left[\frac{\theta_{an} - \theta}{\theta_{an} - \theta_o}\right]^{C_3} \quad (33)$$

L_r [L] is the effective rooting depth of the vegetation, z' [L] is the depth coordinate from the soil surface, and $r_F(z')$ [L^3T^{-1}] is the root extraction function. Based on f_1, transpiration is zero below the wilting point moisture content, and again at the anoxic moisture content when lack of aeration causes transpiration to decrease.

Evaporation is modeled with the following equations:

$$E_s = \alpha^*\left(E_p - E_{can}\right)[1 - f_1(LAI)]EDF \quad (34)$$

$$\alpha^* = \begin{cases} \frac{\theta-\theta_{e2}}{\theta_{e1}-\theta_{e2}} for\ \theta_{e2} \le \theta \le \theta_{e1} \\ 1\ for\ \theta > \theta_{e1} \\ 0\ for\ \theta < \theta_{e2} \end{cases} \quad (35)$$

$$EDF = (E_p - E_{can} - T_p)(1 - f_1(LAI)) \quad (36)$$

Where α^* is a wetness factor for the overland flow domain, and θ_{e1} and θ_{e2} are the moisture contents at the energy limiting stage and below which the evaporation is zero, respectively. The wetness factor expresses the moisture availability for the subsurface domain, and for the overland flow domain will vary between zero and the elevation of flow above depression storage. EDF represents the evaporation distribution function, which represents the subsurface and overland flow domains. It is assumed that the value of evaporation will decrease with depth below the surface. The evapotranspiration fitting parameters used in this model are listed in Table 5.

Table 5 Dimensionless fitting parameters used in the calculation of evapotranspiration

Variable	Description	Value
$\mathbf{C_1}$	Fitting parameter	0.31
$\mathbf{C_2}$	Fitting parameter	0.20
$\mathbf{C_3}$	Fitting parameter	1.00
$\boldsymbol{\theta_{wp}}$	Moisture content at wilting point	0.20
$\boldsymbol{\theta_{fc}}$	Moisture content at field capacity	0.32
$\boldsymbol{\theta_{o}}$	Moisture content at oxic limit	1.00
$\boldsymbol{\theta_{an}}$	Moisture content at anoxic limit	1.00
$\boldsymbol{\theta_{e1}}$	Moisture content above which evaporation can occur	0.20
$\boldsymbol{\theta_{e2}}$	Moisture content below which evaporation is zero	0.32

The LAI and L_r are determined based on the type of vegetation on the surface. While L_r will remain constant over a length of time, LAI is subject to change due to seasonal changes. However, in this model it is assumed that there are no seasonal changes. The land use file discussed previously (Figure 13) provides the base map for determining the LAI and L_r values for each land use type. Values for LAI and L_r were chosen based on research by Asner (2003) and Canadell (1996), respectively, as researched by Guo (2014). To find L_r, Guo (2014) also

consulted with University of Waterloo Department of Biology Professor John C. Semple to determine the most common crops farmed in the Laurel Creek Watershed in order to provide an accurate representation of the vegetation species.

The evaporation depth (B_{soil}) [L] for a particular land use is a function of the EDF described in Equation 36. It is the depth below which evaporation from the land surface will not occur. For example, the agricultural land use has an evaporation depth of 0.3m, which means that evaporation will no longer occur at a depth >0.3m.

Table 6 provides a listing of the LAI, L_r, and B_{soil} values used for each of the land uses in the Laurel Creek Watershed.

Table 6 LAI, L_r, and B_{soil} values used in the calculation of evapotranspiration

Land Use	Leaf Area Index (LAI) (--)	Rooting Depth (L_r) (m)	Evaporation Depth (B_{soil}) (m)
Agricultural	3.600	2.130	0.3
Commercial; Industrial	0.000	0.000	0.0
Forest	5.150	3.930	0.3
Green Space	3.770	3.160	0.3
Institutional	1.545	1.485	0.3
Residential	1.545	1.485	0.3
Road Cover	0.000	0.000	0.0
Water	0.000	0.000	0.0

3.6 Infrastructure

Figure 5 and Figure 6 in Section 2.3.6 give the City of Waterloo water main and sanitary sewer systems. Table 7, Table 8, and Table 9 give the inventory of the water main and sanitary sewer for the according to pipe age, material, and diameter, respectively. Figure 15, Figure 17, and Figure 18 illustrate each of the tables, respectively. The pipe inventory was obtained from the City of Waterloo (2013a).

Table 7 Frequency of City of Waterloo water main and sanitary sewer, by pipe age

Age	Water Main Length (km)	Sanitary Sewer Length (km)
0	0	0
5	446	380
10	744	577
15	1144	830
20	1152	745
25	377	264
30	1762	979
35	689	430
40	776	460
45	493	328
50	1856	534
55	555	474
60	365	216
65	671	362
70	0	0
Unknown	630	520

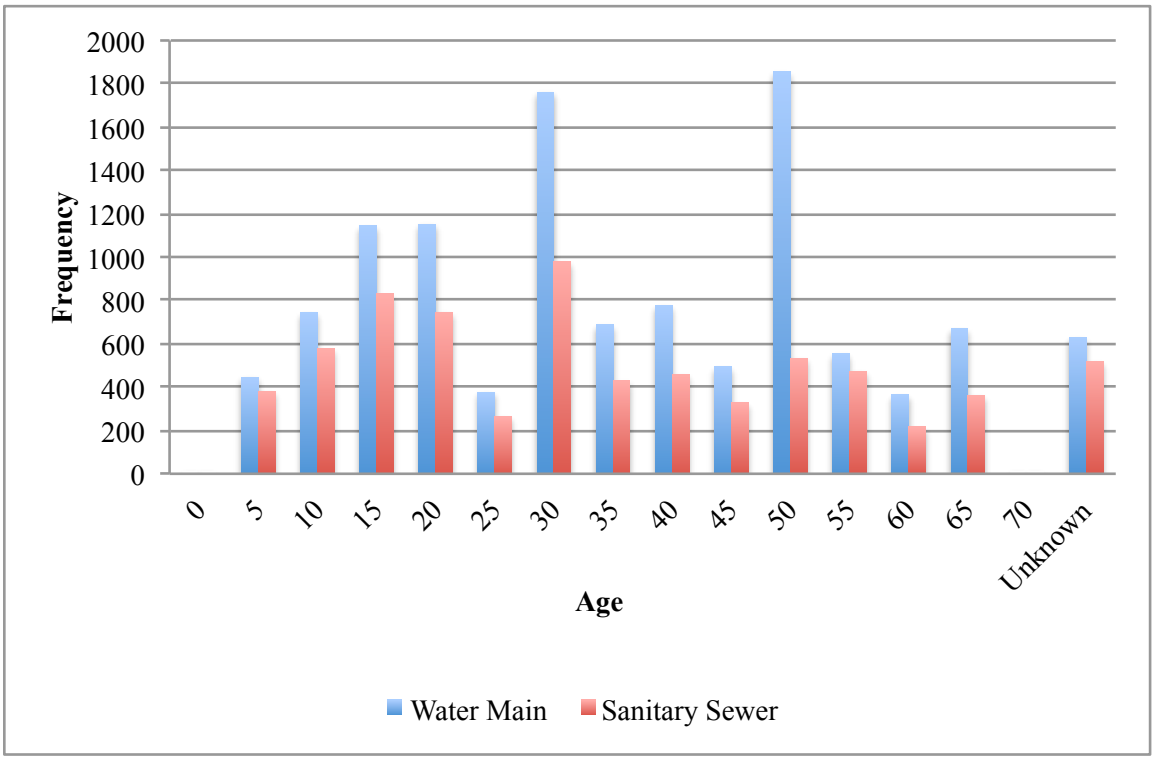

Figure 15 Frequency of City of Waterloo water main and sanitary sewer, by pipe age

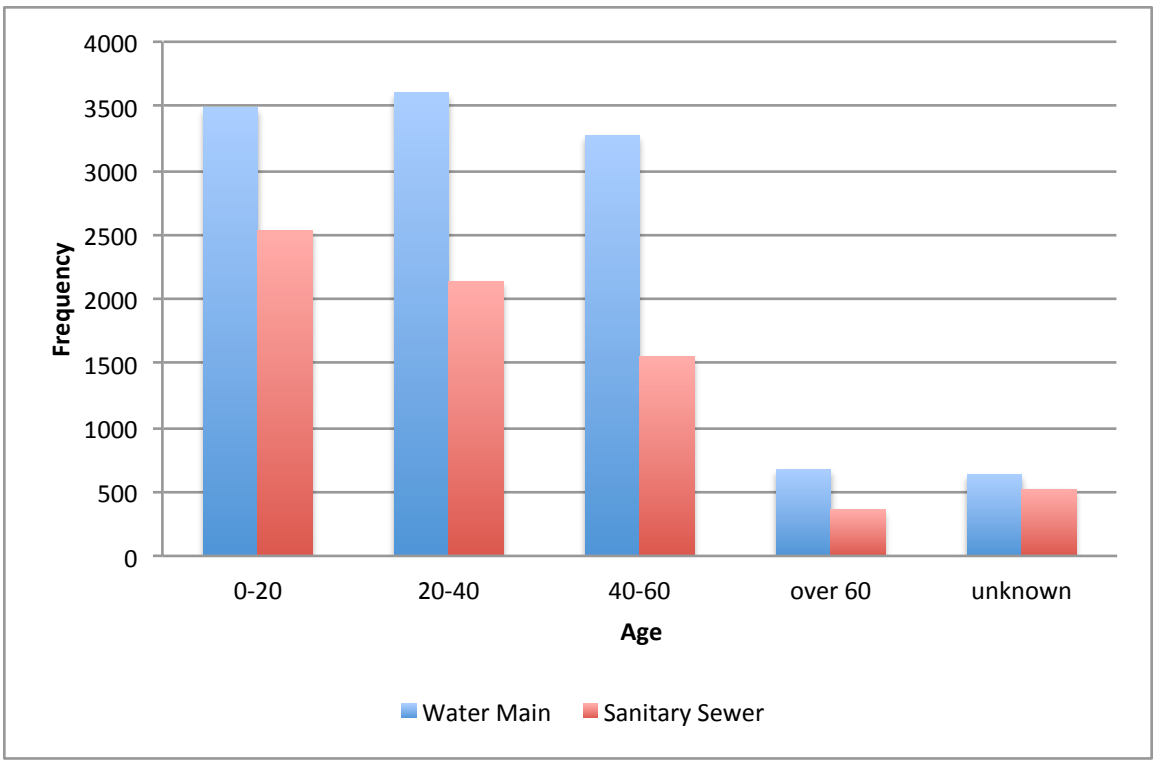

Figure 16 Frequency of City of Waterloo water main and sanitary sewer, by pipe age in 20-year bins

Table 7 and Figure 15 show that most of the water main and sanitary sewer infrastructure is under 60 years old. This is important because as the infrastructure ages, operating and maintenance costs are expected to increase, putting added pressure on the municipality.

Table 8 and Figure 17 illustrate the distribution of pipe material for water main and sanitary sewer.

Table 8 Frequency of City of Waterloo water main and sanitary sewer, by pipe material

Material	Water Main	Sanitary Sewer
Asbestos Cement	30	464
Alkathene	0	375
Cast Iron	3574	0
Concrete	49	992
Ductile Iron	1195	0
PVC	6157	3171
Vitrified Clay	0	893
Other	655	1204

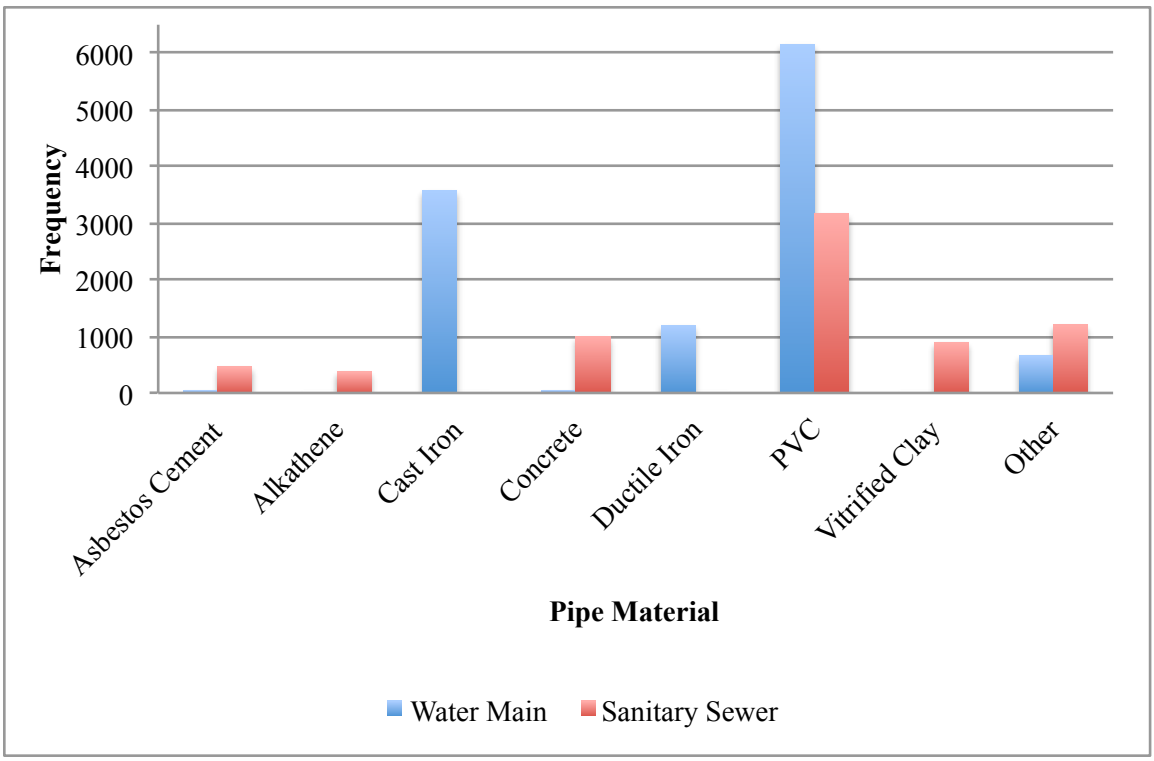

Figure 17 Frequency of City of Waterloo water main and sanitary sewer, by pipe material

Table 9 and Figure 18 show the distribution of pipe diameter for the water main and sanitary sewer. Most water mains are 0-300 mm in size, and the majority of sanitary sewers are 100-300 mm in size with most at 200 mm.

Table 9 Frequency of City of Waterloo water main and sanitary sewer, by pipe diameter

Diameter	Water Main	Sanitary Sewer
100	674	0
200	7246	5202
300	2909	914
400	176	312
500	99	190
600	119	237
More	16	244
Unknown	421	0

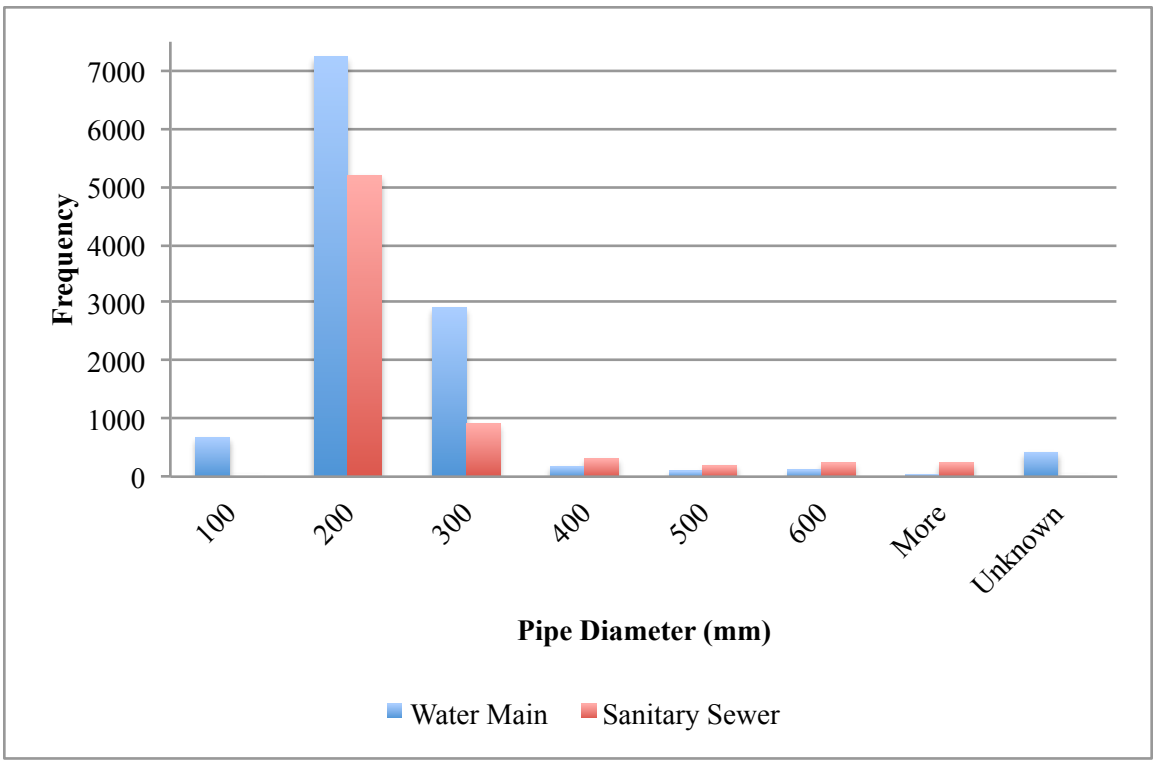

Figure 18 Frequency of City of Waterloo water main and sanitary sewer, by pipe diameter

Figure 19 shows the City of Waterloo sanitary sewer network coloured by the elevation of the upstream invert, with the modeled infrastructure shown in black. Figure 20 shows the ground surface elevation of the Laurel Creek Watershed, with the modeled infrastructure. The modeled infrastructure contained 13.9 km of pipe, which is 3.2% of the total sanitary sewer network for the City of Waterloo. The modeled sanitary sewer system is representative of the City of Waterloo sanitary sewer trunk lines. Based on these figures, it can be seen that the gravity-fed sanitary sewer flows from West to East, discharging into the wastewater treatment plant at the Eastern end of the watershed.

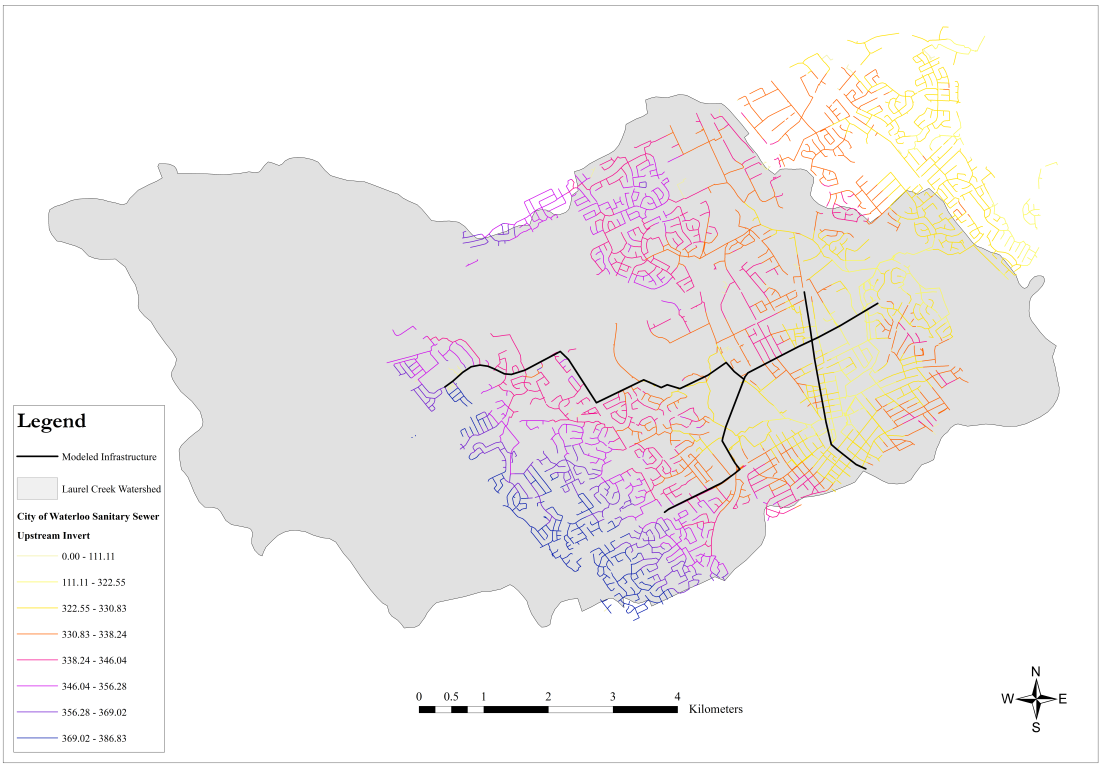

Figure 19 Elevation of City of Waterloo sanitary sewer network and modeled infrastructure

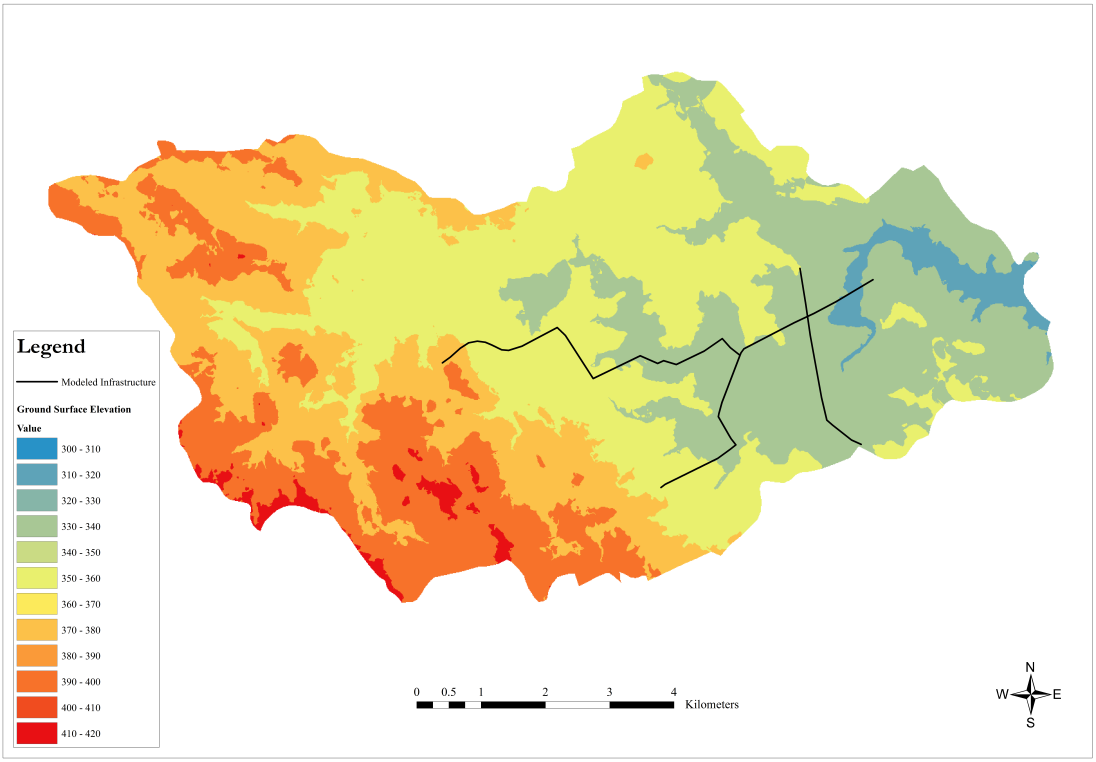

Figure 20 Laurel Creek Watershed ground surface elevation and modeled infrastructure

When inputting a subsection of pipe into the mesh, it was determined that the geometry of the pipes is dependent on the geometry of the mesh. Therefore, a layer was added to ensure the sanitary sewers are input with a continually decreasing elevation.

The infrastructure model was created based on the design criteria from the City of Waterloo (2013b). The sanitary sewers were placed at a minimum of 3.0 m below ground surface with a continually decreasing elevation to allow for gravity drainage. Flow was modeled using Manning's formula (Equation 15 in Section 3.2.5). The modeled sewers were assumed to be 375 mm in diameter with a Manning's roughness coefficient of 0.013. Based on the total measured flow of the sanitary drainage in the City of Waterloo, the cumulative flow through the modeled network was 6.57×10^{06} m^3/yr, or 0.2083 m^3/s. In addition, the pipes were given a coupling length and a coupling conductivity of 0.05 and 0.001, respectively. These parameters define the rate at which water is permitted to flow between the subsurface and infrastructure domains, as described in Equation 17.

Chapter 4: Results

The Laurel Creek Watershed model contained 39 vertical layers, with consistent discretization throughout the mesh. It also contained a layer that was adjusted to accommodate the sanitary sewer network. This layer was adjusted to allow the nodes at the sanitary sewer locations continually decrease in elevation toward the outlet at the site of the wastewater treatment plant. The models described in Table 10 were produced with this discretization.

Table 10 Description of model simulations

Section	Precipitation (Percentage of total annual average)	Evapotranspiration	Infrastructure
4.1	25%	No	No
4.2	100%	Yes	No
4.3.1	25%	No	Yes
4.3.2	100%	Yes	Yes

4.1 Steady State Base Model

A steady state model was created to provide the initial conditions for subsequent models. In order to use a shorter simulation time while simulating the effects of evapotranspiration, the precipitation was modeled as 25% of the total annual average. The results and water balance for this simulation are summarized in Table 11 and Table 12, respectively. Figures illustrating the results are given in Figure 21 to Figure 24.

Table 11 Summary of results for steady state base model

Input	Value	Unit
Precipitation	7.45×10^{-09}	m/s
Potential Evapotranspiration	0	m/s
Flow Through Pipes	0	m^3/s
Output	**Value**	**Unit**
Groundwater recharge	3.97×10^{-01}	m^3/s
Groundwater discharge	-3.97×10^{-01}	m^3/s
Surface Water Evaporation	0	m^3/s
Subsurface Evaporation	0	m^3/s
Subsurface Transpiration	0	m^3/s
Total Evapotranspiration	0	m^3/s
Total Evapotranspiration	0	% of Precipitation
Flow at Laurel Creek Outlet	-5.47×10^{-01}	m^3/s

Table 12 Water balance for steady state base model, all values in m^3/s

Water Sources	Value
Precipitation	0.56
Total Water Sources	0.56
Water Sinks	**Value**
Laurel Creek Outlet	-0.55
Watershed Boundary Outlet	-0.02
Total Water Sinks	-0.56
Mass Balance (Sources - Sinks)	0.00
Mass Balance Error	**0.002%**

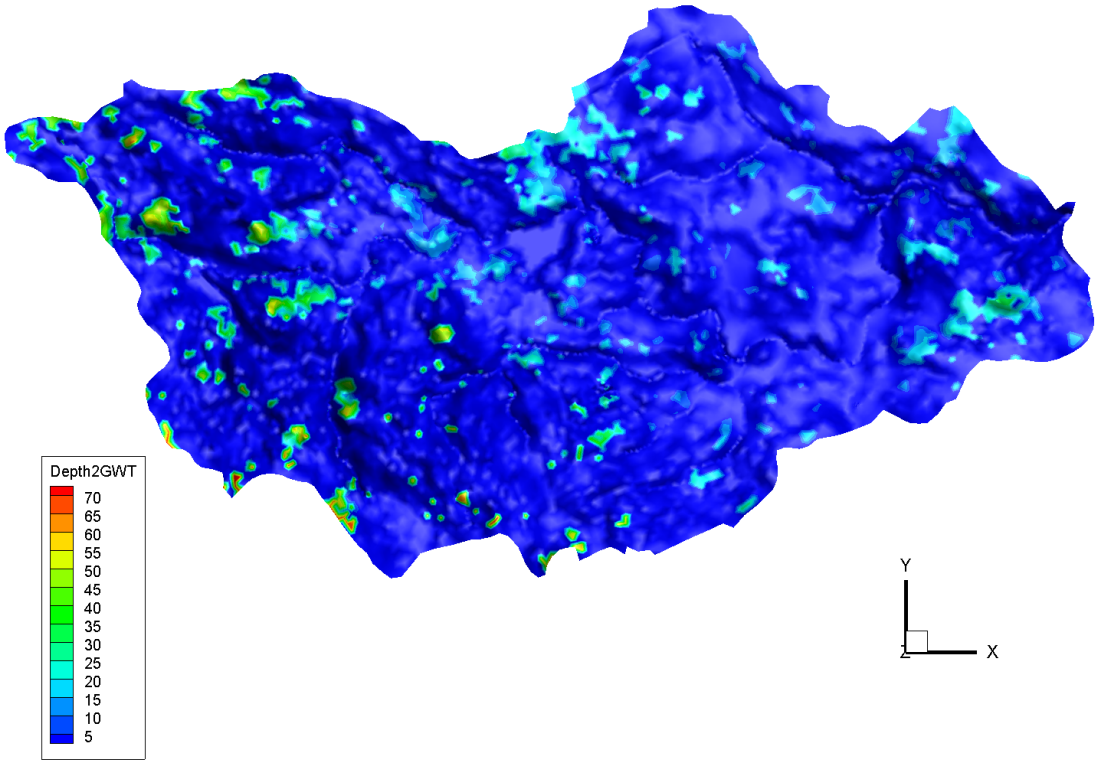

Figure 21 Depth to groundwater table [m], steady state base model

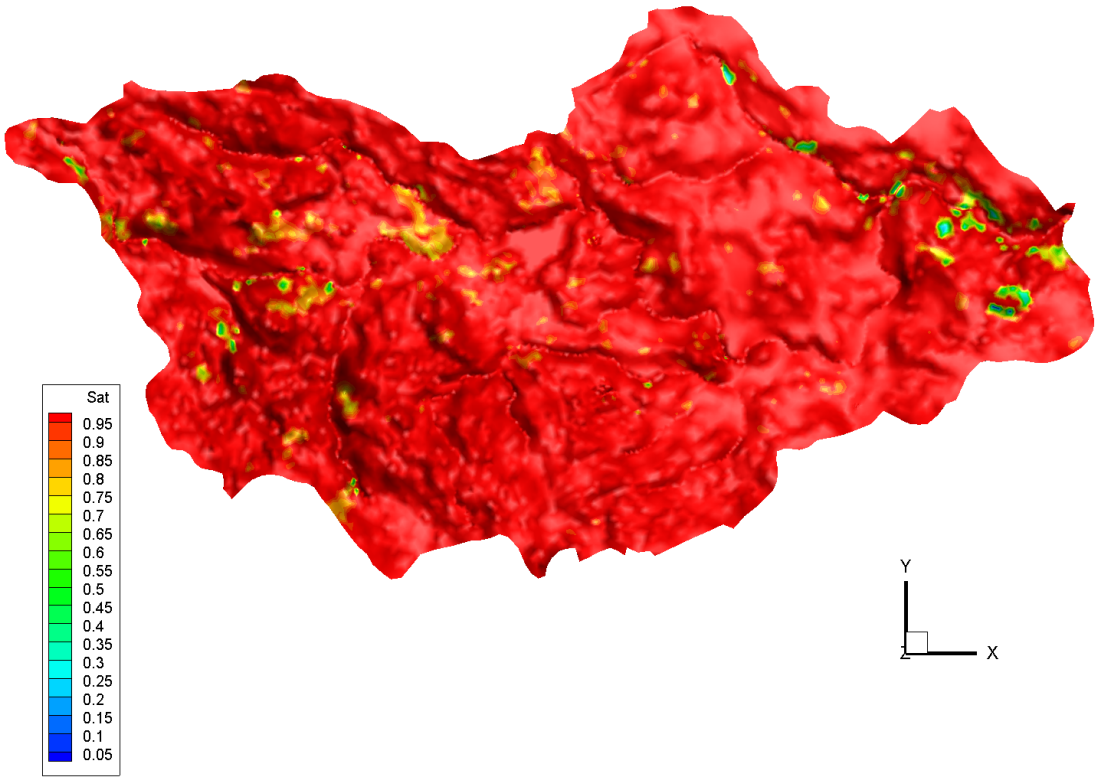

Figure 22 Saturation [m^3/m^3], steady state base model

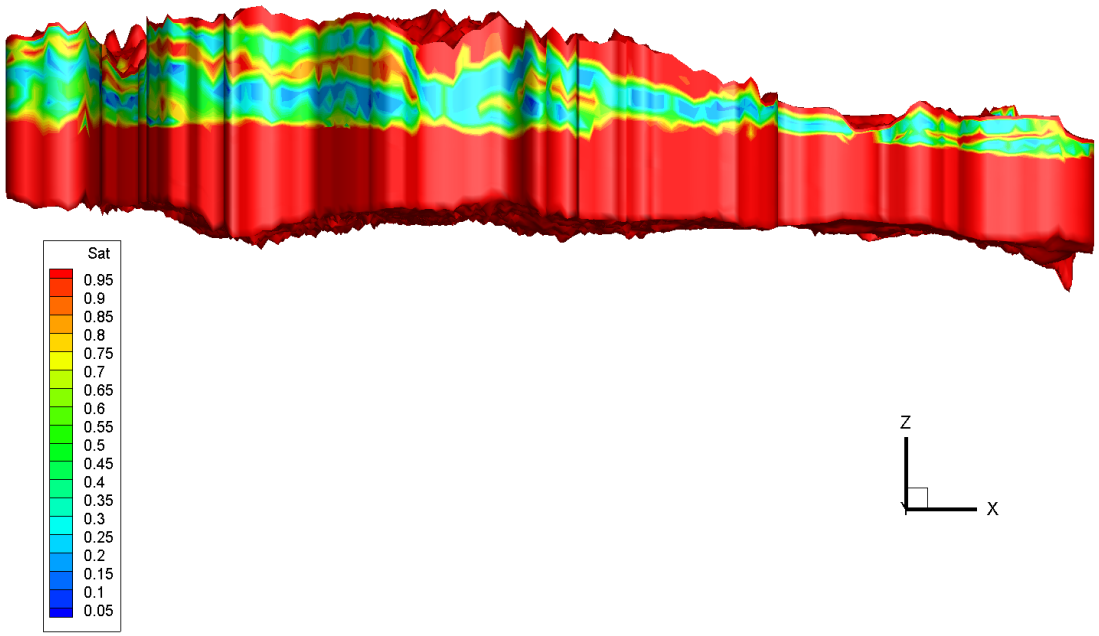

Figure 23 Saturation [m^3/m^3] side view looking North, steady state base model

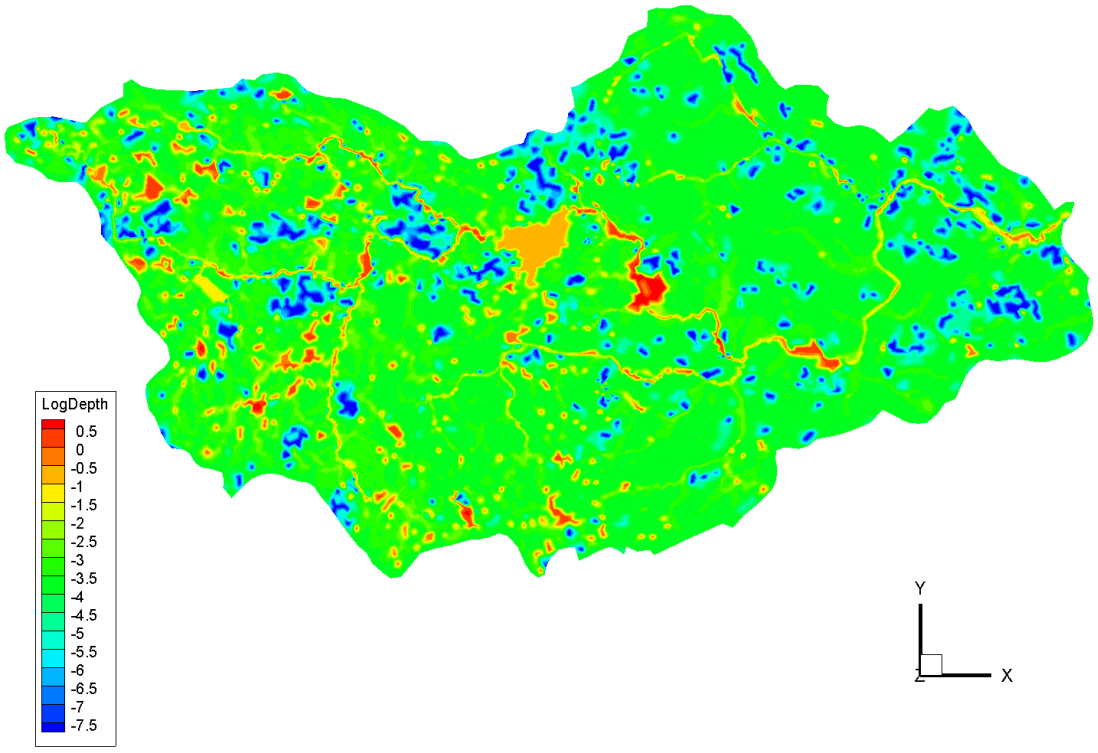

Figure 24 Log depth of surface water [log(m)], steady state base model

Figure 23 provides a well-defined illustration of the water table, and Figure 24 shows the depth of surface water throughout the watershed.

4.2 Evapotranspiration

Using the outputs from the steady state base model as the initial conditions, a model was created with 100% precipitation, and evapotranspiration. The results and water balance for this simulation are summarized in Table 13 and Table 14, respectively. This model resulted total evapotranspiration equaling 63% of the total annual average precipitation.

Table 13 Summary of results for evapotranspiration model without infrastructure

Input	**Value**	**Unit**
Precipitation	2.98×10^{-08}	m/s
Potential Evapotranspiration	2.62×10^{-08}	m/s
Flow Through Pipes	0	m^3/s
Output	**Value**	**Unit**
Groundwater recharge	1.26	m^3/s
Groundwater discharge	-3.23×10^{-01}	m^3/s
Surface Water Evaporation	-4.76×10^{-01}	m^3/s
Subsurface Evaporation	-1.89×10^{-01}	m^3/s
Subsurface Transpiration	-7.49×10^{-01}	m^3/s
Total Evapotranspiration	-1.41	m^3/s
Total Evapotranspiration	62.6%	% of Precipitation
Flow at Laurel Creek Outlet	-8.00×10^{-01}	m^3/s

Table 14 Water balance for evapotranspiration model without infrastructure, all values in m^3/s

Water Sources	**Value**
Precipitation	2.26
Total Water Sources	2.26
Water Sinks	**Value**
Laurel Creek Outlet	-0.80
Watershed Boundary Outlet	-0.05
Total Evapotranspiration	-1.41
Total Water Sinks	-2.26
Mass Balance (Sources - Sinks)	0.00
Mass Balance Error	**0.107%**

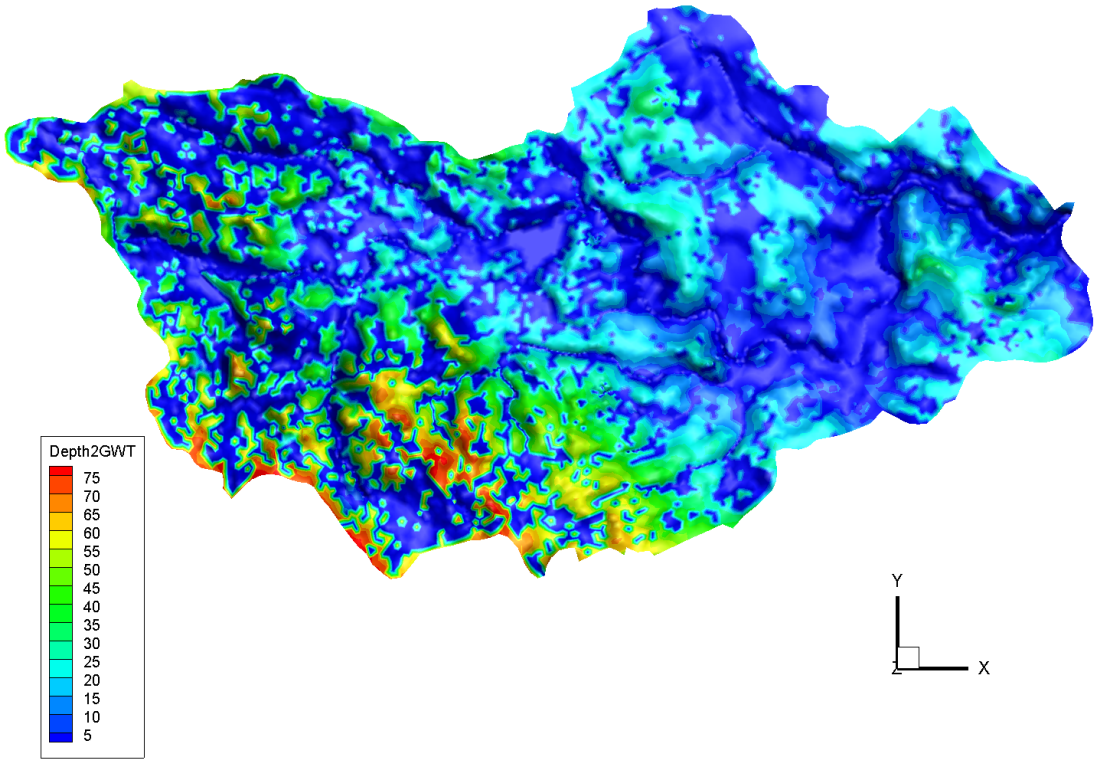

Figure 25 Depth to groundwater table [m], steady state evapotranspiration model

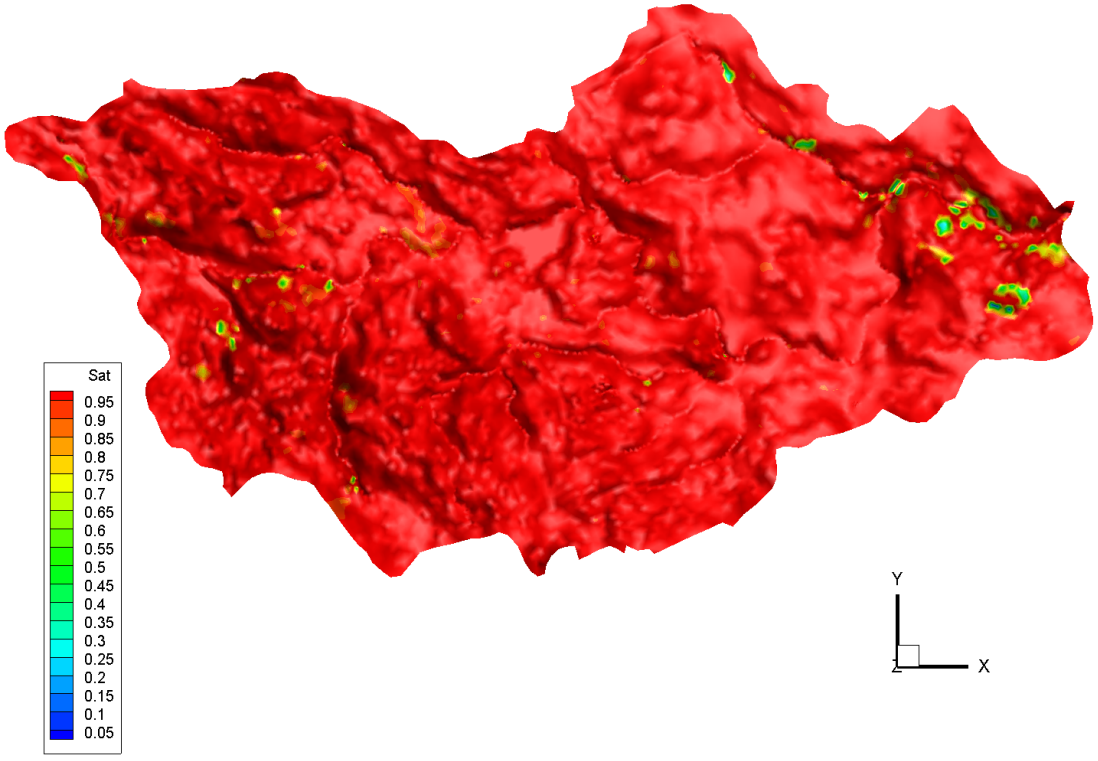

Figure 26 Saturation [m^3/m^3], steady state evapotranspiration model

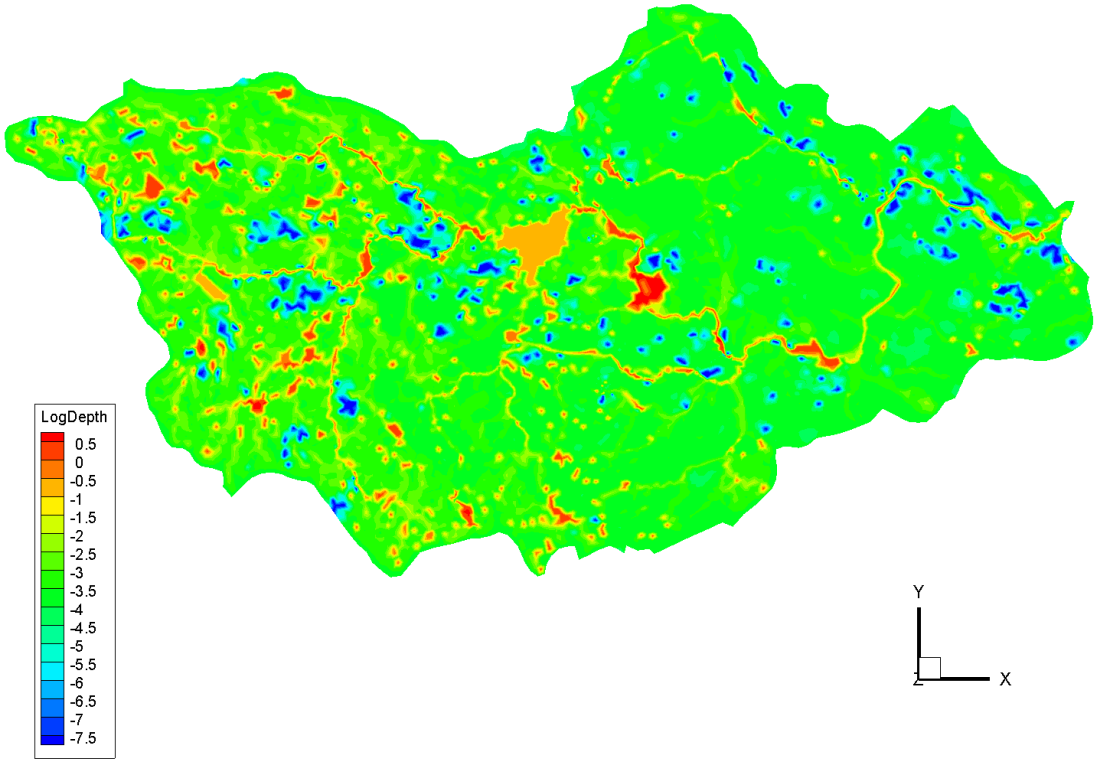

Figure 27 Log depth of surface water [log(m)], steady state evapotranspiration model

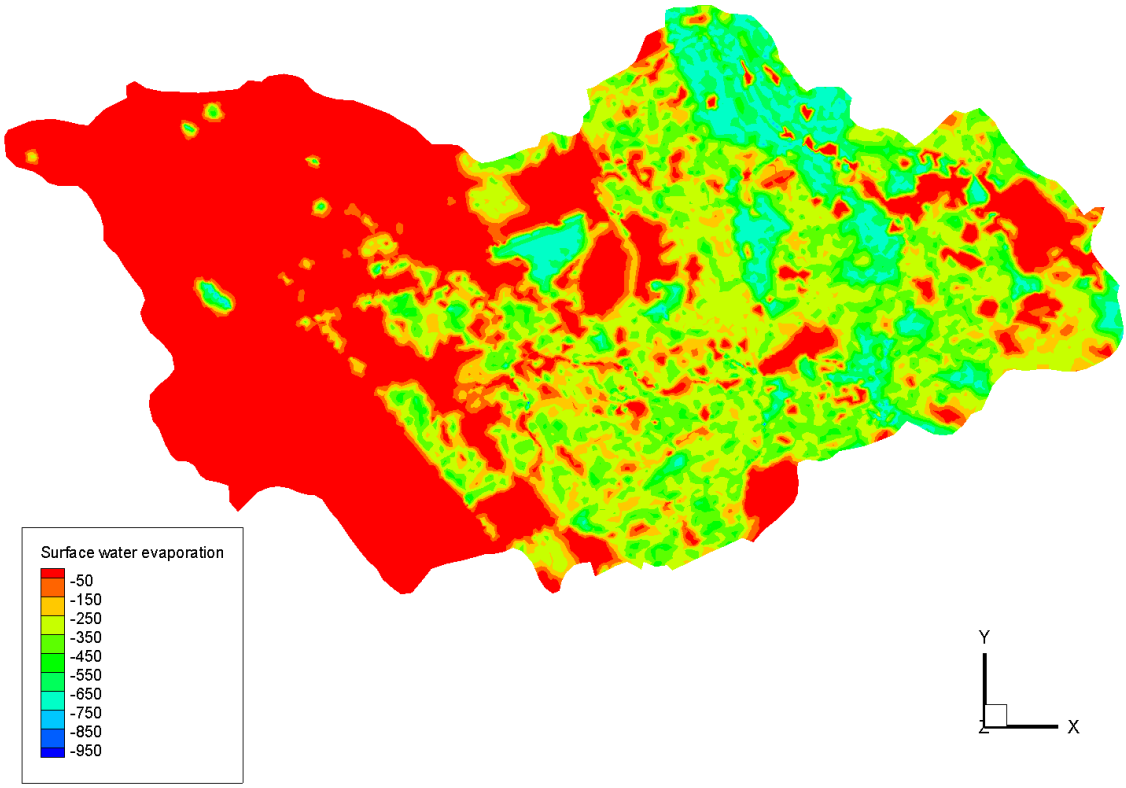

Figure 28 Surface water evaporation [mm/year], steady state evapotranspiration model

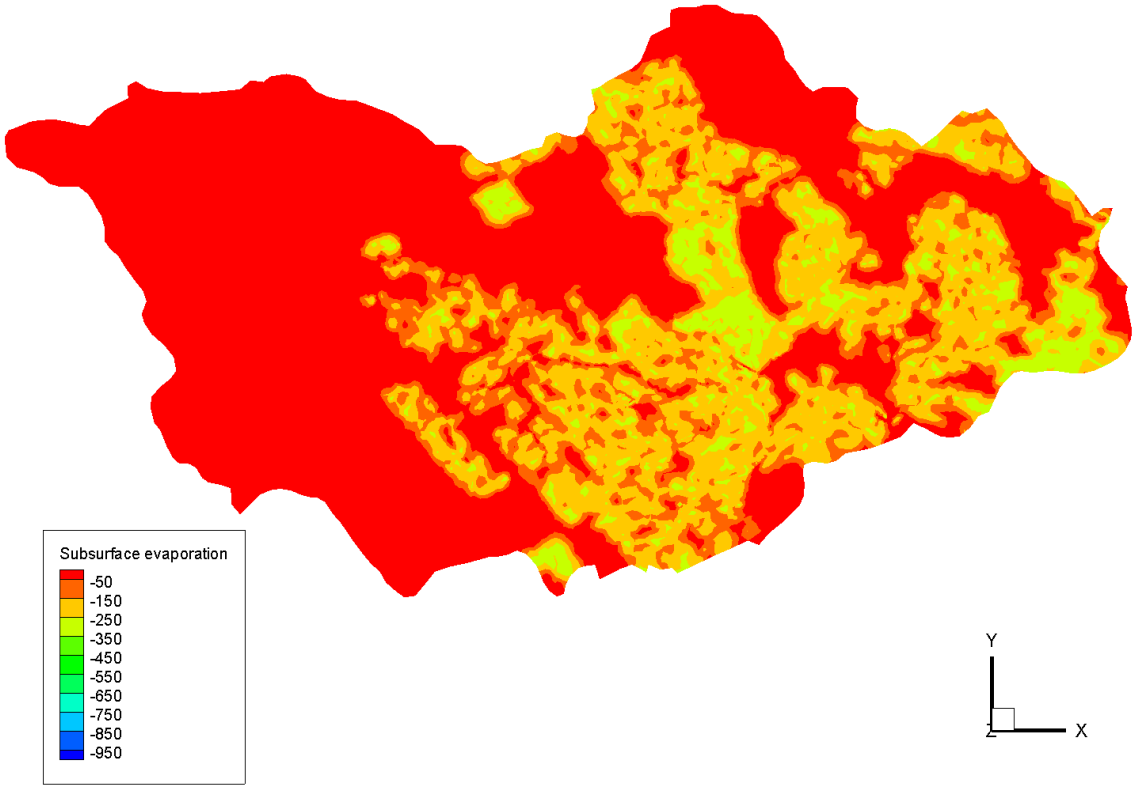

Figure 29 Subsurface evaporation [mm/year], steady state evapotranspiration model

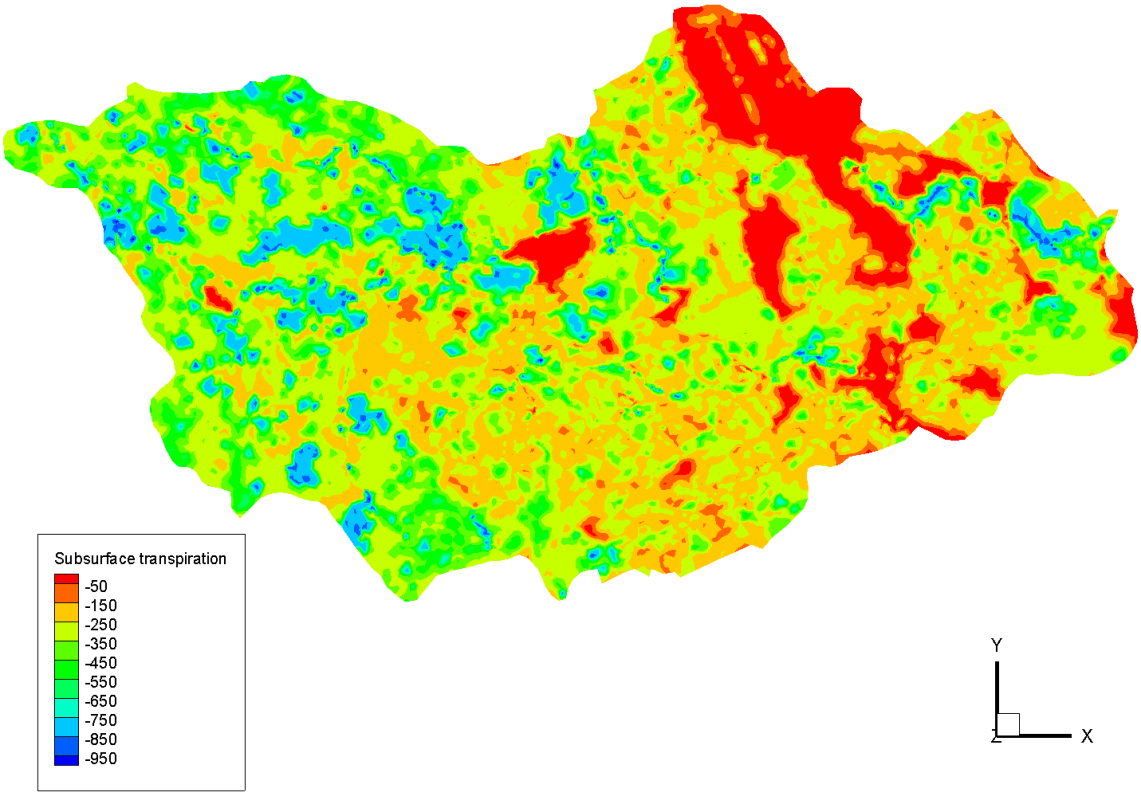

Figure 30 Subsurface transpiration [mm/year], steady state evapotranspiration model

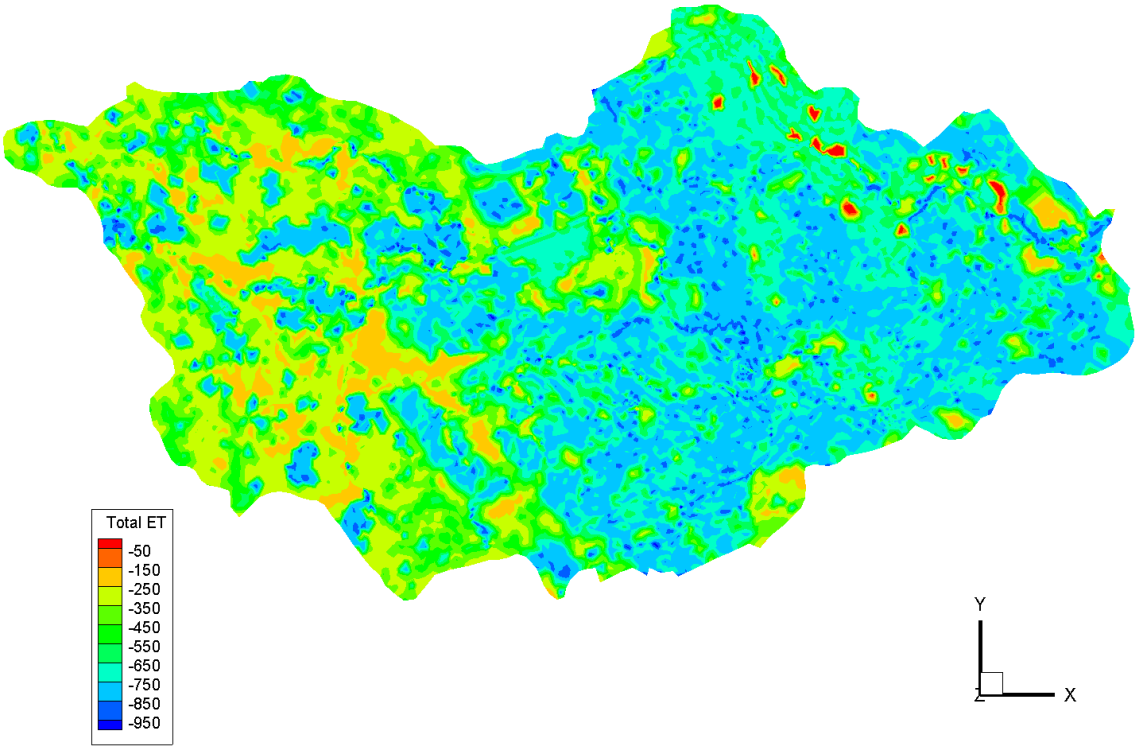

Figure 31 Total evapotranspiration [mm/year], steady state evapotranspiration model

This model provides a realistic representation of evapotranspiration, at 63% of the total precipitation volume. There is a higher amount of evaporation in the Eastern part of the watershed due to the large amount of paved surface. Conversely, more subsurface transpiration, defined on in Section 3.5, occurs in the Western part of the watershed due to the higher amount of agricultural and forested area. This results in evapotranspiration that is evenly distributed throughout the Laurel Creek Watershed.

4.3 Infrastructure

Two models with infrastructure were created. Only the simplified sanitary sewer representing the trunk lines in the City of Waterloo were modeled, as depicted in Section 3.6, and Figure 19 and Figure 20. The first version ran with 25% precipitation and no evapotranspiration; the second version ran with 100% precipitation and included evapotranspiration. The results and figures detailing these models are given in Section 4.3.1 and Section 4.3.2, respectively.

4.3.1 Evapotranspiration Off

This model ran with 25% precipitation to accommodate the absence of evapotranspiration parameters, similar to the model described in Section 4.1. The results and water balance from this model are summarized in Table 15 and Table 16, respectively. Figure 32 through Figure 36 illustrate the results.

Table 15 Summary of results for infrastructure model with 25% precipitation

Input	**Value**	**Unit**
Precipitation	7.45×10^{-09}	m/s
Potential Evapotranspiration	0	m/s
Flow Through Pipes	3.80×10^{-02}	m^3/s
Output	**Value**	**Unit**
Groundwater recharge	3.28×10^{-01}	m^3/s
Groundwater discharge	-6.08×10^{-01}	m^3/s
Surface Water Evaporation	0	m^3/s
Subsurface Evaporation	0	m^3/s
Subsurface Transpiration	0	m^3/s
Total Evapotranspiration	0	m^3/s
Total Evapotranspiration	0	% of Precipitation
Flow at Laurel Creek Outlet	-8.26×10^{-01}	m^3/s

Table 16 Water balance for infrastructure model with 25% precipitation, all values in m^3/s

Water Sources	**Value**
Precipitation	0.56
Infrastructure	0.30
Total Water Sources	0.87
Water Sinks	**Value**
Laurel Creek Outlet	-0.85
Watershed Boundary Outlet	-0.02
Total Water Sinks	-0.87
Mass Balance (Sources - Sinks)	0.00
Mass Balance Error	**0.001%**

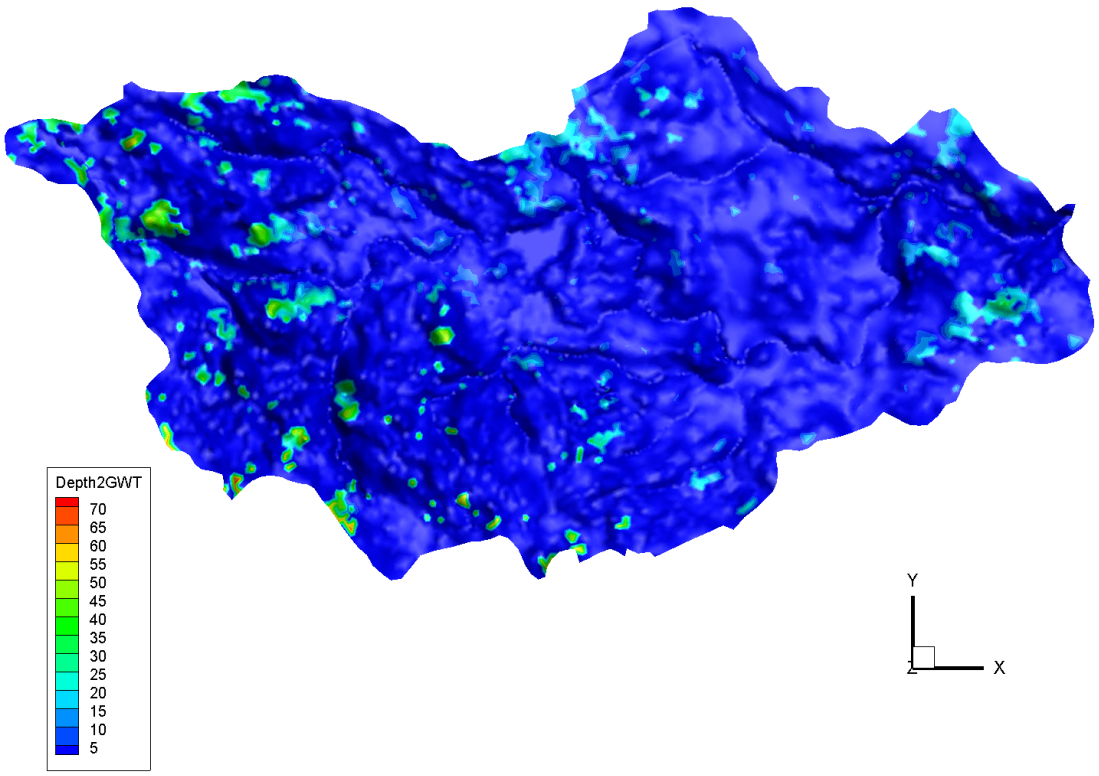

Figure 32 Depth to groundwater table [m], 25% precipitation without evapotranspiration

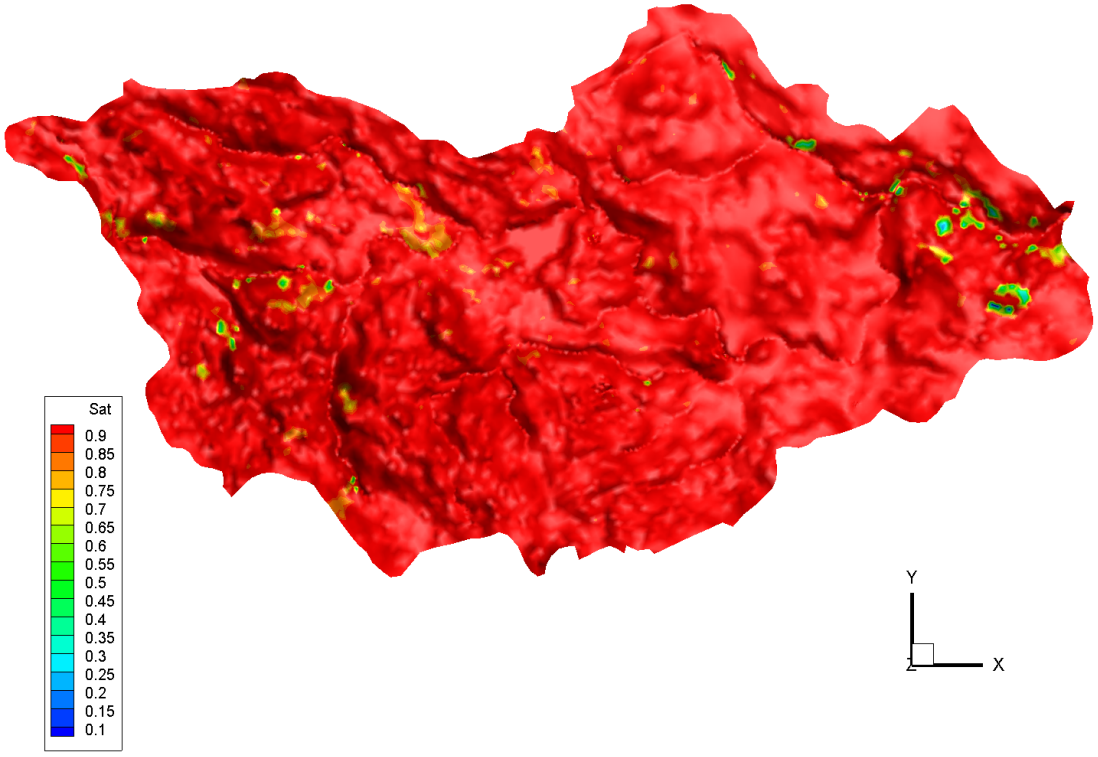

Figure 33 Saturation [m^3/m^3], 25% precipitation without evapotranspiration

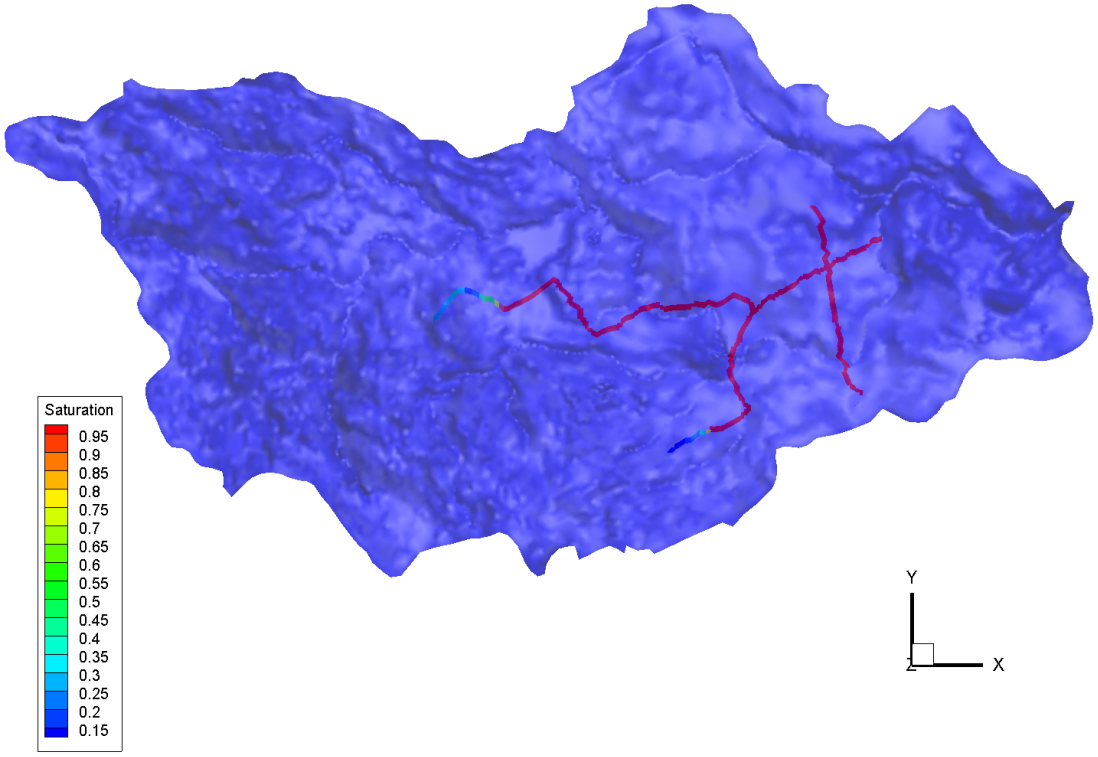

Figure 34 Saturation of infrastructure [m^3/m^3], 25% precipitation without evapotranspiration

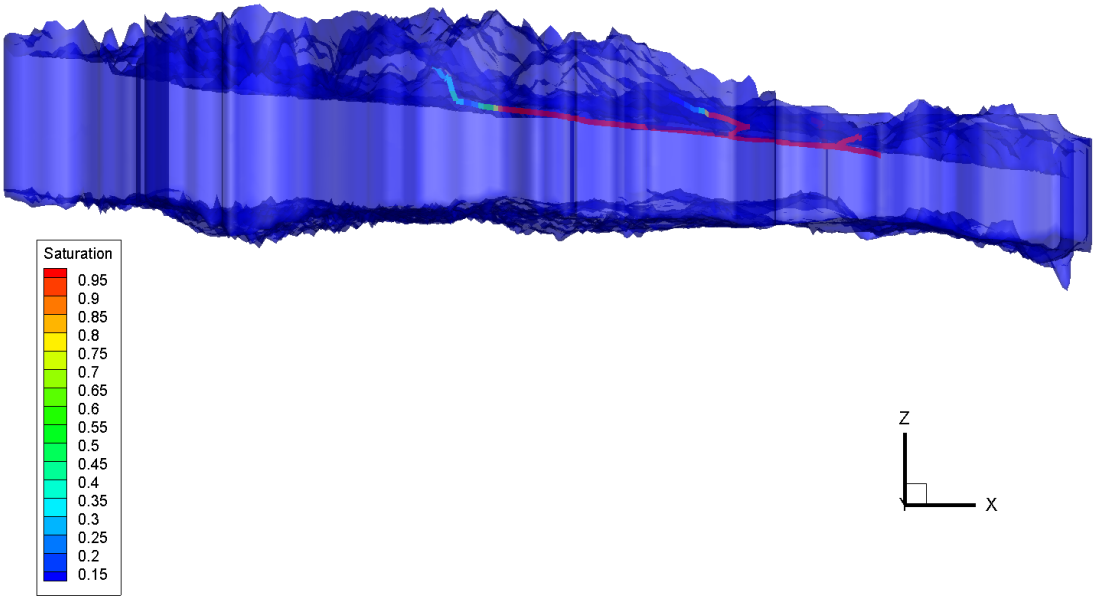

Figure 35 Saturation of infrastructure [m^3/m^3] side view looking North, 25% precipitation without evapotranspiration

Figure 34 and Figure 35 show saturation of the modeled infrastructure. From these figures, it is shown that the sanitary sewer pipes are fully saturated except at upstream ends at higher elevations. The pipes have a continually decreasing elevation.

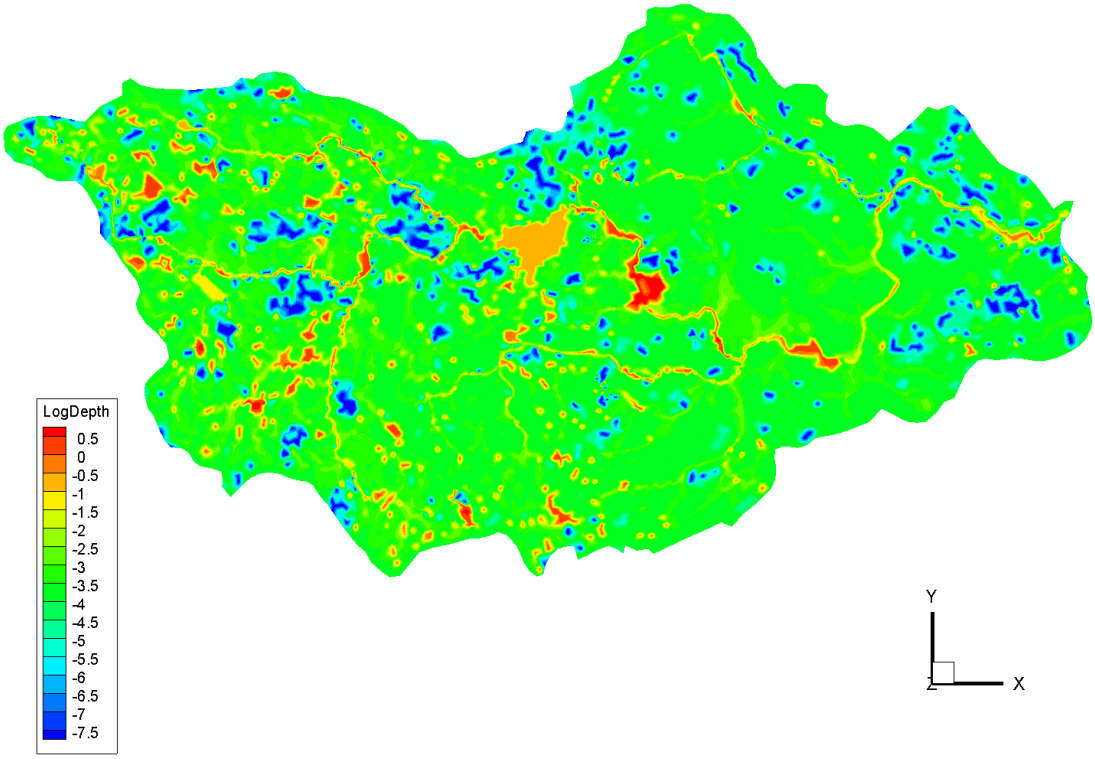

Figure 36 Log depth of surface water [log(m)], 25% precipitation without evapotranspiration

4.3.2 Evapotranspiration On

The final version of the model is a summation of all preceding models. The simulation ran with 100% precipitation, evapotranspiration, and the sanitary sewer infrastructure. The results and water balance are summarized in Table 17 and Table 18, respectively. Figure 37 through Figure 45 illustrate the results.

Table 17 Summary of results for infrastructure model with evapotranspiration

Input	Value	Unit
Precipitation	2.98×10^{-08}	m/s
Potential Evapotranspiration	2.62×10^{-08}	m/s
Flow Through Pipes	2.08×10^{-01}	m^3/s
Output	**Value**	**Unit**
Groundwater recharge	8.82×10^{-01}	m^3/s
Groundwater discharge	-1.55	m^3/s
Leakage Out of Pipes	1.26×10^{-03}	m^3/s
Leakage Into Pipes	-1.67	m^3/s
Surface Water Evaporation	-4.92×10^{-01}	m^3/s
Subsurface Evaporation	-1.89×10^{-01}	m^3/s
Subsurface Transpiration	-8.08×10^{-01}	m^3/s
Total Evapotranspiration	-1.49	m^3/s
Total Evapotranspiration	66.0%	% of Precipitation
Flow at Laurel Creek Outlet	-4.60×10^{-01}	m^3/s

Table 18 Water balance for infrastructure model with evapotranspiration, all values in m^3/s

Water Sources	Value
Precipitation	2.26
Infrastructure	1.67
Total Water Sources	3.92
Water Sinks	**Value**
Laurel Creek Outlet	-2.39
Watershed Boundary Outlet	-0.05
Total Evapotranspiration	-1.49
Total Water Sinks	-3.92
Mass Balance (Sources - Sinks)	0.00
Mass Balance Error	**0.008%**

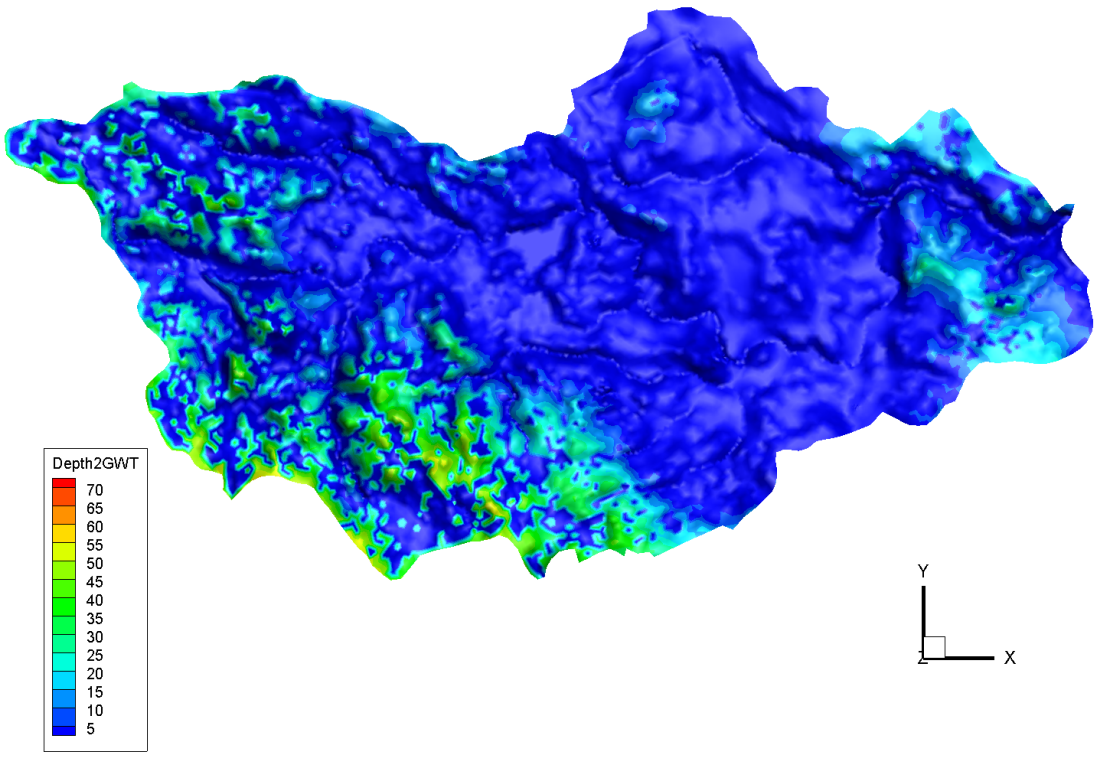

Figure 37 Depth to groundwater table [m], 100% precipitation with evapotranspiration

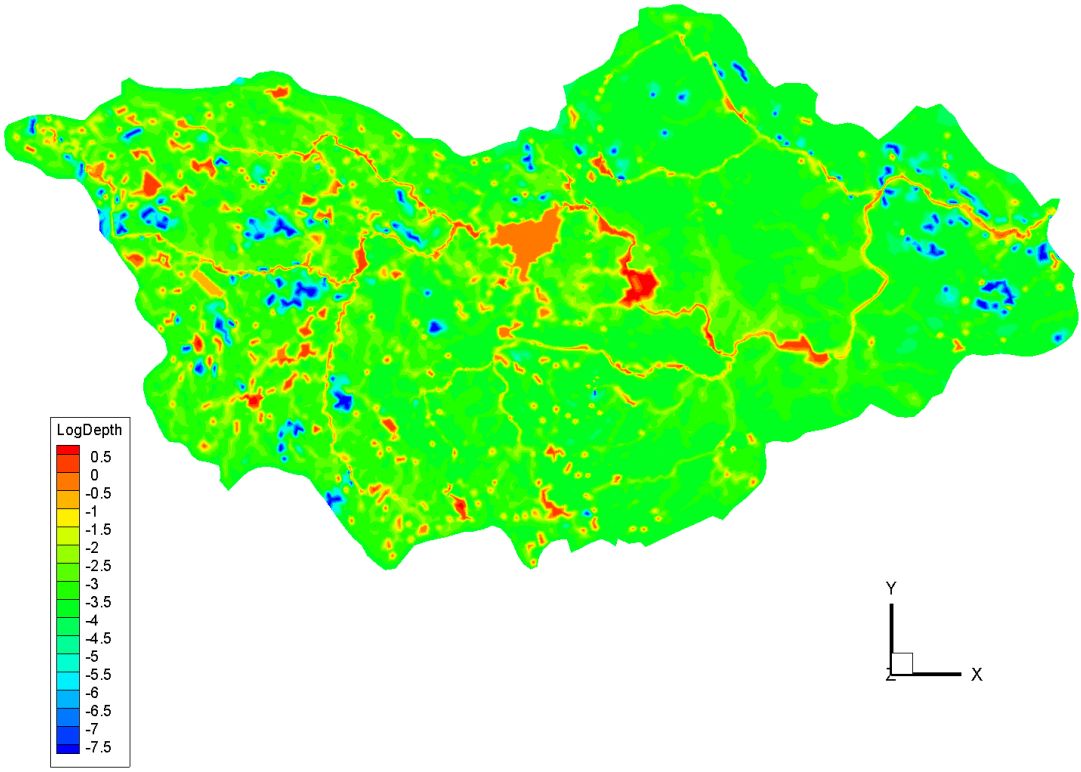

Figure 38 Log depth of surface water [log(m)], 100% precipitation with evapotranspiration

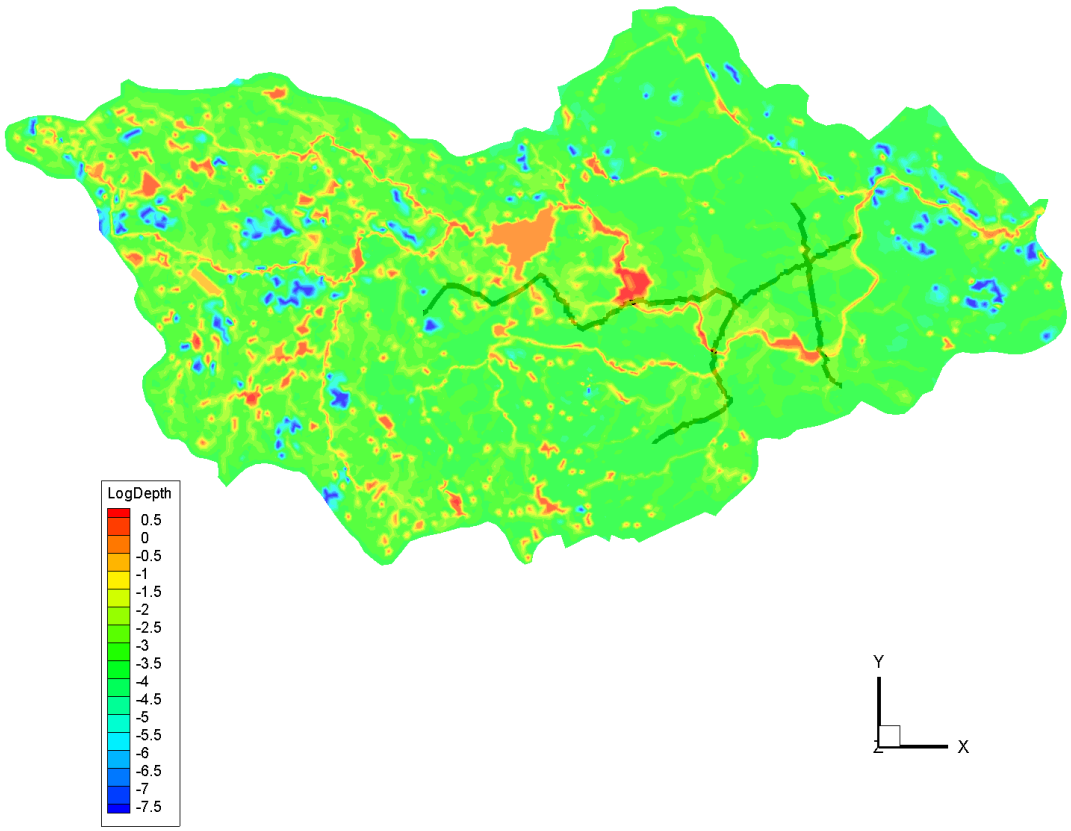

Figure 39 Log depth of surface water [log(m)] with infrastructure, 100% precipitation with evapotranspiration

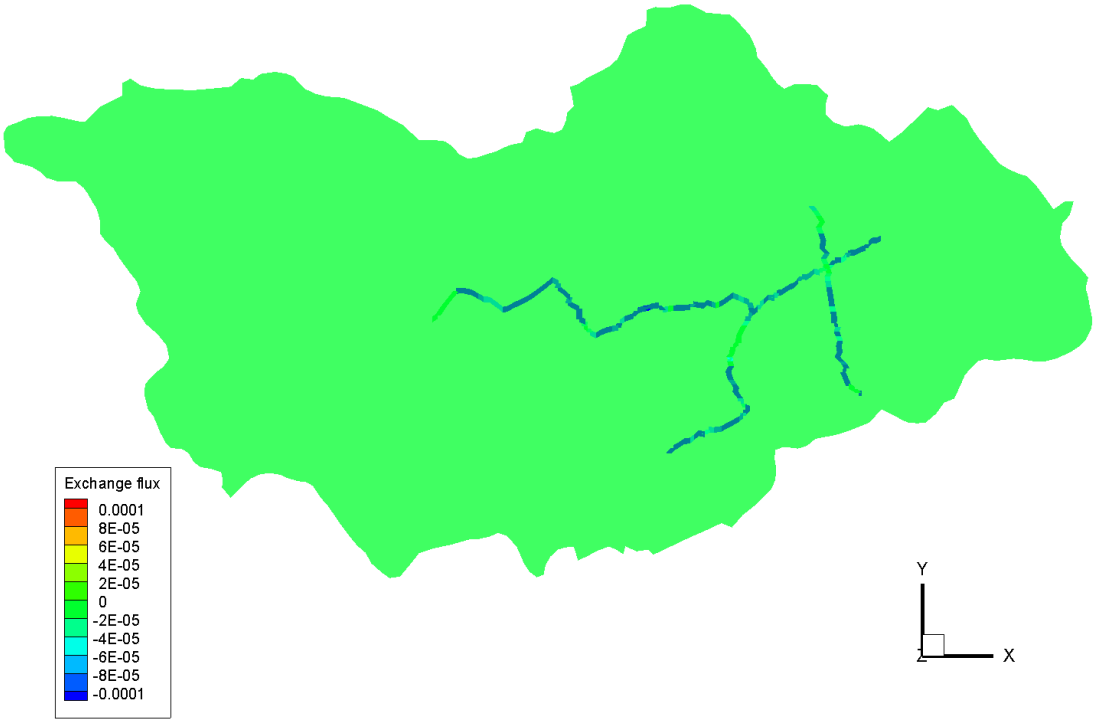

Figure 40 Exchange flux between infrastructure and subsurface domains [$m^3/m^3/s$], 100% precipitation with evapotranspiration

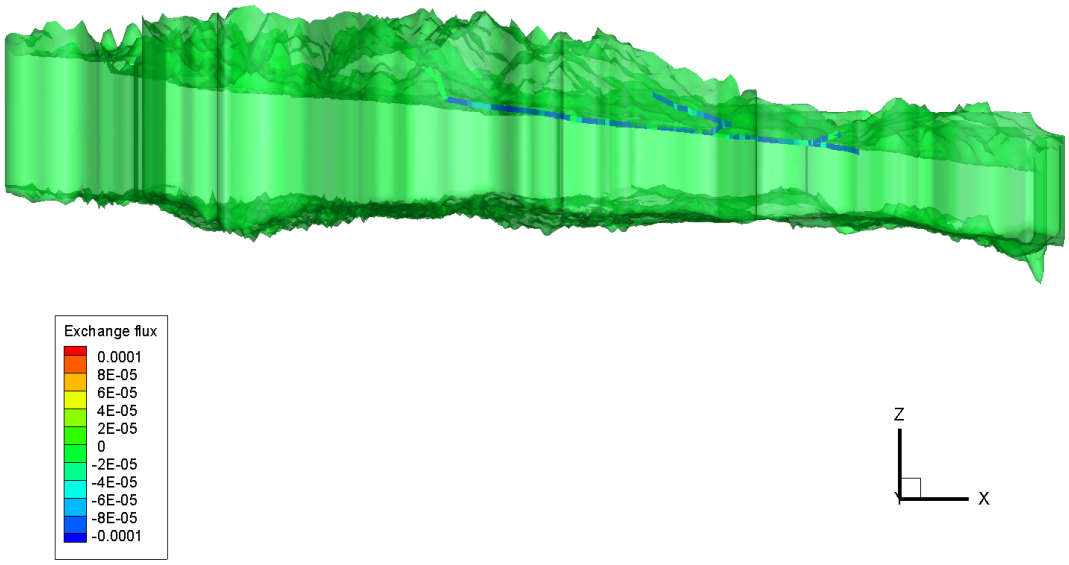

Figure 41 Exchange flux between infrastructure and subsurface domains [$m^3/m^3/s$] side view looking North, 100% precipitation with evapotranspiration

Figure 40 and Figure 41 illustrate the exchange flux between the infrastructure and subsurface domains, with negative values representing flows from the subsurface into the sewers. As depicted in the figures, there is no leakage out of the sewer into the subsurface; there is only infiltration into the sewers from the subsurface. This is expected because sanitary sewers flow via gravity drainage and do not exert a pressure on the pipe walls.

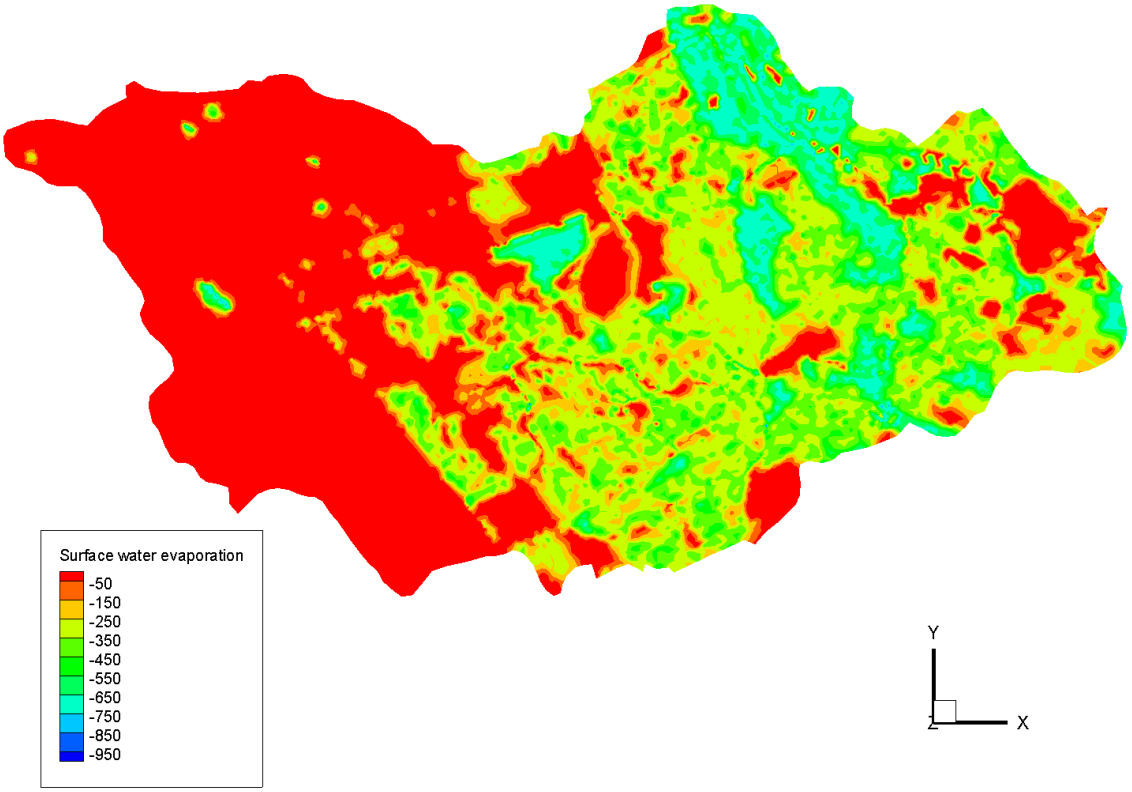

Figure 42 Surface water evaporation [mm/year], 100% precipitation with evapotranspiration

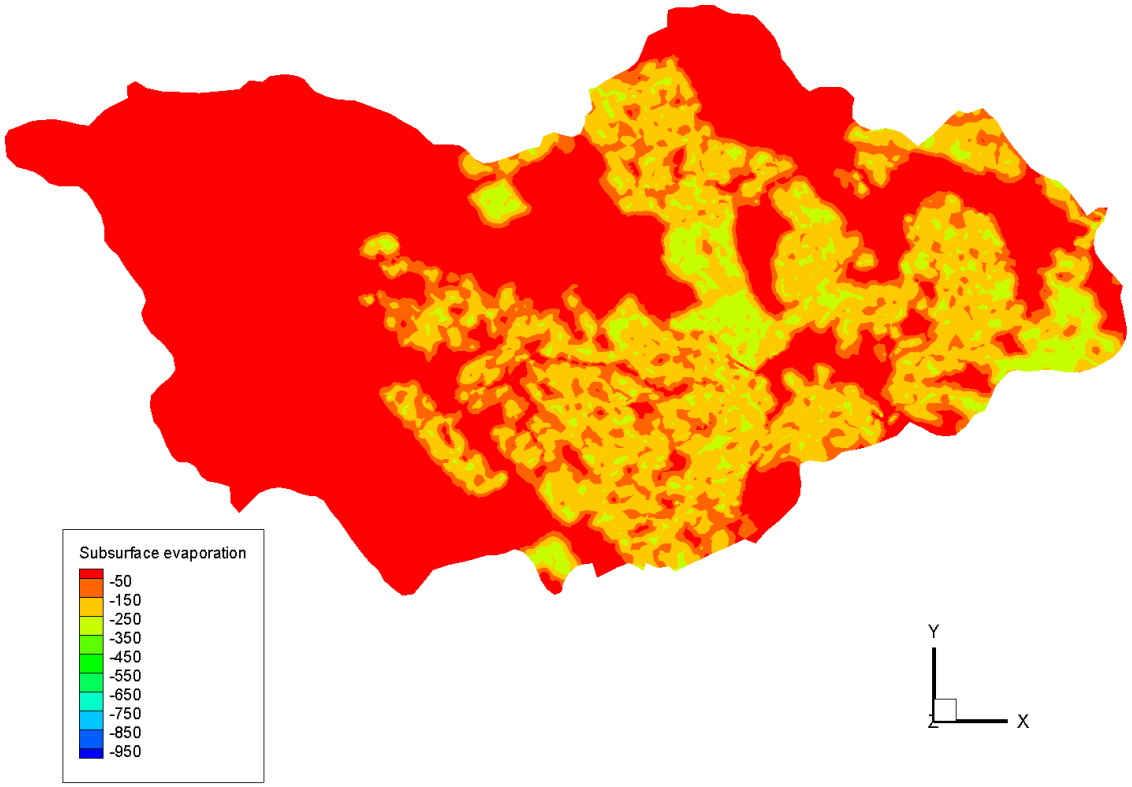

Figure 43 Subsurface evaporation [mm/year], 100% precipitation with evapotranspiration

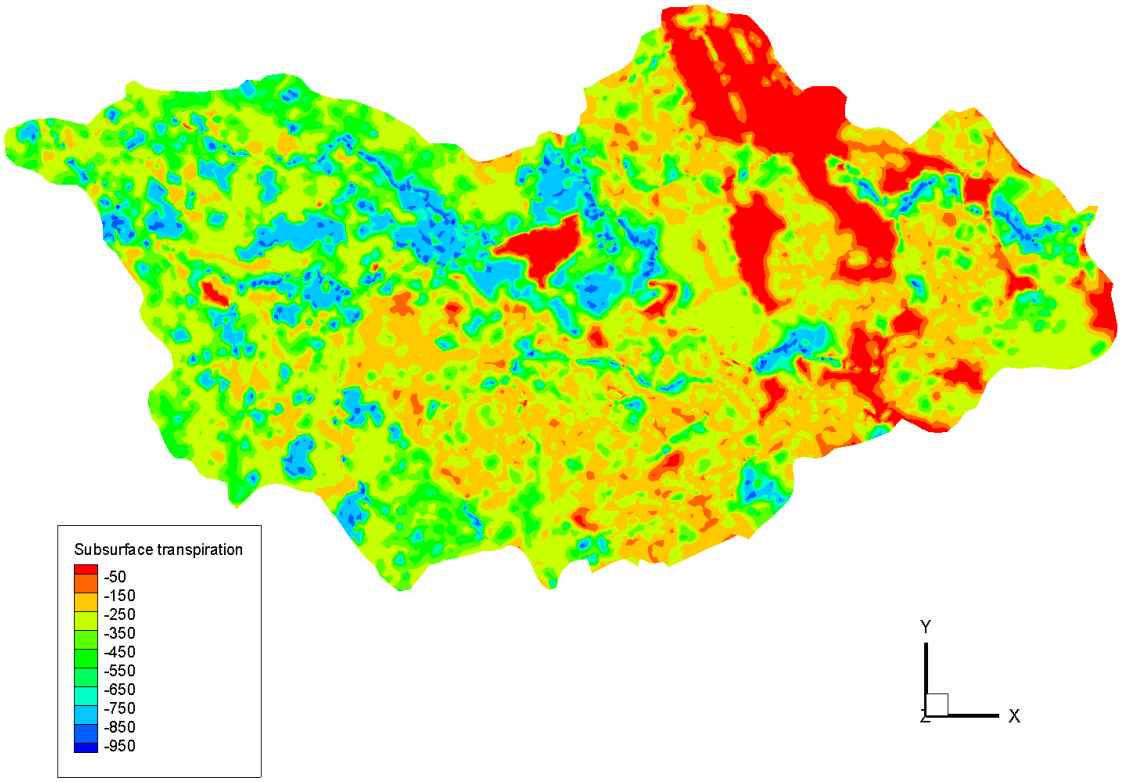

Figure 44 Subsurface transpiration [mm/year], 100% precipitation with evapotranspiration

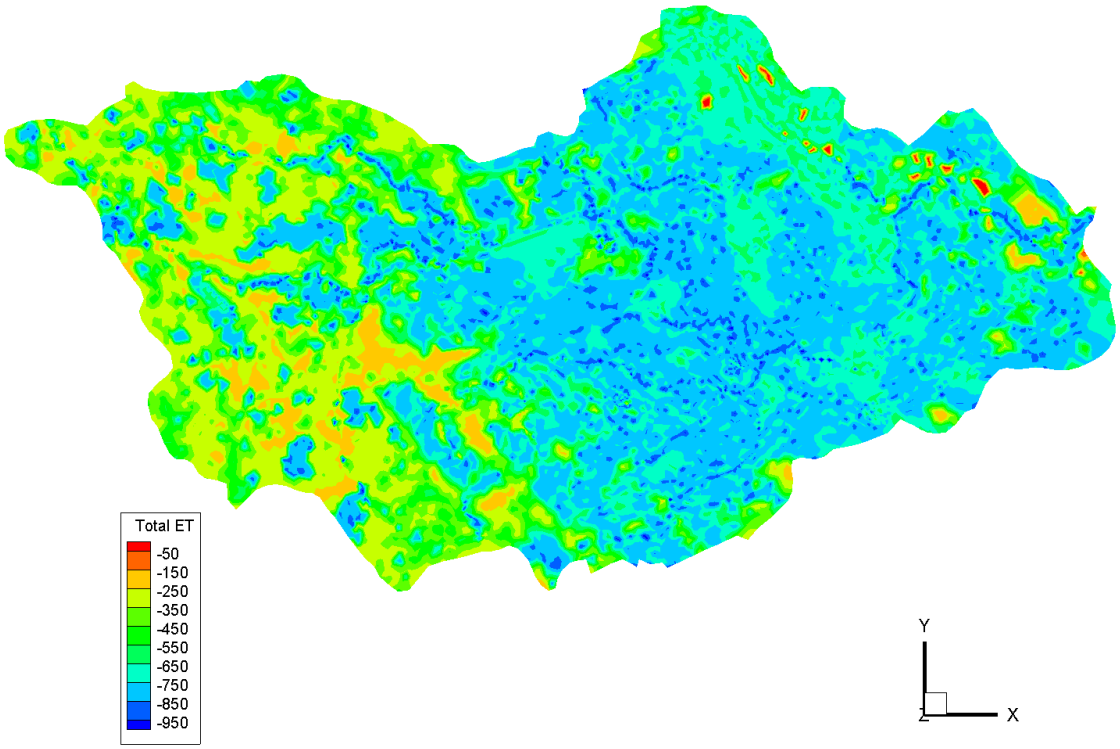

Figure 45 Total evapotranspiration [mm/year], 100% precipitation with evapotranspiration

As expected, most of the surface water and subsurface evaporation occurs in the Eastern end of the watershed, while the majority of the transpiration occurs in the Western end of the watershed due to a higher amount of agricultural and forested areas in the West. This allocation of evaporation and transpiration results in an even distribution of evapotranspiration throughout the watershed, with most occurring in the central region.

4.4 Comparison to Measured Data

Stream flow data for the Laurel Creek Watershed was obtained from Dr. Mike Stone in the Department of Geography and Environmental Management at the University of Waterloo. Base flows were measured weekly at 10 locations, shown in Figure 46. During storm events, storm flows were measured at sites 5, 14, 17, 21, and 23. Two simulations were conducted to compare the hydrographs from measured data and the simulated results, as described in Section 4.4.1 and Section 4.4.2. Pumping wells were pumping at a rate of 0.001 m^3/s during these simulations.

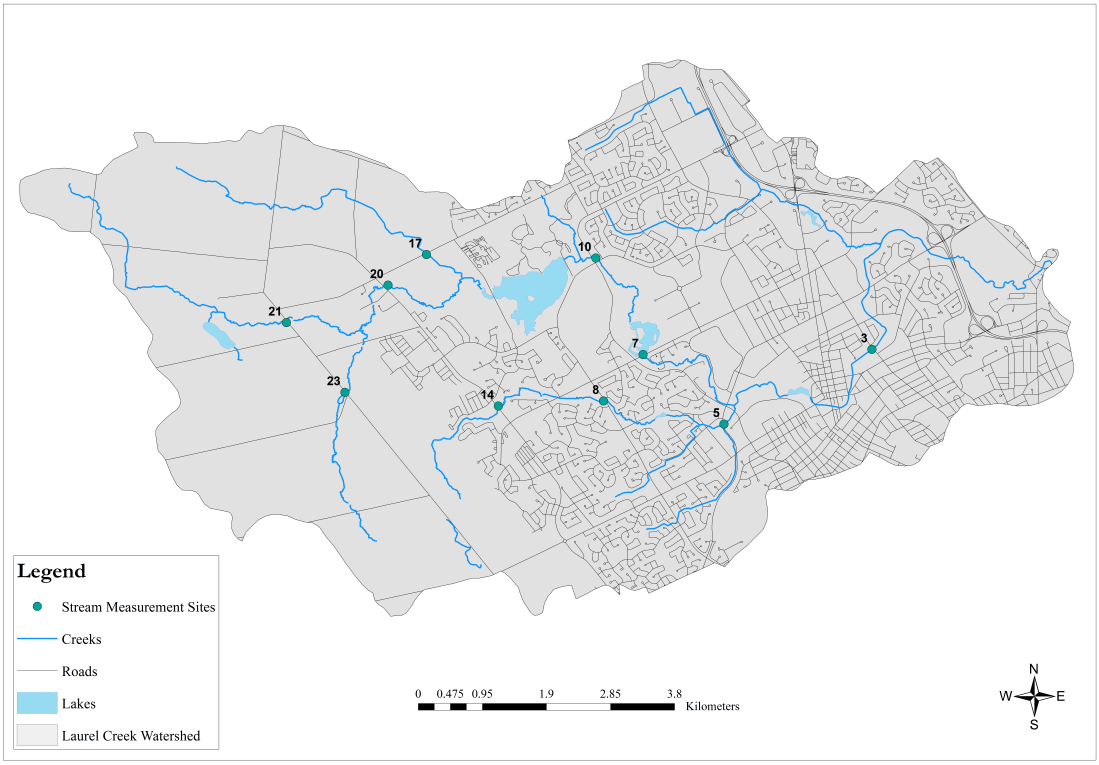

Figure 46 Laurel Creek Watershed stream flow measurement sites

4.4.1 Steady State Comparison

A steady state model was run with hydrographs at all stream measurement locations (Figure 46). The purpose of this model was to compare base flows of each site to the steady state simulated flows. Base flows for each site were obtained by averaging the weekly measurements for the years 2010, 2011, 2012, and 2014. Data for 2013 was unavailable. Measurements were taken between May and August, with 26 to 32 measurements per year. Flows were calculated using the velocity-area method. Table 19 lists the base flows and simulated flows for all site locations.

Table 19 Average measured base flows compared with steady state simulation results

Site	Location Description	Measured Base Flow (m^3/s)				Simulated Flow (m^3/s)	Average (m^3/s)
		2010	2011	2012	2014		
3	Laurel Creek at Weber Street	0.2338	0.4148	0.1424	0.1504	0.4845	0.2614
5	Clair Creek at University Avenue	0.5084	0.0683	0.0312	0.0367	0.0908	0.1278
7	Laurel Creek at Columbia Street	0.1919	0.2215	0.0739	0.0948	0.3839	0.1733
8	Clair Creek at Fischer-Hallman Road	0.0259	0.0584	0.0075	0.0114	0.0528	0.0273
10	Laurel Creek at Westmount Road	0.2557	0.3011	0.0674	0.1231	0.3207	0.1892
14	Clair Creek at Erbsville Road	0.0414	0.0365	0.007	0.0142	0.0527	0.0265
17	Beaver Creek at Conservation Road	0.0379	0.0517	0.0191	0.0198	0.0837	0.0386
20	Laurel Creek at Erbsville Road	0.0994	0.1982	0.1028	0.1225	0.1727	0.1331
21	Laurel Creek at Wilmot Line	0.0349	0.0546	0.0261	0.0328	0.0394	0.0357
23	Monastery Creek at Wilmot Line	0.0244	0.0292	0.0073	0.0076	0.1973	0.0455

Figure 47 illustrates average base flows compared to the steady state simulation result.

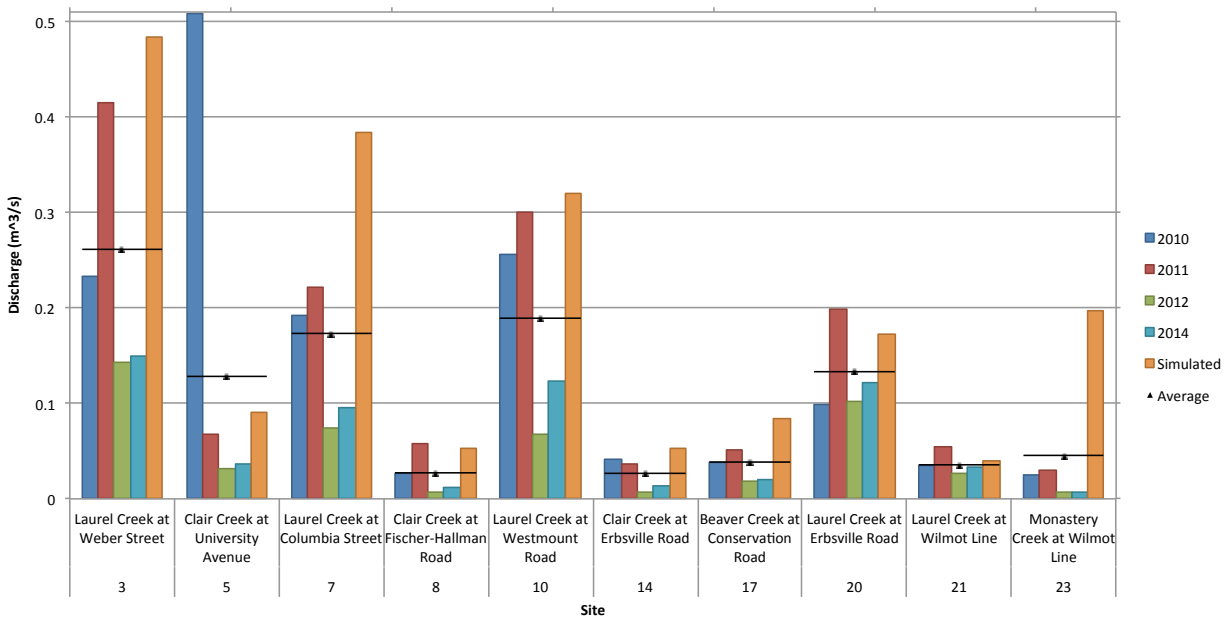

Figure 47 Average measured base flows compared with steady state simulation results

Based on Figure 47, it can be seen that the simulated results are similar to the measured base flows, with the exception of sites 3, 7, and 23 in which the simulated results are much higher than the measured results. It also appears that the model is able to more accurately match base flows at stations that are located upstream of the Laurel Creek Reservoir as they are minimally impacted by urbanization and hydraulic control features. In addition, these areas have more natural rainfall-runoff responses, which this model is able to predict most realistically.

The differences and standard deviations between the average measured base flows and the simulated flow results were calculated for each site, and the results are shown in Table 20. The results show that the steady state model was able to provide an accurate representation of surface water base flows throughout the Laurel Creek Watershed.

Differences between measured and simulated flows are a result of the discretization of the 2-D mesh. The mesh was created using a 10 m DEM, and spacing along the stream network was set to 25 m. Given that the streams may be less than 10 m wide, the streambed detail was lost in the DEM and subsequently in the discretization of the mesh. Differences may also be attributed to the evapotranspiration parameters that were used. Because the model was not calibrated due to time constraints, the evapotranspiration parameters would likely need to be adjusted in order to achieve a perfect steady state result.

Table 20 Standard deviations and differences between average measured base flow and simulated flow

Site	Average Measured Base Flow (m^3/s)	Simulated Flow (m^3/s)	Standard Deviation	Difference (Simulated – Measured)
3	0.2168	0.4845	0.19	0.27
5	0.1352	0.0908	0.03	-0.04
7	0.1312	0.3839	0.18	0.25
8	0.0221	0.0528	0.02	0.03
10	0.1629	0.3207	0.11	0.16
14	0.0212	0.0527	0.02	0.03
17	0.0295	0.0837	0.04	0.05
20	0.1251	0.1727	0.03	0.05
21	0.0349	0.0394	0.00	0.00
23	0.0152	0.1973	0.13	0.18

In addition to comparing stream flow measurements, the simulated hydraulic heads at 42 locations were also compared to measured data. Measured hydraulic head data was made available by Sousa (2013). Figure 48 provides a comparison of measured versus simulated hydraulic head.

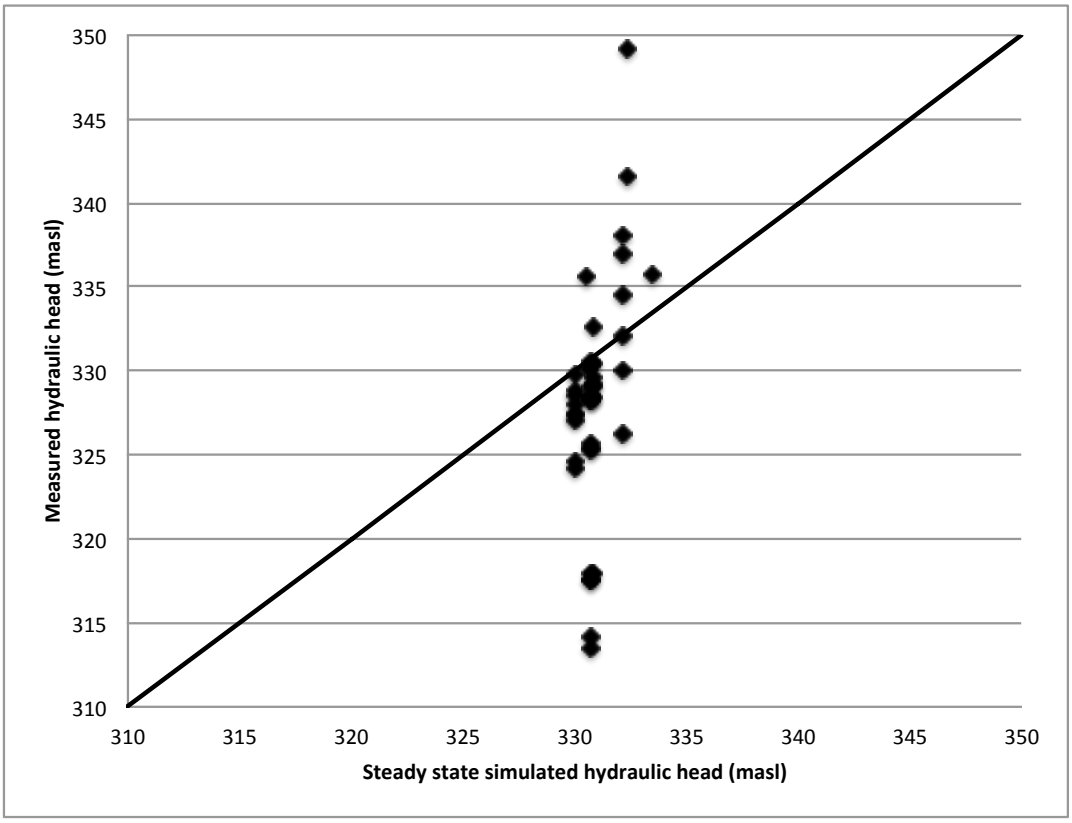

Figure 48 Simulated and measured hydraulic heads at 42 locations throughout the Laurel Creek Watershed

The points in Figure 48 represent the measured versus simulated hydraulic head values. The line represents a perfect fit for the dataset. If all points aligned along this diagonal line, it would indicate that the measured and simulated hydraulic heads were equal at all locations. The figure shows that the simulated hydraulic head values at all locations range between 330.0 m asl to 333.5 m asl, with the most common values being approximately 330.0 m asl, 330.8 m asl, and 332.2 m asl.

Because the simulated hydraulic heads need to be calculated at a specific node within the mesh, the hydraulic heads cannot be calculated at the exact location of the measured heads. To mitigate this in future Laurel Creek Watershed models, the 42 locations of the measured heads should be considered during the mesh generation process.

It is expected that model calibration would result in simulated hydraulic heads having a closer fit to the measured hydraulic heads. Parameterization of the soil properties may be adjusted to achieve hydraulic head values that are representative of the water table. Additionally, this version of the model utilizes no-flow boundary conditions. With the implementation of constant head boundary conditions, a more representative vertical gradient would be achieved throughout the subsurface.

4.4.2 Transient Flow Comparison

A transient flow model was generated for a storm event that occurred on July 27 – July 28, 2014. The precipitation data was obtained from the University of Waterloo Weather Station (Seglenieks, 1998). Measurement data was available for five locations: sites 5, 14, 17, 21, and 23 (Figure 46). Four of the five measurement locations are on tributaries to Laurel Creek, with site 21 being the only measurement location on Laurel Creek.

The storm event began at 6pm on July 27 and finished at 7:30am on July 28. Manual stream flow measurements were taken between 10am and 2pm on July 28. Because the measurements were taken after the storm event, the measurement data may not reflect the peak flows that occurred during the storm event.

Figure 49 illustrates the precipitation event that was used for the transient flow model. Figure 50 through Figure 55 show the hydrograph results from the transient model.

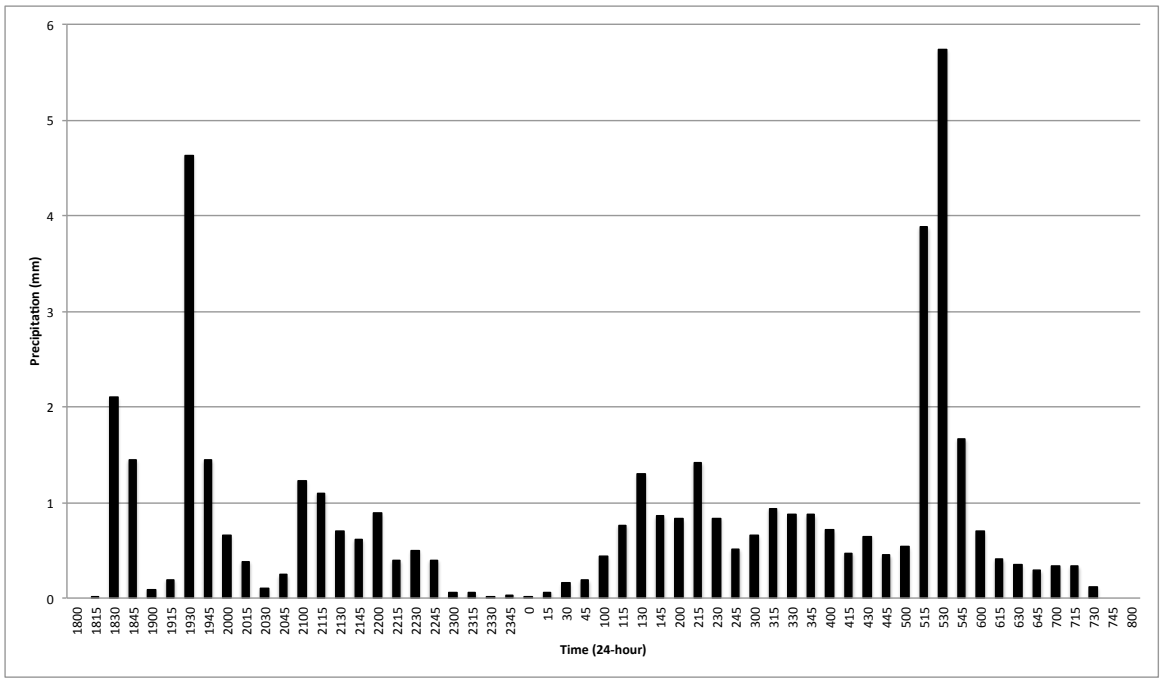

Figure 49 Storm event July 27-28, 2014 used for transient model

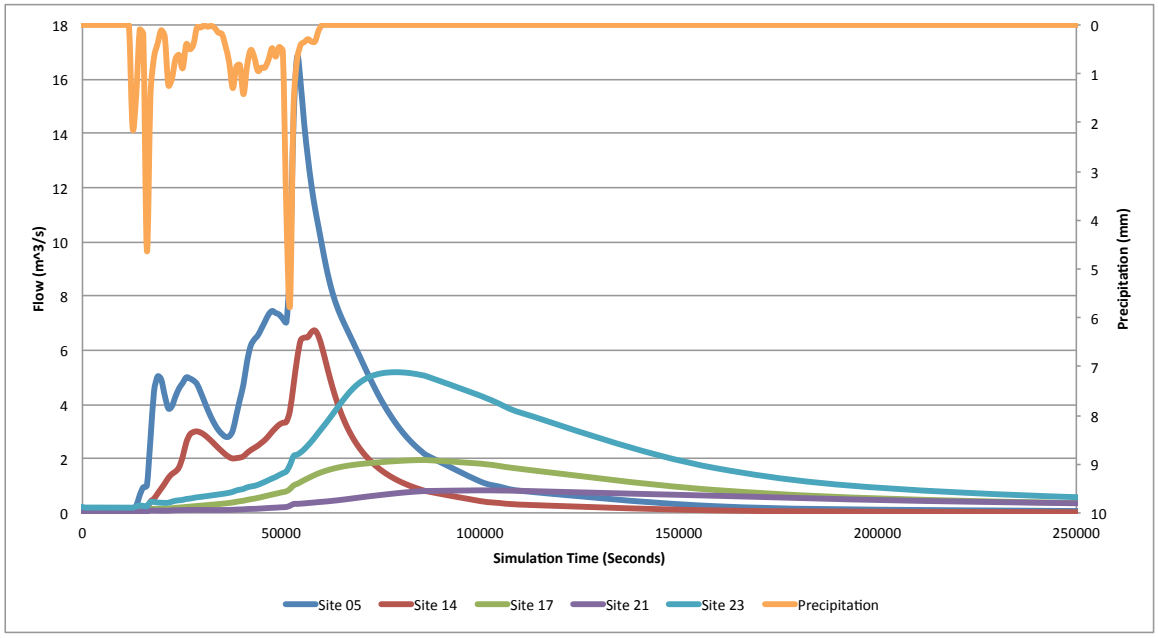

Figure 50 Transient simulation results, all sites

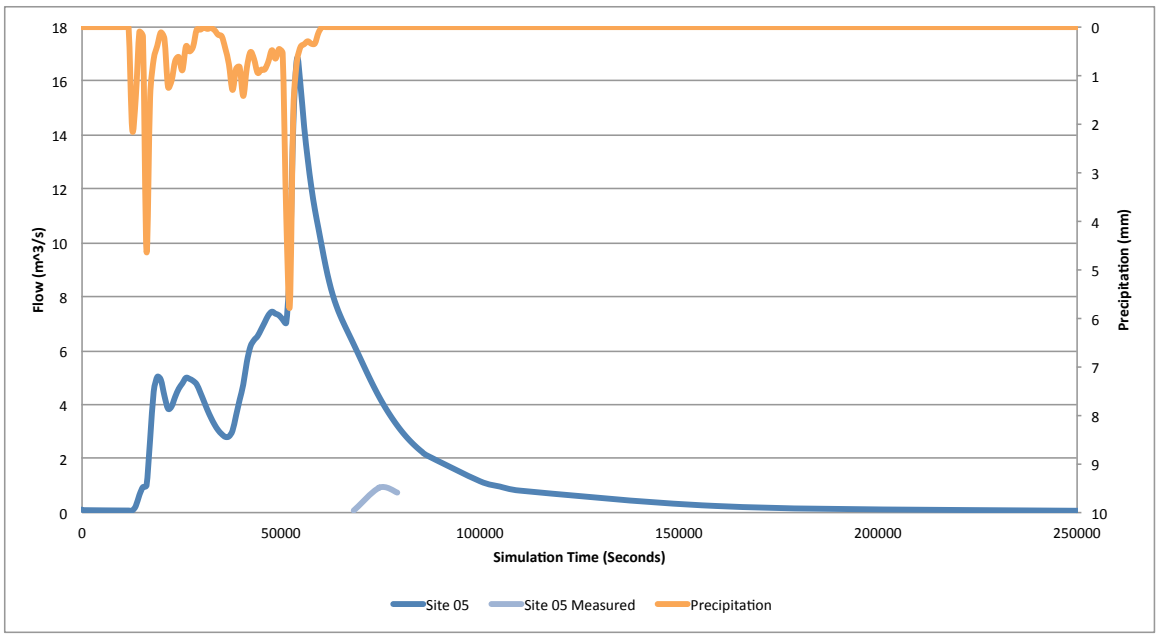

Figure 51 Transient simulation results compared to measured flow, site 05 Clair Creek at University Avenue

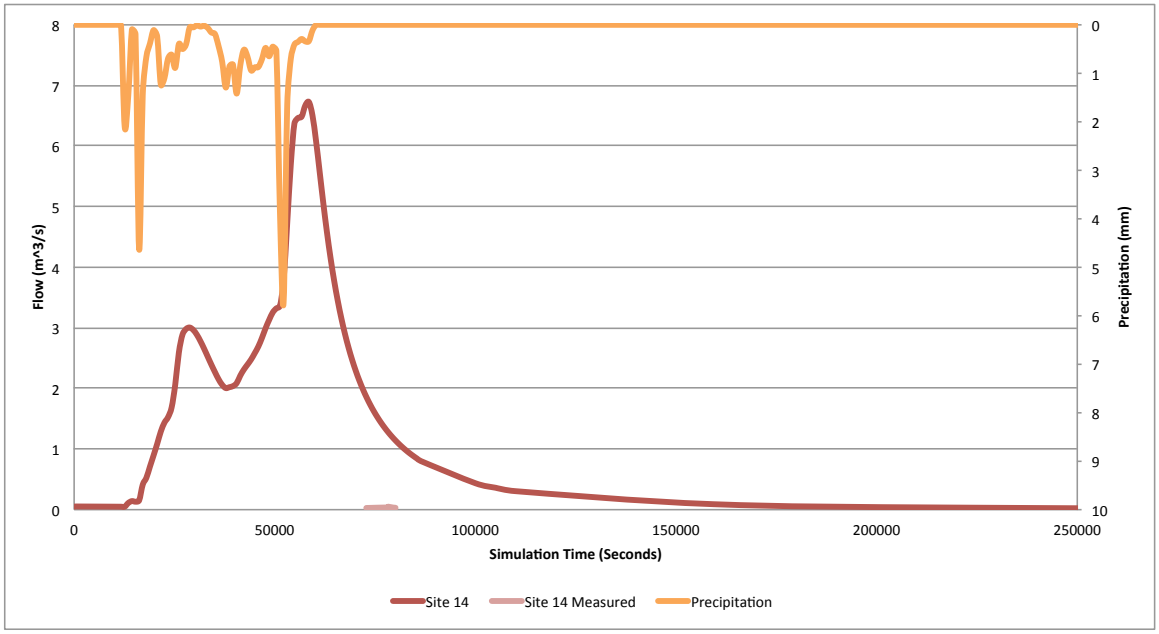

Figure 52 Transient simulation results compared to measured flow, site 14 Clair Creek at Erbsville Road

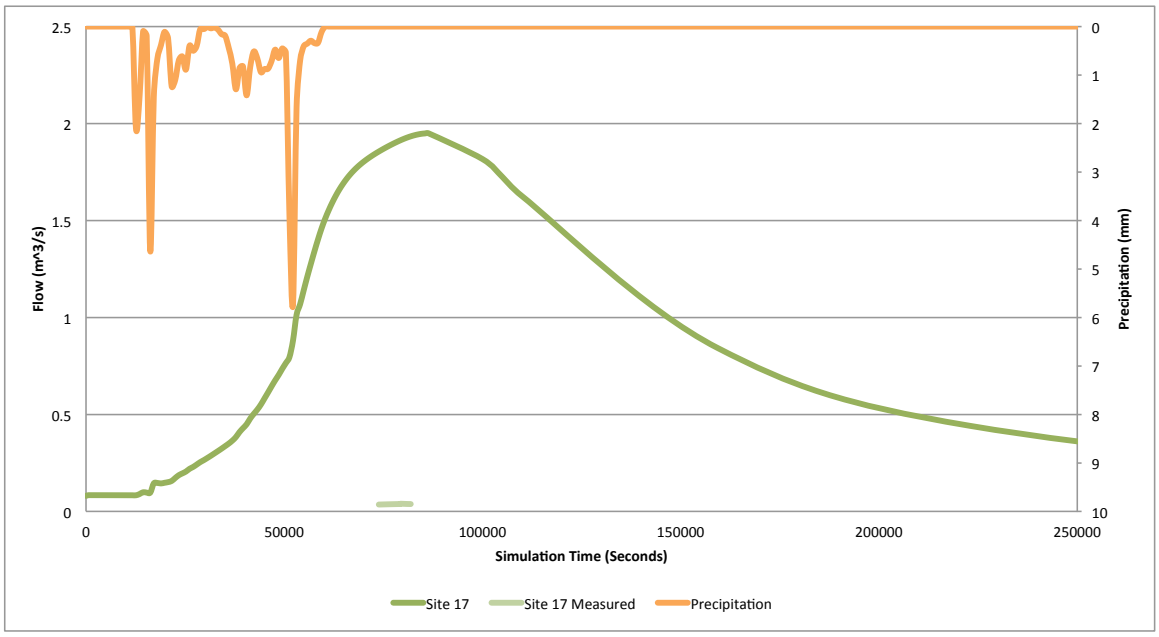

Figure 53 Transient simulation results compared to measured flow, site 17 Beaver Creek at Conservation Road

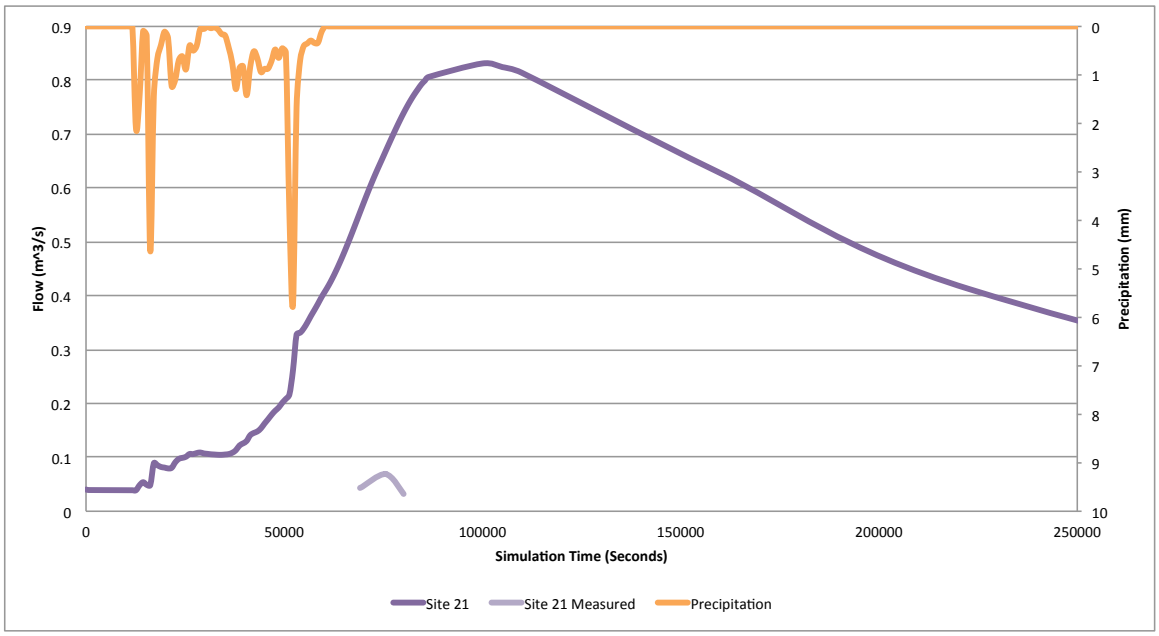

Figure 54 Transient simulation results compared to measured flow, site 21 Laurel Creek at Wilmot Line

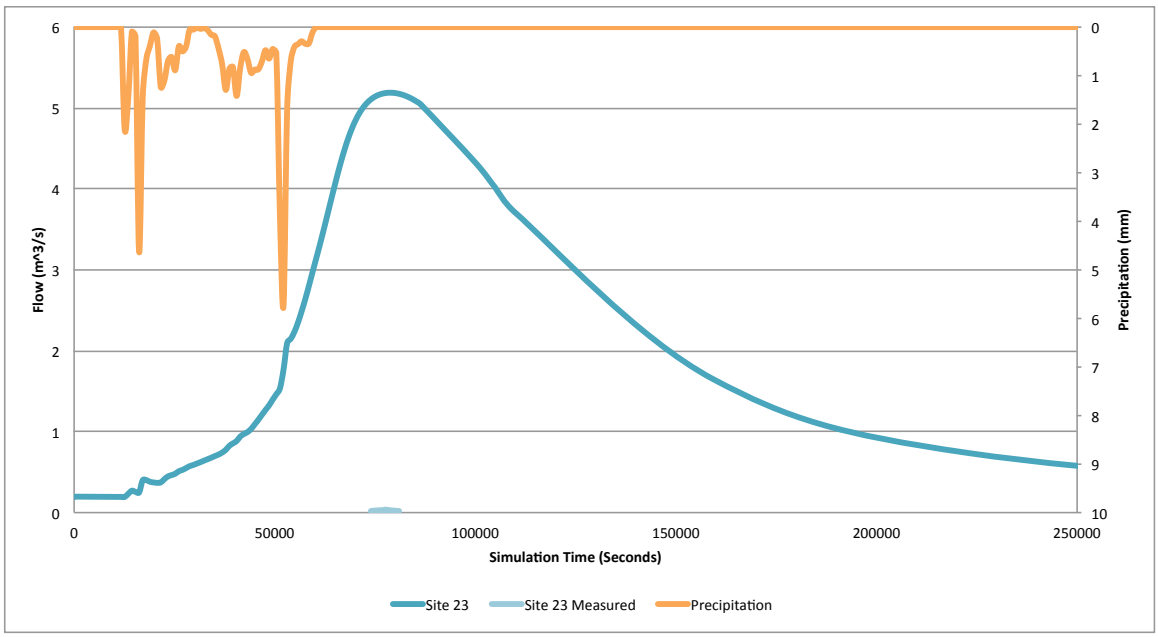

Figure 55 Transient simulation results compared to measured flow, site 23 Monastery Creek at Wilmot Line

As shown in the preceding figures, the transient flow model produced flows that were much larger than the measured flows. It is expected that calibration of the model would reduce the amount of uncertainty in the transient flow model by providing a better fit to the measured data. The simulation at site 21 (Laurel Creek at Wilmot Line) produced the most realistic results as the flows stayed under 1 m^3/s, and were closest to the measured data.

Differences between the measured and simulated flows may also be due to the absence of stormwater management ponds and floodgates on the reservoirs within the watershed, specifically at Columbia Lake and the Laurel Creek Reservoir. The model presented here only generates storage via surface depression, rather than using floodplain management systems. Future versions of the model should include consideration for stormwater management and floodgates that exist within the Laurel Creek Watershed. Additionally, stream reaches in the City of Waterloo are lined with riprap, which influences their natural rainfall-runoff response. The current model is not configured to capture these effects.

Table 21 provides a timeline associated with the outputs of the transient results, depicted in Figure 56 and Figure 57, which show the transient flow results over nine output times for the log depth of surface water and total evapotranspiration, respectively. Figure 56 shows how the depth of the surface water increases throughout the storm event and then decreases following the storm event as a result of surface flow and evapotranspiration. The total evapotranspiration (Figure 57)

remains consistent throughout the storm event, only decreasing when the storm event is finished because of the decrease in evaporation occurring in the Eastern end of the watershed.

Table 21 Timeline of events associated with transient simulation results

Event	Day	Time (12-hr)	Simulation Time (s)
Output 1	July 27	5:15pm	8100
Precipitation Begins	July 27	6pm	10800
Output 2	July 27	7:45pm	17100
Output 3	July 27	10:15pm	26100
Output 4	July 28	12:45am	35100
Output 5	July 28	3:15am	44100
Output 6	July 28	5:45am	53100
Precipitation Ends	July 28	7:30am	59400
Output 7	July 28	8:15am	62100
First stream measurement	July 28	10am	68400
Output 8	July 28	10:45am	71100
Output 9	July 28	1:15pm	80100
Last stream measurement	July 28	1:45pm	81900

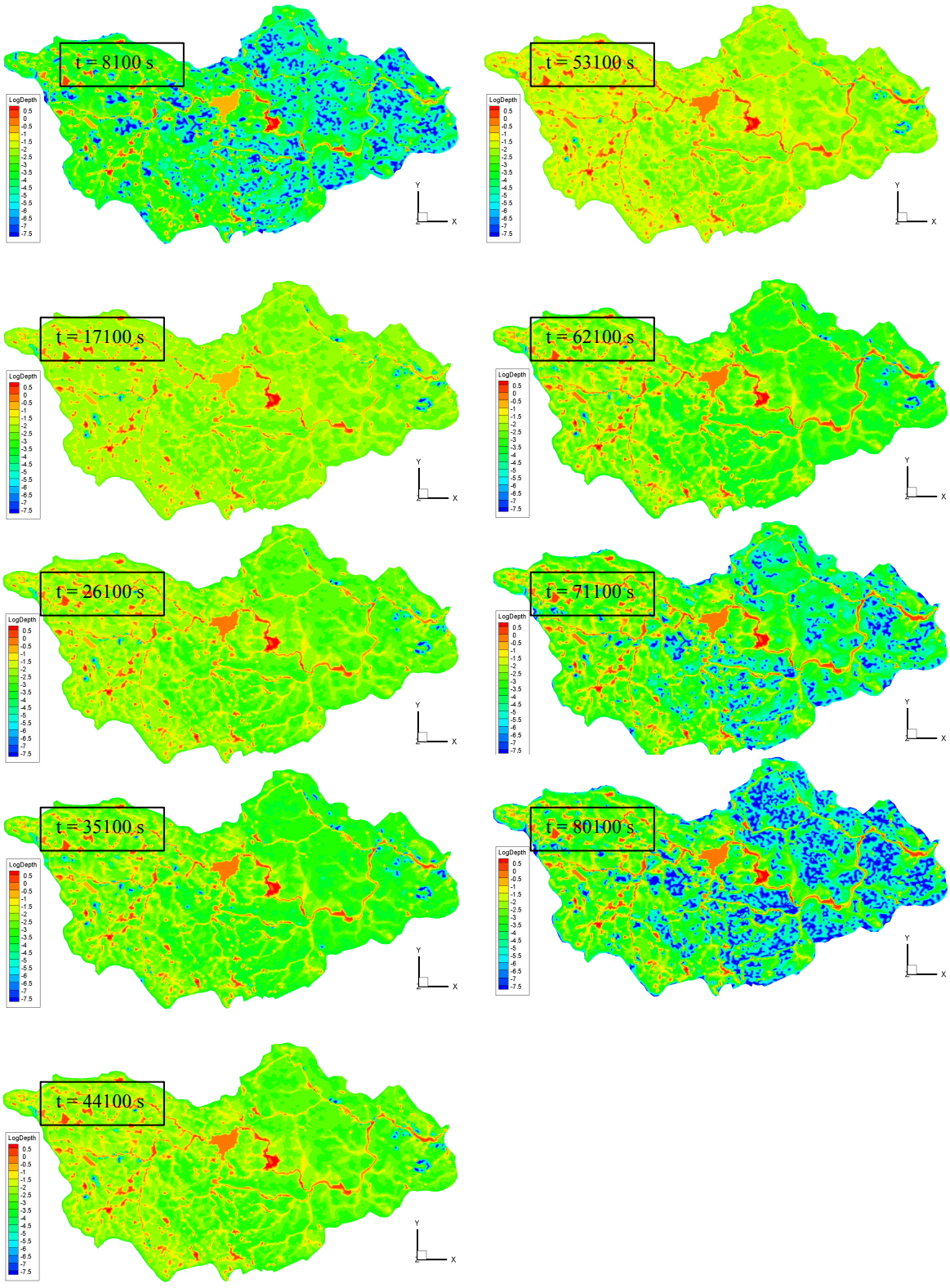

Figure 56 Log depth of surface water [log(m)] for transient flow simulation

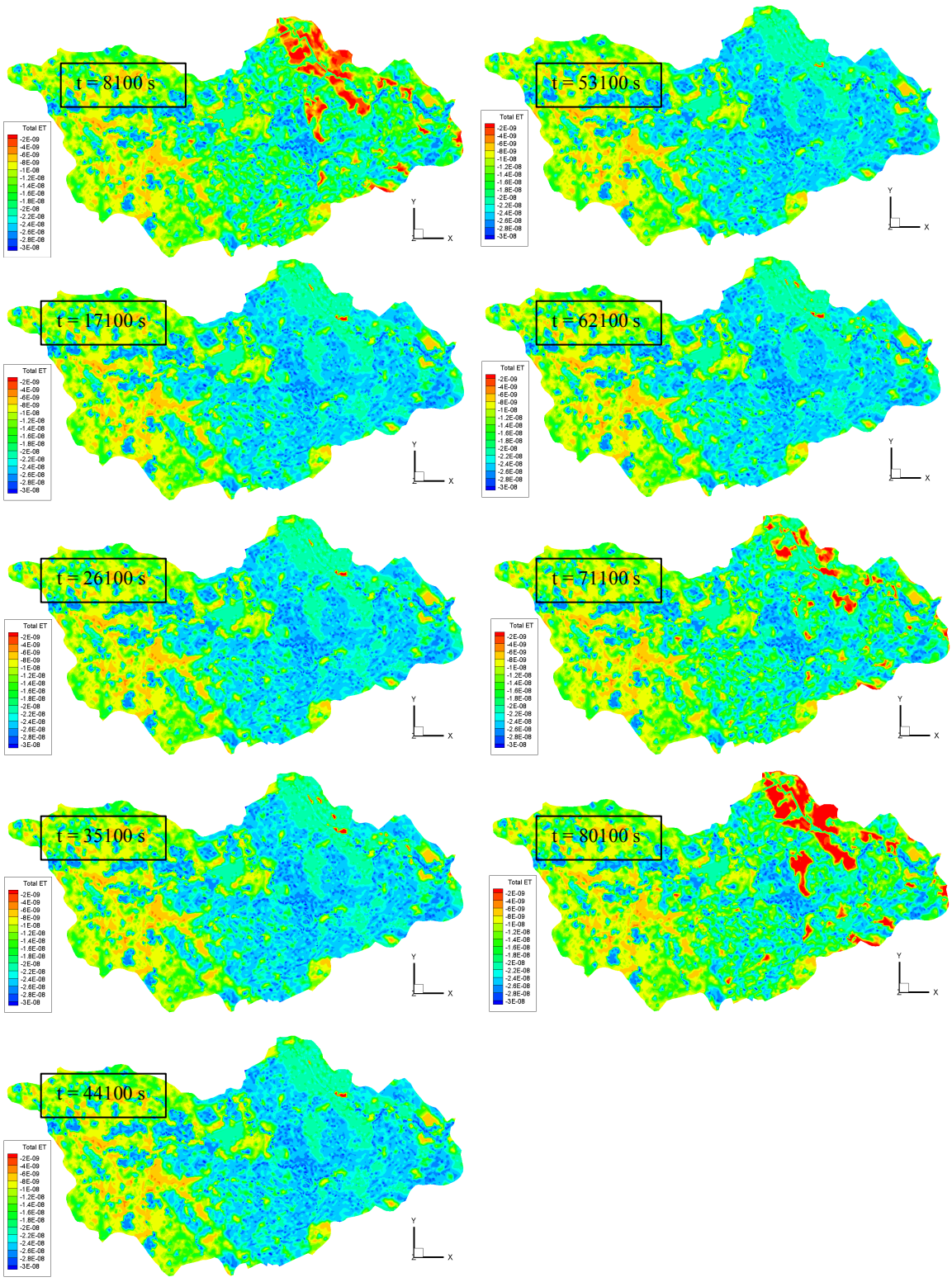

Figure 57 Total evapotranspiration [m/s] for transient flow simulation

Chapter 5: Conclusions

Continued growth of the Canadian economy has led to an increased population, resulting in the progressive urbanization of Canada's watersheds. Additionally, as infrastructure ages, an increasing percentage of drinking water is lost due to leakage from the distribution system. Conversely, groundwater infiltrates into sanitary sewer systems, which results in additional inflow to wastewater treatment plants and increased cost to consumers. As a result, municipal infrastructure asset management is an essential tool to efficiently manage the water and wastewater distribution networks.

To support the City of Waterloo asset management strategies, the primary goal of this thesis was to create an integrated groundwater-surface water model for the Laurel Creek Watershed with the inclusion of sanitary sewer infrastructure. Data was made available by the City of Waterloo, and a simplified version of the sanitary sewer network was created and added to the Laurel Creek Watershed model, which had been updated with a new digital elevation model, hydraulic conductivity field, land use files, and vegetation and evapotranspiration parameters.

Water infrastructure, including sanitary sewers, water mains, and storm sewers represent a large percentage of flow within an urbanized watershed. This amount of infrastructure flow is on the same scale as evapotranspiration; therefore, it is necessary to utilize a full hydrologic model to estimate the impact of the infrastructure on the watershed. Ultimately, a subsection of the sanitary sewer was included to represent the trunk lines throughout the City of Waterloo.

A 2-D mesh was created based on a 10 m DEM of the Laurel Creek Watershed. The mesh had 25 m spacing along the stream network, and 100 m spacing in all other areas. A 3-D mesh was created using the bedrock as the bottom layer, and the 10 m DEM as the top layer. The top 22 layers were based on the 10 m DEM and the bottom 17 layers were generated using the Waterloo Moraine model created by Sousa (2013). An additional layer was added to incorporate the sanitary sewer network in order to ensure the network had a continually decreasing elevation to allow for gravity drainage of the sanitary sewer.

Four steady state simulations were conducted. Two simulations ran with 25% precipitation and no evapotranspiration, with one including the sanitary sewer infrastructure. The next two simulations ran with 100% precipitation and evapotranspiration, with one including the sanitary sewer infrastructure.

The primary conclusion drawn from this thesis is that in order to incorporate the water and wastewater infrastructure into a groundwater-surface water model using HydroGeoSphere, the geometry of the infrastructure network must follow that of the existing mesh. Once the infrastructure is put in to the model with the appropriate geometry, HydoGeoSphere is able to determine the exchange flux between the subsurface and infrastructure domains.

The model results were compared to measured stream flow data made available by Dr. Mike Stone at the University of Waterloo. A steady state model was compared to data collected over four years for measured base flows at 10 sites. The steady state model produced results that were close to the average base flow measurements at all of the sites. A transient model was also created to compare measured flows at five sites from a 2014 storm event. The results from the transient simulation showed that the model produces very high peak flows during the precipitation event. At most, the model predicts a flow that is up to 16 times the measured results. It is expected that calibration of the model would correct this inaccuracy. It was also discovered during simulations that when the model is computing stream flows, it is unable to simultaneously measure the exchange flux between the infrastructure and subsurface domains. Therefore when running transient flow models, no data can be collected for the exchange flux between the subsurface and infrastructure domains. Ideally, the model would be able to provide data for both stream flows and infrastructure.

The model created in this thesis was constructed as a foundational model and is intended for use as the basis of future work. It has created a path toward constructing a practical asset management tool for use by a municipality. More work is required, as described in Chapter 6, in order for this model to be fully functional.

This thesis concludes that sewer infrastructure can be input into an integrated groundwater-surface water model using HydroGeoSphere, on the condition that it must be dependent on the geometry of the 3-D mesh. It also concludes that the updated Laurel Creek Watershed model is able to simulate transient flows, but must be calibrated in order to accurately represent measured stream flows.

Chapter 6: Recommendations for Future Work

A primary conclusion from this thesis is that in order to input water and wastewater infrastructure into an integrated groundwater-surface water model using HydroGeoSphere, the infrastructure must be based on the geometry of the 3-D mesh. The manual reconstruction of the mesh is labour intensive and time consuming. Therefore, manual mesh reconstruction is impractical for the purpose of municipal asset management because the mesh refinement would be required for any potential revisions or updates to the infrastructure.

In order for a model of this magnitude to act as a tool for a municipality in asset management, it is critical that future versions of the model have the ability to input infrastructure geometry independent of the geometry of the mesh. Future versions of the model should also incorporate the water main network in addition to the sanitary sewer network in order to provide a true representation of hydraulic movement in the subsurface.

For practical application of the model, future versions should contain constant head boundary conditions to incorporate regional subsurface flow for the transient system. They could be obtained using the same data as the hydraulic conductivity field, from Sousa (2013). In addition to incorporating constant head boundary conditions, pumping wells should be added to all simulations with average pumping rates for steady state simulations and actual rates for transient simulations.

Future versions of the model should incorporate a smaller mesh. Refinement of this mesh would be based on areas in which there is a sharp transition of hydraulic conductivity, such as a high value directly adjacent to a low value. Refinement should also be based on areas of high hydraulic activity, such as pumping wells, stream flow measurement locations, areas in which groundwater-surface water interactions are expected to be higher. Additionally, the locations of the 42 monitoring wells should be considered when the new mesh is created, such that there is a node placed at each of these locations to provide the most accurate results when comparing measured and simulated water levels. The model presented in this thesis will provide a guideline for where mesh refinement should occur. Outside of these refinement areas, it is suggested that a coarser mesh be incorporated to reduce the mesh size and inspire faster simulation times during calibration, uncertainty analysis, and other scenario-based simulations.

The model should be calibrated with the steady state model calibrating the subsurface to long-term water level averages, and the transient model calibrating the subsurface to well hydrographs. Next, the surface water flows can be calibrated to climate data. Calibration should be conducted manually first, then linked to PEST for polishing. PEST is a software package used for parameter estimation and uncertainty analysis for complex models (PEST, 2015). Anisotropy of the hydraulic conductivity and Manning's roughness coefficient should be considered during the calibration process.

In future models, initial conditions for model scenarios should be based on the realistic hydrology. Ideally, the model would be run with several months of climate and pumping data in order to generate a hydrologic fingerprint of the watershed. This would provide the initial conditions for any hydrologic scenarios.

References

Aquanty Inc. (2013). HydroGeoSphere User Manual. Waterloo, ON: Author.

Asner, G., Scurlock, J., & Hicke, J. (2003). Global synthesis of leaf area index observations: Implications for ecological and remote sensing studies. Global Ecology and Biogeography, 12, 191-205.

Bajc, A., Russell, H., & Sharpe, D. (2014). A three-dimensional hydrostratigraphic model of the Waterloo Moraine area, southern Ontario, Canada. Canadian Water Resources Journal, 39(2), 95-119.

Blackport, R., Meyer, P., & Martin, P. (2014). Toward an understanding of the Waterloo Moraine hydrogeology. Canadian Water Resources Journal, 39(2), 120-135.

Brooks, R.J., and A. T. Corey, 1964. Hydraulic properties of porous media. Hydrology paper 3, Colorado State university, Fort Collins, CO.

Canadell, J., Jackson, R., Ehleringer, J., Mooney, H., Sala, O., & Schulze, E. (1996). Maximum rooting depth of vegetation types at the global scale. Oecologia, 583-595.

Chin, D. (2013). Water-resources engineering (3rd ed.). Upper Saddle River, New Jersey: Pearson Education.

City of Waterloo. *City of Waterloo Infrastructure Geodatabase: ArcGIS 10.1.* Waterloo, ON: Integrated Planning and Public Works Engineering Services, 2013a.

City of Waterloo. (2013b). Design. *Development Engineering Manual,* 64-84. Retrieved from http://www.waterloo.ca/en/business/developmentengineeringmanual.asp

Christensen, J.H., Carter, T.R., Rummukainen, M., Amanatidis, G., 2007. Evaluating the performance and utility of regional climate models: the PRUDENCE project. Climatic Change 81 (Suppl. 1), 1–6.

Cooley, R.L., 1971. A finite difference method for unsteady flow in variably saturated porous media: Application to a single pumping well, Water Resour. Res., 7(6), 1607--1625.

CWWA. (1998). Municipal Water and Wastewater Infrastructure: Estimated Investment Needs 1997 to 2012. Retrieved April 2, 2015, from http://www.cwwa.ca/pdf_files/MWWW Investment Needs 1997-2012.pdf

Darcy, H. P. G.: Les fountaines publiques de la Ville de Dijon, Vic- ton Dalmont, Paris, 1856.

Doorenbos, J. (1977). Guidelines for predicting crop water requirements. FAO Irrigation and Drainage Paper. Retrieved April 1, 2014, from http://www.fao.org/docrep/018/f2430e/f2430e.pdf

Environment Canada. (2011). Municipal water use 2009 statistics. 2011 Municipal Water Use Report. Retrieved September 22, 2015, from http://ec.gc.ca/Publications/B77CE4D0-80D4-4FEB-AFFA-0201BE6FB37B/2011-Municipal-Water-Use-Report-2009-Stats_Eng.pdf

Environment Canada. (2015). Climate Archives. Retrieved April 21, 2015, from http://climate.weather.gc.ca/

Federation of Canadian Municipalities. (2002). A Guide to Sustainable Asset Management. Retrieved from https://www.fcm.ca/Documents/tools/PCP/Guide_to_Sustainable_Asset_Management_for_Canadian_Municipalities_EN.pdf

Federation of Canadian Municipalities. (2004). Managing Infrastructure Assets. Ottawa, ON: National Research Council of Canada. national guide to sustainable municipal infrastructure. Retrieved from http://www.fcm.ca/Documents/reports/Infraguide/Managing_Infrastructure_Assets_EN.pdf

Felio, G. (2012). Canadian infrastructure report card: Municipal roads and water systems(Vol. 1). Ottawa, ON: Canadian Construction Association.

Fetter, C. (2001). Applied hydrogeology (4th ed.). Upper Saddle River, New Jersey: Prentice Hall.

Freeze, R.A. and J.C. Cherry, 1979. Groundwater, Prentice Hall, Englewood Cliffs, New Jersey.

Freeze, R.A. and R.L. Harlan, 1969. Blueprint for a physically-based digitally-simulated hydrologic response model. Journal of Hydrology, 9: 237-258.

Goderniaux, P., Brouyère, S., Fowler, H. J., Blenkinsop, S., Therrien, R., Orban, P., & Dassargues, A. (2009). Large scale surface–subsurface hydrological model to assess climate change impacts on groundwater reserves. Journal of Hydrology, 373(1-2), 122–138. doi:10.1016/j.jhydrol.2009.04.017

Guo, W., 2014. Spatial Mapping of Evapotranspiration Parameters for an Urban Hydrologic Model of the Laurel Creek Watershed. Undergraduate Thesis, Department of Earth Sciences, University of Waterloo, Waterloo, Ontario, 27p.

Hargreaves, G., & Allen, R. (2003). History and Evaluation of Hargreaves Evapotranspiration Equation. Journal of Irrigation and Drainage Engineering J. Irrig. Drain Eng., 53-63.

Houghtalen, R., Akan, A., & Hwang, N. (2010). Fundamentals of hydraulic engineering systems (4th ed.). Upper Saddle River, New Jersey: Prentice Hall.

Jones, J. P., Sudicky, E. a., & McLaren, R. G. (2008). Application of a fully-integrated surface-subsurface flow model at the watershed-scale: A case study. Water Resources Research, 44(3), n/a–n/a. doi:10.1029/2006WR005603

Jones, J.P., 2005. Simulating hydrologic systems using a physically-based, surface-subsurface mode: Issues concerning flow, transport and parameterization. Ph.D Thesis, Department of Earth Sciences, University of Waterloo, Waterloo, Ontario, 145p.

Kalbus, E., Reinstorf, F., & Schirmer, M. (2006). Measuring methods for groundwater – surface water interactions: A review. Hydrology and Earth System Sciences, 10(6), 873-887.

Kilpatrick, F. A. and Cobb, E. D.: Measurement of discharge using tracers, U.S. Geol. Surv., Techniques of Water-Resources Inves- tigations, Book 3, Chapter A-16, 1985.

Li, Q., Unger, a. J. a., Sudicky, E. a., Kassenaar, D., Wexler, E. J., & Shikaze, S. (2008). Simulating the multi-seasonal response of a large-scale watershed with a 3D physically-based hydrologic model. Journal of Hydrology, 357(3-4), 317–336. doi:10.1016/j.jhydrol.2008.05.024

McLaren, R. G. (2011). Grid Builder: A pre-processor for 2-D, triangular element, finite-element programs. Waterloo, ON: Waterloo Centre for Groundwater Research, University of Waterloo

Meyer, P., Brouwers, M., & Martin, P. (2014). A three-dimensional groundwater flow model of the Waterloo Moraine for water resource management. Canadian Water Resources Journal, 39(2), 167-180.

Mirza, S., 2007. Danger Ahead: the Coming Collapse of Canada's Municipal Infrastructure. A report for the Federation of Canadian Municipalities. Retrieved from: https://www.fcm.ca/Documents/reports/Danger_Ahead_The_coming_collapse_of_Canadas_municipal_infrastructure_EN.pdf. April 1, 2015

MOE. (2007). Toward financially sustainable drinking-water and wastewater systems. Financial Plans Guideline. EBR Registry Number: 010- 04920

Neuman, S.P., 1973. Saturated-unsaturated seepage by finite elements, ASCE J. Hydraul. Div., 99(HY12), 2233--2251.

O'Connor, D. R. 2002. Report of the Walkerton Inquiry: The events of May 2000 and related issues. Parts 1 and 2. Toronto, ON: Ontario Ministry of the Attorney General

Perrone, D., Murphy, J., & Hornberger, G. M. (2011). Gaining perspective on the water-energy nexus at the community scale. Environmental Science & Technology, 45(10), 4228–34. doi:10.1021/es103230n

PEST: Model-Independent Parameter Estimation and Uncertainty Analysis. (2015). Retrieved November 20, 2015, from http://www.pesthomepage.org/

Power Applications Group. Ontario municipalities: An electricity profile, 2008. http://www.ieso.ca/imoweb/pubs/sector-specific_ research/Ontario_Municipalities-An_Electricity_Profile.pdf

Province of Ontario. 2006. Clean Water Act. Toronto, ON: Queen's Printer for Ontario.

Rehan, R., Knight, M., Unger, A., & Haas, C. (2013). Development of a system dynamics model for financially sustainable management of municipal watermain networks. Water Research, 7184-7205. http://dx.doi.org/10.1016/j.watres.2013.09.061

Seglenieks, F. (1998). Data Archives. Retrieved April 1, 2014, from http://www.civil.uwaterloo.ca/weather/data.html

Sousa, M. R. De. (2013). Using Numerical Models for Managing Water Quality in Public Supply Wells. Ph.D Thesis, Department of Earth Sciences, University of Waterloo, Waterloo, Ontario, 164p.

Stantec, CH2M Hill. (2014). City of Hamilton Public Works Asset Management Plan. Hamilton, ON. Retrieved April 1, 2015, from https://www.hamilton.ca/NR/rdonlyres/812CACE9-0736-4A0A-8056-BB2E8D25543B/0/COH_AM_Plan.pdf

Stewart, D. (2012, July 1). Municipal Asset Management & Financial Planning in smaller municipalities. Retrieved April 18, 2015, from http://scugog.ca/uploads/1344368167-Municipal Asset Management & Financial Planning Research Paper & Case Study 07-2012 R.pdf

Sudicky, E. A., Jones, J. P., Park, Y.-J., Brookfield, A. E., & Colautti, D. (2008). Simulating complex flow and transport dynamics in an integrated surface-subsurface modeling framework. Geosciences Journal, 12(2), 107–122. doi:10.1007/s12303-008-0013-x

Therrien, R. 1992. Three-dimensional analysis of variably- saturated flow and solute transport in discretely-fractured porous media. Ph.D. thesis, University of Waterloo, Waterloo, Ont.

Therrien, R., R.G. McLaren, E.A. Sudicky, S. Panday, D.T. DeMarco, G. Mantanga, and P.S. Huyakom, 2003. User's guide, HydroSphere: A Three-dimensional Numerical Model Describing Fully-integrated Subsurface and Overland Flow and Solute Transport. Groundwater Simulations Group, Waterloo, Ontario, 230p.

Van Genuchten, M.Th., 1980. A closed-form equation equation for predicting the hydraulic conductivity of unsaturated soils, Soil Sci. Soc. Am. J., 44, 892--898.

VanderKwaak, J.E., 1999. Numerical simulation of flow and chemical transport in integrated surface-subsurface systems. Ph.D Thesis, Department of Earth Sciences, University of Waterloo, Waterloo, Ontario, 242p.

Veale, B., Cooke, S., Zwiers, G., & Neumann, M. (2014). The Waterloo Moraine: A watershed perspective. Canadian Water Resources Journal, 39(2), 181-192.

Zhou, Y., Zhang, B., Wang, H., & Bi, J. (2013). Drops of Energy: Conserving Urban Water to Reduce Greenhouse Gas Emissions. Environmental Science & Technology, 130611081647003. doi:10.1021/es304816h